Design and Evaluation of Elastic Exoskeletons for Human Running

by

Michael S. Cherry

A dissertation submitted in partial fulfillment
of the requirements for the degree of
Doctor of Philosophy
(Mechanical Engineering)
in The University of Michigan
2010

Doctoral Committee:

Associate Professor Daniel P. Ferris, Co-Chair
Professor Sridhar Kota, Co-Chair
Professor Jessy W. Grizzle
Associate Professor Arthur D. Kuo
Assistant Professor Kathleen H. Sienko

If we knew what we were doing, it wouldn't be called research.

— Albert Einstein

To my loving wife, Natalie,
and my angel mother, Penny.

Acknowledgments

This work could not have been accomplished without the guidance and support of Professors Daniel P. Ferris and Sridhar Kota. When I was nearing the end of my undergraduate studies at Brigham Young University, instead of just looking for good schools to attend for my graduate work, I looked for potential advisors. As an undergrad I became interested and involved in compliant mechanism design research. This led me to Professor Kota who graciously took me on as one of his students. Through his guidance I obtained an NSF graduate student fellowship and together persuaded Professor Ferris to take on the role of co-advisor. These two men with their extensive knowledge of mechanism design and human biomechanics, respectively, provided the foundation upon which this dissertation was built.

Continuing on the academic front, I am extremely grateful to the numerous students, both graduate and undergraduate, who assisted me in this research. Back in the early days of my graduate career (2003), I was welcomed into the Compliant Systems Design Laboratory by Charles Kim, Brian Trease, Kerr-Jia Lu, Christine Vehar, Tony Tantanawat, Zak Kriener, Audrey Plinta, and Dragan Maric. These individuals helped me learn the ropes at the University of Michigan, gave me guidance in my research and coursework, and were good friends too.

Throughout my time as a student in the lab I was joined by Youngseok Oh, Girish Krishnan, and Josh Bishop-Moser. I spent a lot of time with these three individuals, working in the CSDL. In particular, Youngseok and I spent many late nights working on our dissertation research and he was instrumental in helping me with finite element analyses. Josh is one of the most creative designers I know and was invaluable in design reviews and brainstorming sessions.

Art Kuo and the students in his Human Biomechanics and Control Laboratory were also extremely helpful during the design stage of my research. Steve Collins, Shawn O'Connor, John Rebula, and Karl Zelik all contributed ideas, support, and information. Peter Adamczyk went above and beyond by spending numerous hours on multiple occasions with me in front of a white board discussing potential designs for exoskeletons. Sometimes I refer to Peter as "the source of all knowledge." Aside from knowing just about everything, he also happens to be one of the nicest guys in the world and an absolute pleasure to associate with.

Other significant contributors on the design side of this research were the two teams of undergraduate mechanical engineers that I had the pleasure of working with. The first team consisted of Dave Choi, Kevin Deng, and Josh Krieger. These three students helped design and implement the elastic knee-ankle-foot orthosis presented in Chapter 2 of this dissertation. Brandon Chan, Sean Mitera, Philip Dowhan, and Joe Cho were on the second team. This team helped design and fabricate the first prototype of the elastic exoskeleton presented in Chapter 4 of this dissertation. Some of their work is also included in the Appendices as it is critical to understanding why the final design concept was used.

The exoskeletons created during this research needed to interface comfortably with human subjects. Needless to say, in my Mechanical Engineering studies we never took courses covering human anatomy, much less how to design mechanisms that attach to it without bruising, blistering, or impinging it. This is where Jake Godak and Anne Manier from the U of M Orthotics & Prosthetics Center came in. They helped me design and fabricate everything between the mechanisms and the subjects. They laid up countless layers of pre-impregnated carbon composite for me in my numerous design iterations.

When it came to precision-machined aluminum, another set of individuals were instrumental in making it happen. It all started with Steve Emmanuel and Jason Moscetti, many years ago with the eKAFO and early prototypes of the eExo. Later on the ME Department acquired a water jet cutter and I quickly became friends with Steve Erskine and Jason Rodgers who ran the machine. I think 80% of the eExo parts were cut on that machine down on the first floor of the Dow building. The rest of them were machined by Kevin Lapprich, a very helpful undergrad who loves to cut metal and make cool things. Thankfully he thought my research was interesting enough that he volunteered to help me out with it. Between him, me, Jason, and Anne, we cranked out the final iteration of the eExo in less than a month. I could not have done it without them.

What good is a prototype with no test data? None at all. This is where the members of Dan Ferris' Human Neuromechanics Laboratory came in to play. During the five years I worked in the HNL I had the privilege of interacting with three separate lab managers. Catherine Kinnaird taught me how to use everything in the lab and helped with all the data collections for the eKAFO study. She was so kind and helpful; everything she touched just seemed to work.

When I started testing the eExo, Evelyn was the lab manager. Those early days of collecting corresponded precisely with the time Antoinette Domingo, Shawn O'Connor, and Cara Lewis were collecting their final data sets. We also had an EEG system in the lab that we were borrowing for a limited term. Consequently the lab was crazy and fully booked. Because I could hardly get in during the day, Evelyn and I spent quite a few late nights

collecting data in the lab, trying to figure out what was wrong with the eExo and how to make it work better.

By the time the eExo was finally complete and ready for the final data collections, Monica Majcher had been hired. Monica, Evelyn, as well as two post-docs, Amy Sipp and Cara Lewis, helped me get through those final collections. Cara deserves special mention. She not only helped with the collections, she was a mentor and a friend. She helped me mature as a graduate student, particularly by helping me learn to be more productive in the lab and in my research. She was one of the most efficient and knowledgeable researchers I've ever met. Whenever there were problems in the lab, Cara showed us how to fix them.

There is a saying that many hands make light work. When collecting data in the lab, this is definitely the case. Aside from the help provided by those already mentioned, there were a number of undergraduate and graduate students from the HNL who helped make the lab run. Joe Gwin, Julia Kline, Ryan Bernstein, Sara Weiss, and Alberto Alfaro are on that list. Alberto was particularly involved in my project. We spent my last summer (2009) working together on the eExo, collecting and analyzing the data. He even helped fabricate and assemble the final iteration of the exoskeleton.

On a more formal note, I could not have completed this dissertation without the help of my graduate committee. In addition to Professors Ferris and Kota, Professors Art Kuo and Kathleen Sienko were on my committee when I presented my prelim document. They gave very helpful feedback and encouraged me in my work. Professor Jessy Grizzle joined the committee for the defense, fulfilling the essential role of a cognate member. His expertise in robotics and controls were a perfect addition to the committee.

From the funding side, this work was supported by an NSF Graduate Research Fellowship and NSF Grant BES-0347479. During my time as a graduate student, I was also supported as a Graduate Student Instructor and a Graduate Student Mentor. I gained valuable experience teaching courses in mechanical design and system dynamics as a GSI in those courses. As a GSM I provided support and assistance to other GSIs in order to help them be better teachers too.

I'd like to finish out this section on a personal note. I am extremely thankful for the support of my family and my Father in Heaven for their support. During my graduate studies our sons Brayden and Caleb were born. It was a significant sacrifice that this happened in Michigan, far away from our families out on the west coast. Completing a Ph.D has been the hardest thing I've ever done in my life, and it was hard on our little family as well. I could not have survived without the help of my loving wife, Natalie.

My Father in Heaven has blessed me in numerous ways during the past years. He has given me insights with my research, and the strength to move forward when challenges arose.

I remember more than one occasion when His Spirit gave me the insight needed to complete a design or an analysis, typically when I took the time to pray or listen to uplifting messages. Probably the most difficult time I had in Michigan was in November of 2007 when my mother Penny passed away. I am so grateful to know that she is resting in Spirit Paradise with friends and family, awaiting the resurrection, and that I will see my mother again after this life. The knowledge that families can be together forever through our Heavenly Father's plan is the most beautiful doctrine in our Lord's restored Gospel. Knowing this helped me to span the gap of sorrow at my mother's passing, and move forward with added faith and confidence. I could not have completed this work without His love, guidance and inspiration.

Table of Contents

List of Figures

List of Tables

List of Appendices

Abstract

When humans hop or run on springy surfaces they alter the stiffness of their legs so that the overall stiffness of the leg-surface system remains the same [Farley 96, Ferris 97, Ferris 98]. Adding a spring in parallel to the ankle joint incites a similar neuromuscular response; humans decrease their biological ankle stiffness such that the overall ankle stiffness remains unchanged [Ferris 06]. These results suggest that an elastic exoskeleton could be effective at reducing the metabolic cost of locomotion. This dissertation presents two elastic exoskeletons that further increase understanding of human locomotion and interaction with elastic mechanisms. The two devices are 1) an elastic knee-ankle-foot orthosis (eKAFO) that adds a stiff spring in parallel to the knee and 2) an elastic exoskeleton (eExo) that adds stiffness in parallel with the leg as a whole. The eKAFO was used as a test platform in ascertaining the neuromuscular effects of adding a parallel knee spring while hopping on one leg. The eExo was similarly used as a test platform to understand the effects of adding parallel leg elasticity while running.

The eKAFO incorporated a custom-built, light, stiff, composite leaf spring attached to the back of the knee joint of the brace. The joints on the spring ends were designed to engage the spring at the knee bend angle corresponding to the point of ground contact and was adjusted accordingly for each subject. On the first day of testing subjects were instructed to hop on their left legs at two frequencies (2.2 Hz and preferred frequency) without the spring attached (No Spring condition) while knee angle at ground contact was measured. The eKAFO provided no stiffness in parallel with any joint in this condition. The spring on the eKAFO was then set to engage at the correct knee angle and subjects were given a chance to practice hopping with the spring attached (Spring condition). The mean brace stiffness across all subjects was 5.6 N-m/°, which was effectively 31.5% of the total knee stiffness when hopping in this condition. On the second day of testing, subjects again hopped under both orthosis conditions while muscle activation levels, kinematics, and ground reaction forces were measured.

Subjects decreased muscle activation levels in the knee extensors in both the controlled and preferred frequency hopping trials in the Spring condition ($P < .01$). For the preferred frequency trials, subjects chose to hop with a higher frequency and had an associated increase in leg stiffness ($P < .05$). Subjects also landed with a more flexed knee but underwent less

knee flexion during stance. This was associated with an increase in the total knee stiffness and a slight but significant decrease in biological knee stiffness in the Spring condition.

In contrast, during controlled frequency hopping (2.2 Hz) subjects maintained constant leg stiffness and kinematics but decreased their ankle stiffness ($P < .05$). As in the preferred frequency trials, subjects increased total knee stiffness and decreased biological knee stiffness ($P < .05$). This shows that subjects choose to modulate stiffness levels of individual joints while hopping under controlled conditions without changing their leg stiffness. At both frequencies the biological knee stiffness decreases ($P < .05$) and knee extensor muscle activation levels decrease ($P < .01$), indicating that elastic exoskeletons may be effective at reducing metabolic cost of locomotion in bouncing gaits.

After completing the study involving the eKAFO, I decided to pursue a separate design rather than modify the eKAFO into a device for running. This was done for a variety of reasons. In the eKAFO study the soft tissue deformation at the posterior thigh was significant—much of the energy that could be stored in the knee brace was lost due to this soft tissue deformation. In running the knee typically does not bend more than 25-30° [Arampatzis 99]. Typical leg deflections however are on the order of 10-15 cm [Farley 96, Ferris 99] and include overall leg length shortening from both knee flexion and ankle dorsiflexion in the first half of stance. As a result, pursuing parallel leg elasticity would allow the soft tissue deformation to have a lesser effect than parallel knee elasticity, while allowing the same potential benefits. In addition, modifying the eKAFO to include a clutch for allowing running would increase the amount of distal mass required. This would drastically increase metabolic cost compared to a device that contains the majority of its weight on the subject's torso. Lastly, the eKAFO had significant unsprung mass, or mass that contacts the ground through rigid links and joints rather than elastic segments. At heel strike these rigid links transmit uncomfortable shock loads which are ameliorated by including an elastic element close to the ground. For these reasons we pursued a whole-leg elastic exoskeleton (eExo) rather than persisting with the joint-based approach.

The eExo relied solely on material elasticity to store and release energy during the stance phase of running. The exoskeleton included a novel knee joint with a cam and a Bowden cable transferring energy to and from a waist-mounted extension spring. A friction-lock clutch released the cable during swing phase for free movement of the leg. A MEMS gyro was used to measure thigh angular velocities and a foot contact switch was used to determine the timing of heel strike and takeoff. A real-time controller used these two inputs to determine the correct times to engage and release the friction-lock clutch by means of a pneumatic cylinder. The design relied upon a composite leaf spring to store and release energy in the distal portion of the exoskeleton about the foot and ankle. In preliminary

subject testing, leg stiffness was measured at 16 kN/m [Cherry 09]. The design goal was to provide 30-50% of this stiffness with the exoskeleton, or 5-8 kN/m. This percentage was chosen based on previous work by Ferris [Ferris 06] and the eKAFO study ([Cherry 06] and Chapter 3). After designing and fabricating the exoskeleton, quasi-static force-deflection experiments showed that the exoskeleton provided 4.8 kN/m in the original configuration (Eng_Spr). In order to provide two stiffness levels, an alternate configuration was also used in which the backpack spring was removed and replaced with a rigid bracket (Eng_NoS). This configuration provided 7.6 kN/m. Both of the achieved stiffness values were in the desired range. The exoskeleton had a mass of 11 kg with 2 kg moving with, but not attached to, each leg.

Six subjects ran at 2.3 m/s with and without (NE) the exoskeleton. In addition to the two Eng conditions mentioned previously, subjects also ran with the controller disengaged (Dis) such that the exoskeleton provided no stiffness at the eExo knee joint during stance. The average exoskeleton stiffness while running was 2.9 kN/m and 3.1 kN/m in the Eng_Spr and Eng_NoS conditions, respectively. These stiffness values are significantly lower than desired. This discrepancy is primarily due to controller behavior and can most likely be rectified through modification of the control method or timing. Average leg stiffness for the six subjects was 12 kN/m while running with no exoskeleton and 16 kN/m while running with the exoskeleton engaged (Eng). In the Eng_Spr and Eng_NoS trials the exoskeleton provided 18.4% and 19.2% of the total leg stiffness. Even though the exoskeleton stiffness was nearly 20% of total leg stiffness, the force provided by the exoskeleton was only 7.0% and 7.2% of the maximum vertical ground reaction force while running in the two conditions. This discrepancy is primarily due to movement of the exoskeleton waist harness with respect to the subjects and can be ameliorated through further improvement to the comfort and fit of the waist harness.

Because the exoskeleton failed to provide the desired assistance, there were no significant differences in metabolic cost between the three exoskeleton conditions (Dis, Eng_Spr, and Eng_NoS), nor were there consistent differences in muscle activation levels. Net metabolic cost and muscle activation in the hip flexors and extensors during swing phase were significantly higher when wearing the exoskeleton than when running normally ($P < .0001$). This is consistent with previous research efforts. Specifically, Myers and Steudel [Myers 85] showed that metabolic cost increased by about 25% when 1.8 kg was added to each ankle and 4% when 3.6 kg was added to the waist. The eExo added 2 kg to each leg and 7 kg to the waist. It is not surprising that metabolic cost increases when the weight of the exoskeleton is borne by subjects while running. It was hoped that when the exoskeleton was engaged the metabolic cost would decrease, but this was not the case for the exoskeleton prototype

presented here. Further improvements to the exoskeleton harness and controller functionality should yield improved results in human performance while wearing the exoskeleton.

Chapter 1

Introduction

1.1 Motivation

The research presented in this dissertation integrates the fields of compliant mechanism design with human locomotion assistance based on human neuromechanical adaptation. The field of compliant mechanisms has been researched for decades. The majority of this research has focused on developing methods for synthesizing compliant mechanism designs. These designs have covered a broad application area ranging from micro-engineered force gauges to adaptive wings on commercial airliners. However, little of this research has been applied to human locomotion assistance.

Locomotion is central to people's ability to function independently in their daily lives. Able-bodied individuals take for granted their ability to move about as they perform daily tasks. Individuals with disabilities that affect their locomotive capacity are well aware of the challenges. However, in a way all individuals are limited in their locomotive capacity. For example we are all bounded by the speeds we can run and the distance we can walk while carrying heavy loads. The high-level aim of this research is to develop wearable mechanisms (exoskeletons) for assisting human locomotion, benefiting both the able-bodied and individuals with disabilities.

1.1.1 Personal Motivation

My personal motivation in performing this research was to merge the fields of compliant mechanisms and human locomotion assistance. I believe that engineering and synthesis tools of compliant mechanisms are capable of making a marked improvement in the design of lower-body exoskeletons. The vast majority of current robotic exoskeleton designs for assisting human locomotion rely on actuators driving rigid link systems and powering individual lower limb joints. Although these devices provide a novel solution to increasing the body's capabilities, more light-weight, inexpensive, simple, and low-profile passive

devices (or compliant mechanisms) can be developed that store and release elastic energy during locomotion. Applying these engineering tools to help people is both exciting and meaningful to me.

1.1.2 Applications

The successful completion of this research hinges on the ability of the human body to adapt neuromechanically to spring-based mechanisms acting in parallel with the lower limbs. Prior research suggests that indeed humans modulate their muscle activation levels to compensate for the addition of elastic surfaces and orthoses [Ferris 98, Ferris 06]. By exploiting this adaptive behavior of the human leg we believe we can reduce the metabolic cost of locomotion, making it possible to restore capabilities to individuals with disabilities and increase the capabilities of the able-bodied.

Specifically, those who are able-bodied would be able to run farther at the same speed before becoming fatigued since their metabolic cost is lower. If the same level of energetic expense is maintained it could also enable running at faster speeds. It is quite foreseeable that the techniques developed in this dissertation could be used to develop exoskeletons capable of carrying large loads with minimal increase in metabolic expense. By transmitting forces through the elastic exoskeleton to the ground the cost of redirecting the carried load with each step can be drastically reduced.

Individuals with disabilities such as muscle atrophy in the lower limb could have locomotive ability restored. For example, an individual with an atrophied quadriceps muscle group could use an elastic knee orthosis to provide a knee extension torque while walking and running, decreasing the demands on the existing muscles and enabling locomotion at higher speeds. Muscle usage for the entire leg is not eliminated however, so muscle groups other than the quadriceps would maintain strength and as the affected muscle group strengthens the amount of assistance provided by the orthosis could be decreased until it is no longer needed. Similarly individuals with injuries such as torn ligaments in the knee or ankle could use an elastic exoskeleton to enable a faster return to exercise regimens that will enable maintenance of strength in their other muscle groups.

Decreasing loads at specific joints in the lower limb might also prove beneficial for individuals suffering from osteoarthritis. A leg exoskeleton capable of sustaining a portion of an individual's body weight would decrease the bone on bone forces at the joints and decrease pain while enabling locomotive ability. In this sense the elastic exoskeleton could take on the role of a body-weight support system that does not need to be used in a laboratory environment. Typical body-weight support systems are large and bulky and not suitable

for daily use. Developing a light-weight low-profile wearable exoskeleton that supports a majority of body-weight could be used for locomotion rehabilitation in the wearer's home and natural surroundings. It could also decrease the metabolic cost of locomotion in healthy individuals as mentioned previously.

1.2 Problem Statement

The overarching goal of this research is to understand the effects of elastic lower-limb exoskeletons that assist human locomotion for all individuals, both with and without disabilities. This includes elasticity in parallel with each of the joints (hip, knee, ankle) as well as in series and in parallel with the leg as a whole for both walking and running. This high-level and general goal has the capacity to benefit all of the aforementioned applications, but significant reduction in the scope of this research was necessary for this dissertation.

1.2.1 Scope

This dissertation focuses specifically on the development of two elastic exoskeletons. The first was an elastic knee-ankle-foot orthosis that provided stiffness in parallel with the knee joint while the second was an exoskeleton that provided stiffness in parallel with the entire leg, extending from the torso to the feet. This research was also limited to bouncing gaits (i.e. hopping and running). This is due primarily to the important role that spring-like function of the leg plays in bouncing gaits. The simplest model for running involves nothing more than a spring representing the function of the legs and a point mass representing body mass (see Figure 1.1 and [Blickhan 89, McMahon 90, McGeer 90]). The simplest model for walking on the other hand is much more dependent on pendular dynamics where the leg behaves more rigidly ([Mochon 80, Alexander 92, Kuo 05]. Human walking dynamics can also be explained using a spring-mass model (see [Alexander 92] , [Geyer 06], [O'Connor 07], and [Whittington 09]). During walking, however, leg deflections are smaller and play a lesser role in the overall energetics of the system compared to running. For this reason we felt that elastic leg orthoses would be more effective for running and therefore bouncing gaits were the focus of this research.

Further, the effects of elasticity in parallel with the hips or coupling the two legs together was not considered. This would be a logical next step in the research but one that will be left for future work. Lastly, the research studies presented herein focus solely on healthy individuals with intact limbs. These individuals would most likely benefit from an elastic leg exoskeleton for either recreational or military use. Understanding the neuromechanical

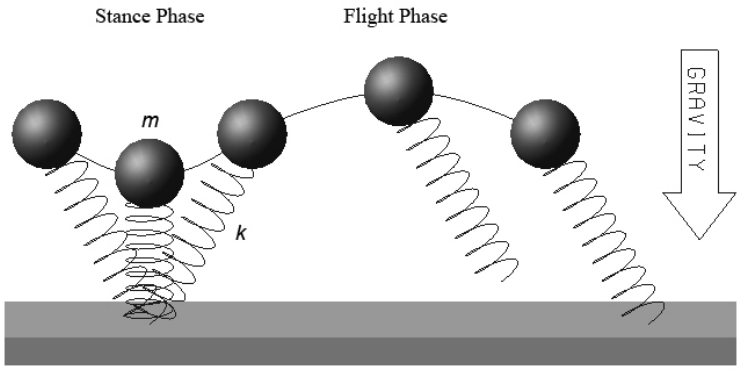

Figure 1.1 The simplest model for running. This model consists of a point mass and a spring representing the weight of the body and the function of the legs respectively. This obvious dependence on energy storage via elastic mechanisms is the primary reason for narrowing the scope of this research to bouncing gaits.

adaptation for healthy individuals, however, will likely aid future work with a wider variety of populations.

1.3 Literature Review

The goal of this research was to design and understand the effects of elastic exoskeletons that assist human running for healthy individuals with intact limbs. In recent years a number of exoskeletons have been built to assist human locomotion. The vast majority of these rely on rigid links and motors to transmit force and torque to the wearer and only address walking with few exceptions. These devices are designed to assist healthy individuals and those with disabilities. Although this research will focus on running and healthy subjects, the rest is relevant as the goal of assisting human locomotion is the same. These devices will be decomposed by intended audience: individuals with disabilities and healthy individuals including devices for recreational use. Rehabilitation robotics will not be included since they are for an entirely different purpose and paradigm. With rehabilitation robotics the intention is to improve gait after using the device but not necessarily to augment capacity while using it. Additionally, they are designed for use in a lab where size and mass are not a concern. The work covered in this literature review is limited to devices that are meant to be portable, although not all have attained that objective.

1.3.1 Locomotion Assistance

Individuals with disabilities

Possibly the most visible exoskeleton for assisting individuals with disabilities is HAL. This device was developed by Professor Sankai from the University of Tsukuba in Japan [Kawamoto 02, Kawamoto 05] for use with the elderly and individuals with disabilities. The rigid links and joints on this device span both the upper and lower body and are controlled by motors while being powered by batteries. This is a good example of an active device, or one in which the forces and torques are provided directly by motors.

A semi-active device is one in which the actuator is used only to set parameters of the system such as stiffness or damping, but not to provide forces or torques to the user. Hollander's ankle-foot orthosis (AFO) is such a design [Hollander 04, Hollander 05a, Hollander 05b]. This design uses a motor and lead screw to set the stiffness of a spring that stores and releases energy during the gait cycle. Similarly, the active ankle-foot orthosis (AAFO) developed by Blaya and Herr [Blaya 04] utilizes elasticity in series with a motor to decrease the peak motor torque and total power required. This device is designed for individuals with drop foot gait while walking.

Entirely passive devices also exist. These devices are much simpler as there is no need for a power supply or actuator. Consequently they are typically much lighter and low-profile. Also designed for assisting drop foot gait while walking, Ossur (Ossur hf., Iceland) has designed a commercial posterior leaf spring AFO called the AFO Dynamic [Ossur 08]. This light-weight elastic ankle support stores and releases energy during stance and provides support of the foot during swing. Similarly, the Protonics®knee brace provides an adjustable stiffness at the knee joint to assist individuals suffering from osteoarthritis [Empi 08]. Studies by Earl et al. have shown that this device is effective at decreasing quadriceps muscle torques during step-down exercises [Earl 04]. Although the stiffness is variable in this device it cannot be actively modulated during gait.

A major consequence of having a passive device at the knee or ankle is that users cannot vary from the set point without overcoming the stiffness. For hopping, as presented in Chapters 2 and 3, this is perfectly functional. However, while walking and running this is problematic since the knee needs to bend freely during swing phase to maintain toe clearance and avoid tripping. For this reason although a passive device is preferred for its light weight and simplicity there needs to be a means whereby the stiffness can be modulated and turned off completely during the swing phase for running. This was a basic design requirement for the exoskeleton presented in Chapters 4 and 5. Nevertheless, we also desired a mechanism as simple as possible, so we did not pursue a series elastic actuator based design like the

ones discussed above. Instead we developed a simple clutching system that engaged and disengaged the elastic element at the appropriate times in the gait cycle, simplifying the demands on both the motor and control system.

Another notable passive mechanism that merits mentioning is the gravity-balancing leg orthosis developed by Banala et al. at the University of Delaware [Banala 06]. This mechanism is based on the theory of gravity balancing developed by Herder [Herder 01] in which elasticity is used to store potential energy and statically balance potential energy changes over a given range of motion. The statically balanced orthosis is used to counteract the effects of gravity on the leg during its range of motion and is meant to be used for rehabilitation of patients with stroke. Although this then falls under the category of rehabilitation robotics one embodiment of this device is a portable mechanism connected to a backpack and consequently is included here.

Healthy individuals

The most well-known exoskeleton designed for augmenting the performance of healthy individuals is BLEEX [Kazerooni 05, Zoss 05, Chu 05, Amundson 06, Ghan 06, Zoss 06b, Zoss 06a, Kazerooni 07]. This device attaches at the foot and waist with additional straps added to each shank and thigh. It allows a user to carry heavy loads in a backpack that also houses the power supply and control system. While original designs relied on noisy gasoline engines for power, more recent versions include battery power for quiet operation and energy recycling through regenerative braking [Zoss 06a]. Equally impressive is the design developed by Sarcos [Jacobsen 04, Guizzo 05]. Although videos have been posted of this exoskeleton, details on this design have not been forthcoming and consequently cannot be discussed here. Both of these designs were sponsored by the military and aimed at augmenting human endurance and load-carrying capacity while walking and running.

A similar design called the Power Suit was developed by Yamamoto et al. [Yamamoto 03, Yoshimitsu 04] but for a very different purpose. This design is intended for use in the healthcare industry where nurses are required to lift and carry patients on a frequent basis. Like the Sarcos exoskeleton this device also provides assistance at both the upper and lower body and is hydraulically powered. Current versions do not appear to have addressed the need for a low-profile design but this may be forthcoming. Again these powered exoskeletons offer a degree of control and assistance not found in passive devices but are far more complex since they require a power source and complex control hardware. Active devices may also benefit from the energy storage and release provided by elastic systems since they can drastically reduce power requirements.

Another class of exoskeletons for assisting healthy individuals incorporates elasticity into the system with the actuators and control system. The RoboWalker [Pratt 04b, Pratt 04a] uses a series elastic actuator at the knee to assist with walking and carrying loads. This device extends from the ground to the upper thigh and does not have any actuation at the hip. Similarly the powered exoskeleton being developed by Low et al. aims to incorporate elasticity in series with a motor at the knee joint [Low 04, Low 05, Low 06] but connects instead to a hip harness. This device is designed specifically for carrying heavy loads and although it includes elasticity the control system and power requirements from the motor are still quite high. Another exoskeleton concept that includes both actuators and elasticity is the device developed by Walsh et al. [Walsh 06]. This mechanism is also designed to carry heavy loads while walking but incorporates a variable damper at the knee and elastic elements at the ankle and hip. They also designed the system to include an actuator at the hip to test both concepts. Although this almost entirely passive device was successful at supporting the external load, metabolic cost increased over carrying the load in a conventional backpack. This is most likely due to the large amount of added mass on the legs and constraints imposed on the wearer by a rigid-link mechanism being used.

Another concept developed by Herr [Carr 08, Grabowski 09] is a simple leaf-spring with a clutch in the vicinity of the knee. This device is entirely passive and does not constrain the motion of the wearer. This embodiment also does not maintain low profile during motion. Results presented to this point have included subject-less testing of the device with the knee joint locked and a hopping study in which individuals were able to hop with significantly less metabolic cost than hopping with no exoskeleton. Two exoskeleton stiffnesses were tested in this study, one that aimed to provide the full leg stiffness when hopping at 2.0 Hz and the other to provide about half of that. The exoskeleton with less stiffness provided over 20% savings in metabolic rate while the stiff exoskeleton provided around 10% savings. Their future work will include measuring muscle activation levels while hopping in the device and running by actuating the clutch near the knee. This device most closely resembles the exoskeleton presented in Chapters 4 and 5.

Herr and Dollar also developed an elastic exoskeleton for assisting human running [Dollar 08a]. This device adds stiffness in parallel with the knee in a very similar manner to the elastic knee orthosis presented in Chapters 2 and 3 and published in [Cherry 06]. Their device used a heavy coil spring to provide the desired stiffness but included a clutch to allow free flexion of the knee during swing phase. The results published to date for this device only include bench-top testing but no data from human subject testing.

An additional concept proposed for passively decreasing the cost of locomotion is based on the observation that equines such as horses use long tendons in their legs to store and

release elastic energy during running, resulting in up to a 50% decrease in energy cost per kg of body weight compared to humans [Biewener 98]. With this in mind van den Bogert developed simulations suggesting that implementation of an elastic polyarticular (passing over multiple joints) tendon can theoretically result in up to a 70% decrease in power consumption in human walking [van den Bogert 03]. Similar calculations have not been done for running nor has this device been fabricated and tested to verify the claims.

Lastly, over 15 years ago Dick and Edwards developed an entirely passive, spring-based, mechanism for aiding human running (SpringWalker [Dick 91]). This monolithic mechanism connects to the user's feet and trunk, holding the user off the ground and transmitting the ground forces almost entirely through the mechanism. Energy is transferred from the many kinematic links through cables to springs mounted on the backpack frame. Although this device was demonstrated successfully running at 24 km/hr and carrying a 90 kg load at a fast walk it is still awaiting commercialization [Guizzo 05]. In addition to the large size of this device, one possible reason for it not progressing in development is the fact that there is elasticity placed between the user and the ground. This raises the user's center of mass which has an affect on stability and also decreases the bandwidth of the user as all forces to the ground must first pass through the elastic system, decreasing agility. For this reason it is desired to include elasticity between the user's center of mass and ground, but not between the feet and ground.

The final category of locomotion-assisting devices is recreational. These passive devices make no claims of decreasing metabolic cost or allowing carriage of large loads, but they do claim to increase jumping height and running speed. Both the Powerskip [Bock 04] and the Kangoo Jumps [RDM 06] place springs in series with the feet, as did the SpringWalker, but have significantly smaller profiles. The benefits to this approach include the storage of energy typically lost at impact and the reduction of impact forces applied to the legs. They also increase the effective leg length which could increase stride length and decrease the metabolic cost of locomotion. However, as stated previously, they also reduce stability and agility making it difficult to change speed or direction of travel.

Ferris et al. have also contributed to the knowledge base of human locomotion assisting devices by developing and testing an elastic ankle orthosis [Ferris 06]. The elastic ankle orthosis consisted of a spring in parallel with the ankle that provided a plantar-flexor torque when the foot was dorsiflexed beyond the spring's set point (original un-stretched length). The spring was set to engage very closely to the ankle angle at ground contact in hopping. Consequently, during the stance phase of hopping the spring stiffness aided the ankle plantar-flexors and subjects decreased both muscle activation and biological joint stiffness, suggesting that an elastic exoskeleton could be effective for reducing the metabolic cost of

locomotion with bouncing gaits. These purely passive light-weight orthoses were low-profile as they were custom-fit to the leg of each subject. The orthoses were only used in hopping and not running since there was no mechanism incorporated for turning off the spring during swing phase to allow uninhibited dorsiflexion to maintain ground clearance of the toe.

Summary

In summary, the existing literature and applications give numerous examples of exoskeletons designed to assist human locomotion. The best features contained in these devices are the ability to elastically store and release energy, maintain a low profile on the user's body throughout the gait cycle, and control the stiffness of the elastic member. Although the goal of all these devices is to decrease the cost of walking and running, no published research to date has shown results that achieve this objective. The majority of these devices fail in this respect due to their excessive weight and power requirements, as well as rigid links attaching to the legs that constrain motion of the wearer. Elastic exoskeletons require very little energy to operate, with actuators only required to vary the stiffness of the exoskeleton during the stride cycle. This is known as a quasi-passive or semi-active design. Using this approach, Grabowski and Herr [Grabowski 09] achieved a decrease in metabolic cost while hopping with an elastic leg exoskeleton, but the device has not been shown to work while running. They kept as much mass off the legs as possible by designing an almost entirely passive elastic system. We also used a quasi-passive design that relied solely on material elasticity to store and release energy during gait. In addition, the elastic exoskeleton presented in this dissertation remains closer to the legs of the wearer during running, helping to maintain a low profile of the exoskeleton. In addition, their design includes a clutch at the exoskeleton knee joint that moves with the legs. Our design moves this clutch to the subject's torso where the metabolic penalty for carrying the mass is a minimum. Aside from these differences, the most obvious contribution of this work compared with all others is that we present results from running with the exoskeleton. Although hopping and running can both be described by the same fundamental spring-mass model, running is significantly more complex. This is partly due to the inclusion of forward velocity, but more importantly due to the need for making the exoskeleton provide minimal resistance during the swing phase. To our knowledge this document is the first publication of results from a human running in an exoskeleton.

In order to study the effects of elastic knee and leg exoskeletons it was necessary to design compliant systems to interact with the human body. Specifically, two compliant mechanisms were designed as part of this dissertation. The design of the elastic knee-ankle-foot orthosis (eKAFO) is presented in Chapter 2 while the design of the elastic exoskeleton

(eExo) is presented in Chapter 4. Compliant mechanism design approaches were used in both of these devices. With this in mind the following section is provided to give background on compliant mechanisms to those who are unfamiliar with that area of research.

1.3.2 Compliant Mechanisms

Historical Applications

Since the days of medieval warfare compliant mechanisms have been used to store and transfer energy. Both the catapult and the bow are used to store energy over an extended period of time to reduce peak input power requirements but then release energy quickly to convert the stored strain energy into kinetic energy of the projectile. Similarly, the human body, when walking, uses the Achilles tendon to store energy over an extended period of time during stance while the weight of the body bears down on it. This allows the ankle plantar-flexors to efficiently activate isometrically. Then at the end of stance the energy stored in the tendon is released to propel the body forward into the next step [Ishikawa 05, Fukunaga 01]. Likewise birds and insects that flap their wings rapidly utilize elasticity to aid the cyclic motion [Vogel 98].

Another important lesson we learn from nature is that stiffness is not equivalent to strength. In nature very few structures are rigid. Trees are flexible so that during high winds they can bend and not break. Maple leaves morph in the wind, curling up on themselves to reduce drag and avoid being torn off their branches [Vogel 98]. Nature teaches us that flexible systems can be made strong and compliant to perform their function.

Modern Applications

Modern applications of compliant mechanisms include force transducers and motion amplifiers in microelectromechanical systems (MEMS) [Wittwer 02, Kota 00] all the way up to large-scale devices such as adaptive airplane wings (FlexSys, Inc, Ann Arbor, MI). They are also being used in medical devices such as compliant grippers for surgical applications and stents that expand and conform to the shape of the arterial wall.

Benefits

One of the major benefits of compliant mechanisms lies in the concept of design for no assembly. A traditional wiper blade assembly for an automobile consists of over a dozen parts. This assembly is quite easily redesigned as a single part to drastically decrease material and assembly costs (see Figure 1.2) [Kota 01]. Compliant mechanisms also boast

the ability to benefit high precision instruments. For many years flexure-based mechanisms have been used for precision positioning systems [Awtar 07]. They are effective in this application because compliant systems don't have backlash or friction. They also reduce wear, weight, and maintenance.

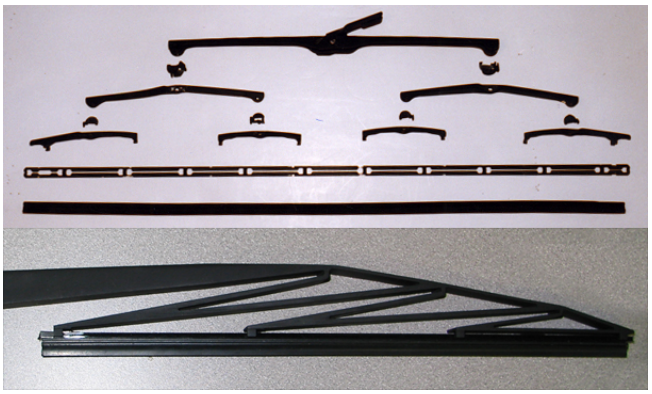

Figure 1.2 Redesign of a conventional windshield wiper. Using a compliant mechanism design reduces the complexity and number of parts dramatically [Kota 01].

Kinematics-Based Synthesis

There are two major categories for the design approach of compliant mechanisms. The first is a kinematics-based synthesis while the second is an automated synthesis methodology. The kinematics-based approach began with work by Howell and Midha and led to the development of the Pseudo-Rigid-Body Model [Howell 01]. This method models compliant mechanisms as rigid-body mechanisms with elasticity applied at the revolute joints as torsion springs. This approach allows the use of decades of research in mechanical systems and unifies compliant mechanism and rigid-body mechanism theories. One can design a compliant mechanism using this approach by first synthesizing a rigid-link mechanism using traditional kinematic synthesis techniques [Erdman 01] and then translating that design into a compliant mechanism with equivalent behavior.

This method requires that the topology of the mechanism be predetermined just as the traditional rigid-link kinematic synthesis does. On one hand this limits the variety of designs that are possible to those proposed by the designer, but on the other hand it allows the designer to use intuition and experience in the synthesis process. This is the approach that was used in developing the elastic knee orthosis found in [Cherry 06] and Chapters 2 and 3.

Another synthesis technique that allows a compliant mechanism designer to use intuition and understanding in the design process is the instant center approach originated by Kim et al. [Kim 06]. This design methodology utilizes building blocks for performing displacement amplification and attenuation, providing an intuitive and systematic methodology for gener-

ating initial compliant mechanism designs. The building blocks presented to date include a compliant four-bar and a compliant dyad (two straight beams) but more building blocks are being developed. Understanding how these building blocks behave enables them to be used intuitively in the design process.

Automated Synthesis Methodologies

The other major category of compliant mechanism synthesis techniques is the automated or systematic approach. This typically follows the design approach from structural optimization which determines the topology, shape, and size of a compliant mechanism. The topology refers to the number, arrangement and interconnectivity of the mechanism's elements while the size and shape refer to the dimensions such as thickness and width as well as the specific locations of the mechanism's elements. Ananthasuresh et al. [Ananthasuresh 94] showed that the topology of a compliant mechanism largely influences the kinematics. Since the structural optimization determines the topology in this synthesis method it also determines the kinematics unlike the previous two methods discussed.

There are typically four steps involved in the automated synthesis approach. First, the design space is defined by selecting overall size and boundary conditions for input, output, and ground. Second, the design space is parameterized to represent all possible solutions, or topologies. Third, using an optimization scheme, designs are generated and evaluated according to a defined objective function. Fourth, and finally, the physical compliant mechanism is interpreted into a complete system based on the optimal geometry from the third step. A complete description of these steps is found in the work by Lu and Kota [Lu 06].

Jutte and Kota recently used this methodology to formulate a new generalized synthesis approach for nonlinear springs [Vehar 06]. In this method the design space was discretized as numerous splines whose existence, thickness, connection points, and path were all parameterized (step two above). The objective function defined for step three was to match a desired stiffness function or force-displacement curve without failing due to stress. The design approach used in Chapter 4 is most similar to this approach but is scaled back considerably. Initial design efforts showed that the desired stiffness and safety factor were achievable with a simple topology and the size and shape of the spline were the only variables considered in the compliant segment optimization. Additionally, a Design of Experiments (DOE)-based approach was used rather than a genetic algorithm due to the complexity of the three-dimensional design and time involved to simulate the force-deflection behavior.

Chapter 2

Design of an Elastic Knee Orthosis

This chapter was written by Michael S. Cherry, Dave J. Choi, Kevin J. Deng, Sridhar Kota, and Daniel P. Ferris. It was published as a paper with the title "Design and fabrication of an elastic knee orthosis — preliminary results" in the proceedings of the ASME International Design Engineering Technical Conferences in September 2006 [Cherry 06].

2.1 Abstract

When humans hop or run on compliant surfaces they alter the stiffness of their legs so that the overall stiffness of the leg-surface system remains the same. Adding a spring in parallel to the ankle joint incites a similar neuromuscular response; humans decrease their biological ankle stiffness such that the overall ankle stiffness remains unchanged. These results suggest that an elastic exoskeleton could be effective at reducing the metabolic cost of locomotion. To further increase our understanding of human response we have developed an elastic knee brace that adds a stiff spring in parallel to the knee. It will be used as a test platform in ascertaining the neuromuscular effects of adding a parallel knee spring while hopping on one leg. This paper focuses primarily on the mechanical design and implementation of our elastic knee orthosis. Results of the forthcoming studies of human subjects wearing this knee orthosis will be presented in a separate article that will focus on the biomechanics and the neuromuscular adaptations of the human body. Prior research found that the neuromuscular response to hopping on compliant surfaces was the same when running on compliant surfaces. We expect that our results from hopping with springs in parallel with the knee will also be applicable to running. This elastic knee brace represents the first phase of an ongoing research project to develop a passive compliant lower-body exoskeleton to assist in human running. It is expected that this research will benefit healthy individuals as well as those with disabilities causing decreased muscle function.

2.2 Introduction

Limitations of the human body play an important role in the research and development of devices that assist human locomotion. Clinical lower limb devices such as prosthetics (artificial limbs) and orthotics (braces) increase mobility for a wide range of individuals. In total, there are currently more than 1 million individuals living in the United States with lower limb amputation [CDC 06]. About 156,000 Americans lose a limb each year and this number is climbing with ongoing military operations abroad [CDC 06]. There are more than 6.3 million Americans using orthoses to assist with paralysis, deformities, or orthopedic impairments [NCOPE 06]. More broadly, there are 6.1 million people in the United States living outside of institutions using canes, crutches, or walkers on a regular basis [UCSF 06]. Other devices such as performance-enhancing exoskeletons could benefit individuals in the military or search and rescue. Although these devices may not be designed specifically for those with physical impairments, the technology is likely to benefit clinical orthoses and prostheses.

Much of the research done in exoskeletons involves the use of active devices that require a power source and expensive control hardware. Although these devices provide a novel solution to increasing the body's capabilities, more light-weight, inexpensive, simple, and low-profile passive devices (or compliant mechanisms) can be developed that store and release elastic energy. This class of devices is best suited for running and hopping since these gaits already involve the storage and release of elastic energy. These bouncing gaits can be modeled as a simple spring-mass system composed of a compression spring and a point mass (Fig. 2.1). The spring represents the legs, while the point mass represents the lumped body mass (see [Cavagna 77], [Blickhan 89], [McMahon 90], and [Geyer 05]). Although this model qualitatively describes why passive elastic devices would be useful for running and hopping, it fails to account for the human neuromuscular response.

Human neuromuscular response to passive elastic systems has been the subject of prior research by Farley and Ferris (see [Farley 96], [Ferris 97], and [Ferris 98]). These studies indicate that the addition of a spring in series with the leg (see Fig. 2.2(a)), such as in the case of running or hopping on a compliant surface, results in an increase in leg stiffness. This is done such that the combined stiffness of the leg-surface system matches the leg stiffness from the basic model shown in Fig. 2.1. Similarly, the human body adapts to an added stiffness about the ankle (see Fig. 2.2(b)) when hopping by reducing the biological stiffness of the ankle joint [Ferris 06]. This is accomplished by reducing the muscle activity in the ankle plantar flexors in such a manner that the combined ankle stiffness and the overall leg stiffness remain the same.

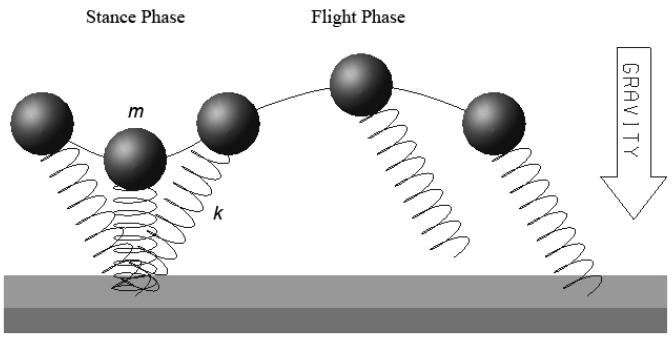

Figure 2.1 Spring-mass model for running. m—point mass, k—spring constant representing leg stiffness. This model accurately describes the center of mass motion and ground reaction forces for bouncing gaits. Adapted from [McMahon 90].

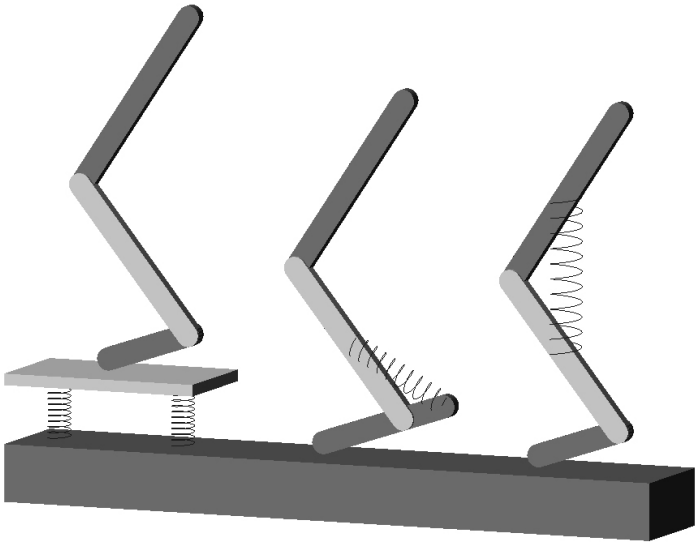

Figure 2.2 Simplified models of human interaction with springy surfaces and orthoses. Hopping and running on compliant surfaces can be modeled as a (a) spring in series with the leg (see [Farley 96], [Ferris 97] and [Ferris 98]). Hopping with an elastic ankle orthosis can be modeled as a (b) spring in parallel with the ankle joint [Ferris 06]. Both of these cases illicit a neuromuscular response such that the combined stiffness remains the same as the spring in the simplest spring-mass model (see fig. 2.1). Hopping with an elastic knee orthosis can be modeled as a (c) spring in parallel with the knee joint and is presented in this paper.

By exploiting this adaptive behavior of the human leg, we predict that placing a spring in parallel with the knee as seen in Fig. 2.2(c) will result in a reduction of biological knee stiffness and muscle activation of the knee extensors. In order to verify this hypothesis, we have developed an elastic knee orthosis which we can use as a testing platform to easily sample a range of stiffness values on the knee. We initially focus on unilateral hopping rather than running since both running and hopping can be modeled using the spring-mass model,

but the model is simpler for hopping because it is primarily uniaxial. Also, assuming that kinematics are unchanged, running requires a more complex mechanism since the knee must also be allowed to rotate freely during swing phase to achieve foot-ground clearance, which indicates the need for a triggering mechanism. We plan to implement such a triggering mechanism in our knee brace and conduct experiments on running in future studies. We hope to use the data from these studies to develop a more comprehensive lower-body elastic exoskeleton that will benefit human running. We emphasize that our current knee brace is simply a testing platform and is just one step toward understanding the human neuromuscular response to elastic locomotion-assisting devices.

2.2.1 Organization of Paper

In the remainder of this paper we give a brief summary of related research after which we discuss the conceptual layout and overview of the two knee braces we have designed to date, the first of which uses torsion springs while the latter uses a composite leaf spring. We then show a validation of our analytical leaf spring model with experimental testing and describe how this knee orthosis will serve as an important biomechanical test platform. Finally, we discuss our conclusions and future plans in this ongoing project.

2.3 Background

2.3.1 Passive Devices

Utilizing elastic energy to assist in human locomotion is not a new concept. The pogo-stick and various other commercially available products exploit elastic energy to propel the human body. Equines such as horses use long tendons in their legs to store elastic energy during running, resulting in up to a 50% decrease in energy cost per kg of body weight compared to humans [Biewener 98]. Simulations suggest that implementation of an elastic polyarticular (passing over multiple joints) tendon can theoretically result in up to a 70% decrease in power consumption in human walking [van den Bogert 03].

There are a number of commercial products that demonstrate the range of devices available to passively assist human locomotion. Devices such as the SpringWalker [Dick 91] support the user and translate the user's motions to an external structure much like a bicycle. Other devices such as the Powerskip [Bock 04] and the Kangoo Jumps [RDM 06] have a smaller profile and use springs placed in series with the legs. The benefits to this approach include the storage of energy typically lost at impact and the reduction of impact force

imparted to the legs (up to 80% by the Kangoo Jumps). The Springwalker and the Powerskip also increase the user's effective leg length. This enables increased stride length which can potentially reduce the metabolic cost of locomotion by increasing the distance traveled per stride rather than decreasing muscle activation. However, this also reduces stability and agility, making it difficult to change speed or direction of travel.

Orthotics and prosthetics that implement elastic energy systems are also becoming more prevalent. For example, leg braces with torsion springs at the knee joint (see [Deharde 04] and [Earl 04]) show how elastic energy can be used to assist stance-leg support in walking for individuals with patellofemoral pain syndrome. However, the stiffness of these springs is generally too low to assist in running since that is not their intended function. On the other hand, prosthetics that implement compliant mechanisms have been developed successfully for walking and running. In particular, the Flex-Foot® improves comfort for walking and can also provide energy storage and release to enable both running and sprinting [Ossur 06a]. These examples illustrate how using passive mechanisms can assist human locomotion.

2.3.2 Active Devices

Powered exoskeletons such as BLEEX [Zoss 06b] and HAL [Kawamoto 02] show the potential of using an active device to assist in locomotion. Recently these exoskeletons have been redesigned to be more light-weight and low-profile (see [Guizzo 05] for a summary of recent advances in powered exoskeletons including details on HAL-5). Additionally, an active ankle-foot orthosis (AAFO) was designed to assist clinical treatment of drop-foot gait [Blaya 04] and the RoboKnee [Pratt 04b] was created to benefit healthy individuals by sensing their intent and assisting knee extension. All of these devices offer a level of control and adaptability not found in passive devices but are more complex since they require a power source and complex control hardware. We feel that active devices may also benefit from the energy storage and release provided by elastic systems since it can reduce the power required.

2.3.3 Semi-Active Devices

Semi-active designs such as the AMASC actuator [Hurst 04] and Hollander's ankle-foot orthosis (see [Hollander 05a] and [Hollander 06]) also offer a degree of control not found in purely passive devices while maintaining lower power costs when compared to purely active devices. These semi-active devices rely on elastic energy to assist the user much like passive devices do, however, unlike passive devices, they offer dynamic adjustment of stiffness which provides more robust assistance. Another class of semi-active devices adjusts

damping in prosthetic knee joints, quickly adjusting to changes in speed, load, and terrain (see [Ossur 06b] and [Herr 03]). The commercially available Rheo Knee^{TM}is light-weight, low-power, and highly adaptable, however, it cannot be used to store and return energy.

2.4 Conceptual Design

Our primary goal was to design a test platform to validate our hypothesis that augmenting the knee with a parallel spring reduces muscle activity in the knee extensors resulting in a decreased biological knee stiffness. As discussed in the introduction, we aim to reduce muscle activation without changing the kinematics of hopping similar to the elastic ankle orthosis created by Ferris et. al. [Ferris 06].

Preservation of kinematics served as a starting point in the required characteristics of our testing platform, among which were: device weight, comfort, and simplicity. Device weight, as seen in our beta prototype test trials, plays an important role in keeping the device in place on the user's leg during data acquisition. Comfort plays a large role in kinematics, since an uncomfortable device can cause the user to deviate from his or her natural kinematics. A simple design reduces device weight by implementing fewer components and makes the device easier to manufacture. The testing platform must also be able to provide the range of stiffness values we would like to test and be able to change stiffness by swapping springs.

Most of these requirements were subjective since little data is available regarding weight and its effect on human hopping kinematics. Comfort, simplicity, and manufacturability are also subjective since a value cannot be attributed to describe them. However, data on knee stiffness and level of augmentation to joints was readily available in existing literature (e.g. [Kuitenen 02]). Data from a similar experiment implementing an elastic AFO [Ferris 06] showed that a 25% increase in stiffness about the ankle resulted in a statistically significant difference in muscle activation. We used this percentage of joint stiffness as a starting point in finding a stiffness to use in our preliminary studies. We plan to test multiple stiffness values in order to assess the effects of elastic augmentation of the knee.

2.4.1 Beta Prototype & Modeling

The goal for our beta prototype was to try the proposed 25% stiffness and subjectively judge whether the effects of a spring in parallel with the knee could be felt. We would then conduct a full biomechanics evaluation in order to quantify the effect and validate our numbers for predicted reduction of biological knee joint stiffness.

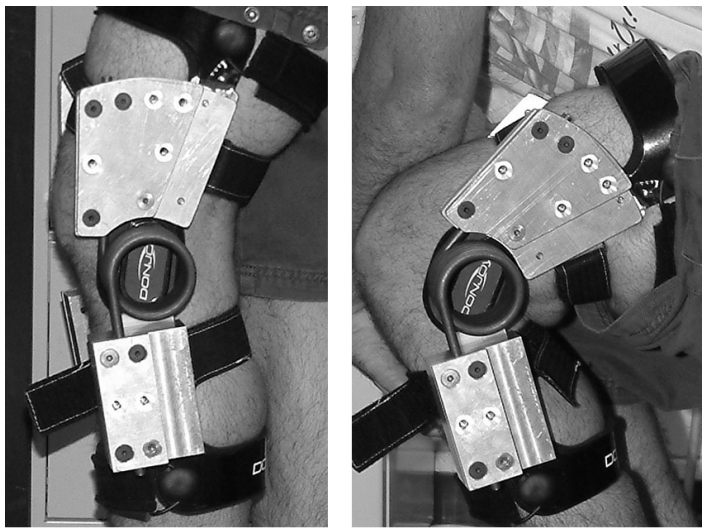

(a) (b)

Figure 2.3 Beta prototype of elastic knee brace shown in (a) extended and (b) flexed positions. Total brace weight—3.4 kg (7.5 lbs). Net rotational stiffness—1.5 N·m/deg (1.1 ft·lbf/deg).

We used a commercially available knee brace and attached two torsion springs (combined rotational stiffness, K =1.5 N·m/deg) at a predefined angle of 25 degrees knee flexion where 0 degrees is defined as a fully extended knee. This value was derived from prior studies [Ferris 06] where a knee angle of 25 degrees knee flexion at ground contact in hopping was observed. The torsion springs were attached to the brace via a set of aluminum fixtures (see Fig. 2.3).

We manufactured the brace and performed preliminary biomechanical studies, but were unsuccessful in obtaining meaningful data for a number of reasons. We calculated the biological leg stiffness of our subject via inverse dynamics and found that our spring was 15% as stiff as the biological knee joint and not the 25% we had aimed for. We also had problems keeping the brace in place due to its weight. We tried to remedy these problems by tightening the brace about the subject's leg; however, this restricted blood flow and caused discomfort. Also, due to our implementation of the torsion spring, the brace mandated a starting knee angle of 25 degrees which prevents full knee extension without some effort by the user. These problems ultimately affected our kinematics and we took them into account when designing our final test platform.

2.4.2 First Generation Prototype

Taking into account the problems we experienced with our beta prototype, we constructed our test platform using pre-impregnated carbon fiber for its high rigidity/weight ratio. We

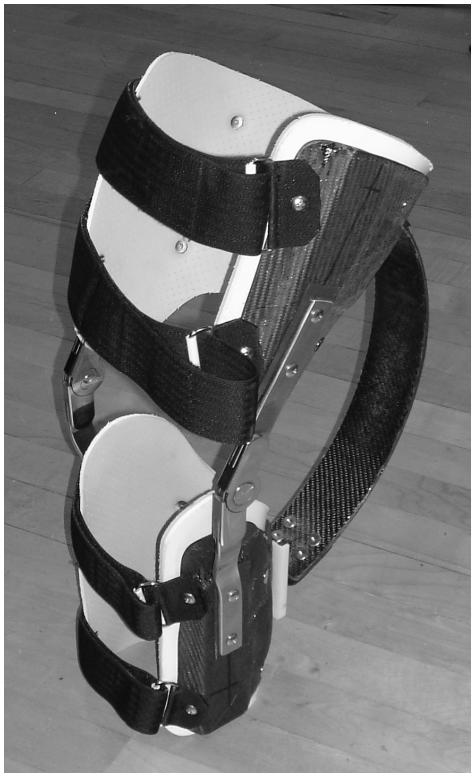

Figure 2.4 First generation prototype utilizing pre-impregnated carbon composite for the brace and leaf spring. Total brace weight—1.6 kg (3.5 lbs). Net rotational stiffness—2.8 N·m/deg (2.0 ft·lbf/deg).

fabricated a custom fit, shell-style knee brace to remedy fitting and relative rotation issues, and used a composite leaf spring for its high stiffness/weight ratio and ease of manufacture (Fig.2.4).

Leaf Spring Design and Optimization

We began designing the leaf spring by first applying size constraints. Based on the size and geometry of the subject's leg, we chose limits for acceptable locations of the two pin joints which mount the leaf spring onto our knee brace. This placed limits on the maximum and minimum length of the spring given the amount of flexion the knee was to undergo. We then used an initially curved pinned-pinned segment pseudo-rigid-body model (PRBM) to approximate the force-deflection relationship of the leaf spring [Howell 01]. This model consists of three rigid links connected by conventional pin joints with torsional stiffness prescribed by the beam geometry as shown in Fig. 2.5 and defined in equations (2.1) through (2.3).

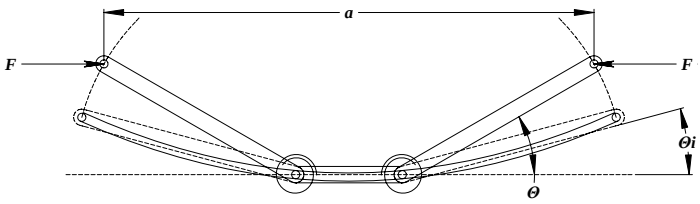

Figure 2.5 Pseudo-rigid-body model for an initially curved pinned-pinned segment used to model the force-deflection relationship of the composite leaf spring. f—spring force, a—spring length, Θ—pseudo-rigid-body angle, Θ_i—initial pseudo-rigid-body angle. Adapted from [Howell 01].

$$F = \frac{2K(\Theta - \Theta_i)}{\rho l \sin\Theta} \tag{2.1}$$

where

$$\Theta = \cos^{-1}\left(\left(\frac{a}{l} + \gamma - 1\right)\Big/\rho\right) \tag{2.2}$$

and

$$K = 2\rho K_\Theta \frac{EI}{l}. \tag{2.3}$$

This model produces accurate approximations (0.5% maximum error) and is computationally efficient due to its closed form analytical equations.

This model was used to select the thickness and width of the leaf spring as well as the exact pin joint locations for a resulting stiffness of 25% of normal biological knee stiffness. Preliminary testing of our subjects indicated that a typical knee stiffness value is around 10 N·m/deg so our desired stiffness was 2.5 N·m/deg. Since there were an infinite number of solutions that satisfy this design goal, we narrowed down our solutions by optimizing our design such that the torque vs. rotation curve was as linear as possible. This was done by maximizing the R^2 value of the linear regression. A summary of these design variables, constraints, and the objective function are found in Table 1.

Figure 2.6(a) shows plots of the resulting leaf spring force-deflection curve as well a plot of how the moment arm of the spring changes as the knee rotates. The product of these two curves was used to obtain the torque provided by the knee brace which is shown plotted against knee joint rotation in Fig. 2.6(b). A best linear fit of this torque-rotation plot provided the value for the effective brace stiffness (K =2.8 N·m/deg). Figure 2.7 shows the key dimensions and brace configuration that resulted from this design optimization. Although the stiffness of this brace is higher than expected ($\approx$ 10%), this error is not critical since knee stiffness varies between individuals and the value used for this design is an

approximation. However, knowing the exact value of the brace stiffness is critical because it is the primary variable that affects neuromuscular response.

Using the parameters we found from our model, we fabricated the leaf springs using pre-impregnated carbon fiber and validated our model using data from force vs. deflection tests. We conducted two trials of force vs. deflection tests using an Instron machine (Model 5585 with a 4.45 kN (1000 lb) load cell at a deflection rate of 1 in/min (2.5 cm/min) as shown in Fig. 2.8). We used this data (see Fig. 2.9) to refine our analytical model and found excellent agreement between the new analytical approximation of our model and the test data ($R^2 = 0.999$). Note that this data only validates the force-deflection model for the leaf spring starting at 0 cm deflection. Also note that this force-deflection data differs from the torque-rotation curve since torque must account for the moment arm of the force about the knee joint which changes with knee rotation. We validated the torque-rotation model by physically measuring the fabricated geometry of the brace to determine the actual pin joint locations and calculating the effective moment arm of the leaf spring.

Implementation

We implemented a novel hinge to attach the leaf spring to our brace by using Dacron® straps (see Fig. 2.10). One end of the leaf spring is attached using a loose length of strap which becomes taut at a knee angle of 25 degrees and loads the spring. The other end of the leaf spring is also attached with a Dacron® strap, but with no slack. Note that the knee angle and the angle of the brace are not necessarily equal due to soft tissue deformation. In preliminary testing we have observed a 7.5 degree discrepancy which has been accounted for in the design model by setting the brace angle at 17.5 degrees when the spring engages.

Table 2.1 Setup of design problem for the leaf spring.

Maximize:	
R^2	: Linear regression coefficient of torque vs. rotation curve
Subject to:	
$K \approx 2.5 N{\cdot}m/deg$	: Brace stiffness approximately 25% of knee stiffness
x_A, y_A *min/max*	: Position of pin joint A on thigh within specified range
x_B, y_B *min/max*	: Position of pin joint B on thigh within specified range
Variables:	
t	: Thickness of leaf spring
w	: Width of leaf spring
a_i	: Initial un-deflected length of spring
κ	: Curvature ratio of the spring

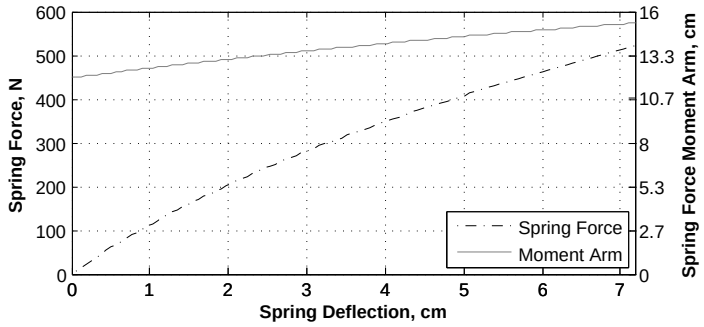

(a)

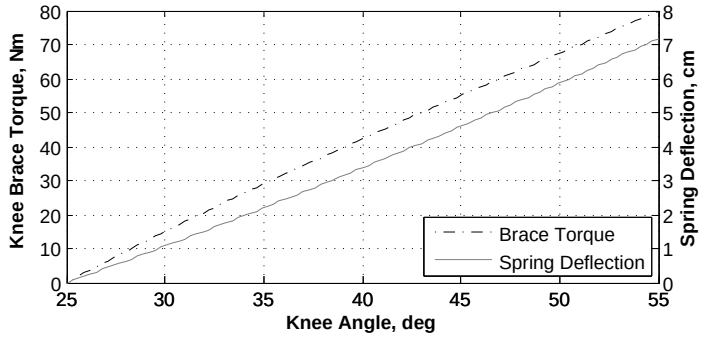

(b)

Figure 2.6 Multiplying the spring force by its moment arm (distance from leaf spring force line of action to knee joint) yields the torque for the knee brace. (a) shows the force and moment arm as a function of spring deflection. (b) provides the relation between spring deflection and knee angle, and plots the knee brace torque as a function of knee rotation. The rotational stiffness of the orthosis is 2.8 n·m/deg. The R^2 value for a linear best fit is 0.997, indicating that the rotational stiffness is practically linear as desired.

The test data shown in Fig. 2.9 illustrates this behavior as the flat region on the left of the force-deflection curve. The benefits of this approach are two-fold: 1) it is lighter than commercially available conventional hinges but is strong enough to withstand the required loads, and 2) users are now able to move their legs freely between knee angles of 0 and 25 degrees and are no longer restricted to a mandated starting knee angle. This design fits well with our original requirements by being simple and easy to implement, and increases comfort by allowing users to stand straight. Although the spring abruptly transitions from off to on, preliminary testing indicates the transition is smooth enough that we do not sacrifice comfort. This design also grants us the option of changing the spring engagement angle by modifying the strap length or moving the mounting brackets.

This design also has other benefits over more traditional pin joints and hinges. Traditional pin joints and hinges add a rigid segment between the flexible portion of the leaf spring and the joint. This introduces error in our pseudo-rigid-body model for a pinned-pinned segment since the model assumes that the entire pin-to-pin length of the spring is flexible. Although

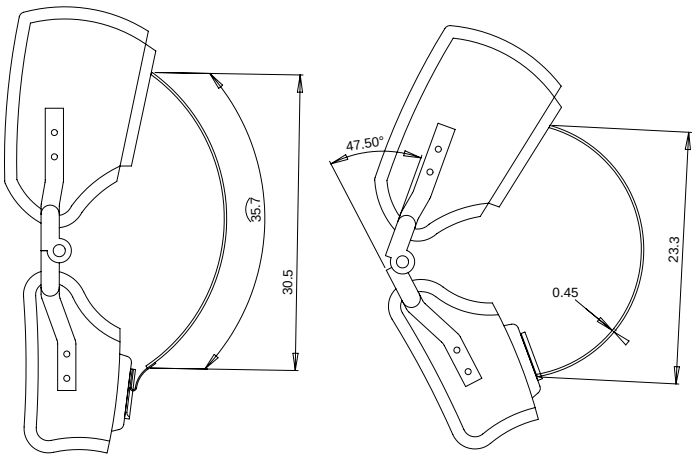

Figure 2.7 Sketch of the first generation prototype. The orthosis is shown at maximum extension (a) and at 47.5 deg brace rotation which corresponds to 55 deg knee flexion due to deformation of soft tissue on the legs. All linear dimensions are in cm.

Figure 2.8 Quasi-static (1 in/min) compression testing was used to refine and validate the analytical model. Testing was performed on an Instron Model 5585 with a 4.45 kn (1000 lb) load cell.

the model can be modified to account for this error, the dimensions of the hinge must be known beforehand, and the mountings of the hinge may be incompatible with the dimensions of the resulting spring, making the modeling a more iterative process and difficult to use. Our design uses Dacron® straps that fit closely over the end of the spring which maintains the flexibility of the entire length of the spring and provides a true one-to-one correspondence to our model.

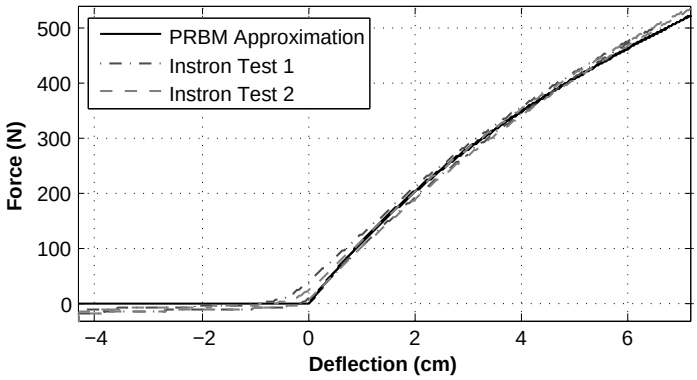

Figure 2.9 Empirical data and refined analytical pseudo-rigid-body model show a close correlation ($R^2 = 0.999$).

(a) (b)

Figure 2.10 Use of traditional pin joints mandate a single equilibrium knee joint angle. The novel joint design shown here provides a single point at which the spring will engage (25 deg knee flexion), resulting in a range of free joint rotation where the strap is slack (a) to the point where the strap becomes taut (b).

2.5 Biomechanical Test Platform

Currently, we have successfully designed and fabricated a light-weight custom-fit knee brace that can provide a rotational stiffness that is large enough to create a felt effect. Using this brace, we can proceed with performing necessary biomechanical studies, and we expect testing a large number of subjects will reveal general trends and provide further insight into human adaptive neuromuscular behavior while hopping with knee joint augmentation.

We will be primarily collecting data regarding muscle response and kinematics in these studies. Data such as muscular response will be collected using Electromyography (EMG) by attaching surface electrodes on the skin over the major external muscles. Preliminary EMG results from a pilot study we conducted can be seen in Fig. 2.11. Data for kinematics will be collected using reflective markers and motion capture cameras. Additional data required for inverse dynamics will be collected using force plates. Inverse dynamics will be

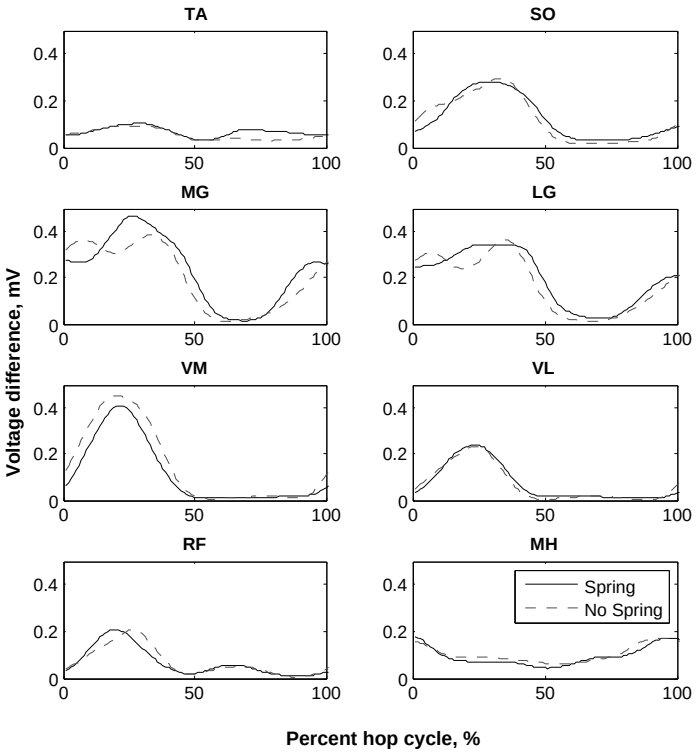

Figure 2.11 Electromyography (EMG) is used to measure the muscle activation level during the hop cycle beginning with ground contact. Curves shown here are at a hopping frequency of 132 bpm (2.2 hz). TA—Tibialis anterior, SO—Soleus, MG—Medial gastrocnemius, LG—Lateral gastrocnemius, VM—Vastus medialis, VL—Vastus lateralis, RF—Rectus femoris, MH—Medial hamstrings.

used to calculate joint torques at the ankle and knee, and the slopes of these curves will be used to find joint stiffness. An example of the torque vs. rotation curves and joint stiffness values generated from the same pilot study can be seen in Fig. 2.12 for a hopping frequency of 132 BPM which is typical for human bouncing gaits.

Currently we do not have a statistically significant number of data points and cannot make any claims as to what effects this knee brace has on the human neuromuscular system. However, the results shown here demonstrate the viability of using this knee brace as a testing platform which will allow us to collect a statistically meaningful number of data points and present our findings in future publications.

2.6 Conclusions & Future Work

Light-weight passive exoskeletons can provide one of the simplest ways to augment the human body. Passive exoskeletons are also one of the more economical options available

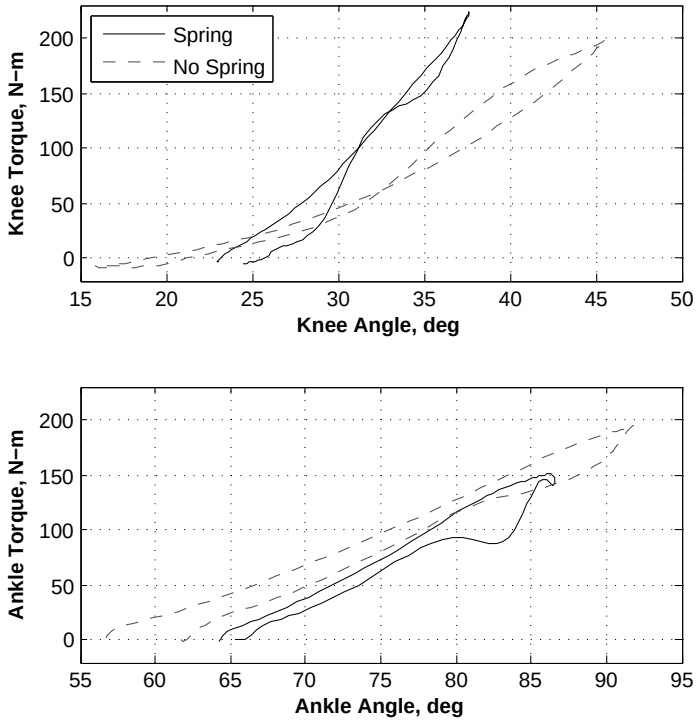

Figure 2.12 Knee and ankle moments vs. joint angles for a subject hopping at 132 bpm (2.2 Hz). Slopes of curves represent joint stiffnesses. Positive values represent knee extension and ankle plantar flexion torques.

since they do not require a power source or complex control hardware like their active counterparts. In previous studies, elastic orthoses have demonstrated the capacity to reduce muscle activation and associated metabolic costs, however, data on human neuromuscular response to a passive orthosis designed to augment the knee joint is currently lacking. In order to gain a greater insight on such a device we developed an elastic knee orthosis to use as a test platform, the development and designs of which we have presented in this paper.

The immediate future plans for this project are to test a greater number of subjects to reach statistically significant values. The results of these studies will be published in a separate article that emphasize the biomechanics and neuromuscular response of elastic knee joint augmentation in hopping. We will eventually test the effects of our exoskeleton in running applications by developing a triggering system to disengage the spring during swing phase which will allow users to maintain ground clearance of the swing leg.

In later phases of this project, we plan to combine our work with previous studies [Ferris 06] and design a device that would augment both ankle and knee joints simultaneously. We suspect that coupling the two joints together, as is done with the gastrocnemius muscle, will result in a greater reduction of muscle activation and metabolic cost.

2.7 Acknowledgments

The authors wish to acknowledge the assistance of Jacob Godak in fabrication and modification of the braces and leaf springs as well as Catherine Kinnaird for her continued assistance in data collection and Steven Emanuel for guidance in machining operations. This research is supported by NSF BES-0347479 and an NSF graduate research fellowship for the first author.

Chapter 3

Neuromechanical Adaptation to Hopping with an Elastic Knee Orthosis

This chapter was written by Michael S. Cherry, Daniel P. Ferris, and Sridhar Kota as a manuscript for publication as a journal article.

3.1 Abstract

When humans hop or run on springy surfaces they alter the stiffness of their legs so that the overall stiffness of the leg-surface system remains the same [Farley 96, Ferris 97, Ferris 98]. Adding a spring in parallel to the ankle joint incites a similar neuromuscular response; humans decrease their biological ankle stiffness such that the overall ankle stiffness remains unchanged [Ferris 06]. These results suggest that an elastic exoskeleton could be effective at reducing the metabolic cost of locomotion. This paper presents an elastic knee-ankle-foot orthosis (eKAFO) that adds a stiff spring in parallel to the knee. The eKAFO was used as a test platform in ascertaining the neuromuscular effects of adding a parallel knee spring while hopping on one leg.

The eKAFO incorporated a custom-built, light, stiff, composite leaf spring attached to the back of the brace's knee joint. The spring ends were designed to engage the spring at the knee bend angle corresponding to the point of ground contact and was adjusted accordingly for each subject. On the first day of testing, subjects were instructed to hop on their left legs at two frequencies (2.2 Hz and preferred frequency) without the spring attached (No Spring condition) while knee angle at ground contact was measured. The eKAFO provided no stiffness in parallel with any joint in this condition. The spring on the eKAFO was then set to engage at the correct knee angle and subjects were given a chance to practice hopping with the spring attached (Spring condition). The mean brace stiffness across all subjects was 5.6 N-m/°, which was effectively 31.5% of total knee stiffness when hopping in this condition. On the second day of testing, subjects again hopped under both orthosis conditions while muscle activation levels, kinematics, and ground reaction forces were measured.

Subjects decreased muscle activation levels in the knee extensors in both the controlled and preferred frequency hopping trials in the Spring condition ($P < .01$). For the preferred frequency trials subjects chose to hop with a higher frequency and had an associated increase in leg stiffness ($P < .05$). Subjects also landed with a more flexed knee but underwent less knee flexion during stance. This was associated with an increase in the total knee stiffness and a slight but significant decrease in biological knee stiffness in the Spring condition.

In contrast, during controlled frequency hopping (2.2 Hz) subjects maintained constant leg stiffness and kinematics but decreased their ankle stiffness ($P < .05$). As in the preferred frequency trials, subjects increased total knee stiffness and decreased biological knee stiffness ($P < .05$). This shows that subjects chose to modulate stiffness levels of individual joints while hopping under controlled conditions without changing their leg stiffness. At both frequencies the biological knee stiffness decreased ($P < .05$) and knee extensor muscle activation levels decreased ($P < .01$), indicating that elastic exoskeletons may be effective at reducing metabolic cost of locomotion in bouncing gaits.

3.2 Introduction & Background

The human leg behaves in a spring-like fashion while hopping and running [Blickhan 89, McMahon 90, Farley 91, Farley 93, Farley 96, Farley 96, Ferris 97, Farley 98b, Farley 99]. The simplest model for these bouncing gaits is a spring-mass model where the overall behavior of the leg including bones, tendons, ligaments, and muscles is modeled as a linear spring. The entire mass of the human body is modeled as a point mass connected to the top of the spring. Although an obvious over-simplification, this model has been shown to accurately predict and describe running and hopping behavior in a large variety of species [McMahon 90]. During the first half of stance the muscles and tendons in the lower leg store elastic energy which is then released during the second half of stance leading towards take-off. Providing this spring-like function incurs a metabolic cost as the muscles are required to activate and sustain loading in order to store energy in the tendons. However, this energetic cost is far less than it would be without the spring-like behavior of the tendons as they allow the muscles to take advantage of the stretch reflex and provide force in an isotropic fashion which is less costly from a metabolic perspective [Novacheck 98]. Mechanical springs on the other hand require minimal energy to provide their spring-like function where they store and release energy in the form of elastic strain. The fundamental concept is then to use mechanical springs to provide a portion of the spring-like function of the leg. Hypothetically this would decrease the amount of effort required of the human leg and result in decreased leg muscle activation levels and metabolic cost.

A wide variety of experiments have been performed over the past two decades to understand how humans interact with elastic mechanisms. McMahon and others began work in this field by looking at how the springiness of an elastic surface affects running performance [McMahon 79]. Further work showed that humans adjust the stiffness of their legs while hopping and running on elastic surfaces [Kerdok 02]. This is done to achieve a constant overall stiffness of the leg-surface combination. Similarly, Ferris et al. created an elastic ankle orthosis that provided stiffness in parallel with the ankle joint. When hopping, subjects decreased the stiffness of their biological ankle joint to compensate for the additional stiffness provided by the device. This was done to maintain a constant total ankle joint stiffness and resulted in a 30% decrease in muscle activation levels of the ankle plantar-flexors [Ferris 06]. More recently, Grabowski and Herr built an elastic leg exoskeleton that provides stiffness in parallel with the entire leg while hopping. Again, subjects decreased leg stiffness to compensate for the additional stiffness provided by the exoskeleton and maintained a constant overall stiffness while hopping. More importantly, while hopping in the device subjects had a significant decrease in metabolic cost [Grabowski 09]. The results of these studies suggest that an elastic exoskeleton could be effective at reducing the metabolic cost of locomotion.

In this paper we present the results of hopping with a stiff spring in parallel with the knee. The design of this device was presented in [Cherry 06]. We hypothesized that subjects would compensate for the additional stiffness at the knee by reducing biological knee stiffness in order to maintain constant combined knee stiffness. We also hypothesized that subjects would maintain a constant leg stiffness while hopping with and without the additional stiffness at the knee. We expected that subjects would decrease muscle activation levels in the knee extensors (quadriceps muscle group) in order to provide this modulation of biological knee stiffness. In order to maximize similarity between the hopping task and running, we chose to have subjects hop on one leg. Due to the difficulty of hopping on one leg for an extended duration of time it was not possible to measure metabolic rate during this study.

3.3 Methods

3.3.1 Subjects

Ten healthy subjects participated in this study [8 men, 2 women; age 26 yr (SD 3.8), mass 86 kg (SD 9.5)]. The University of Michigan Institutional Review Board granted approval for this project and all participants gave informed, written consent.

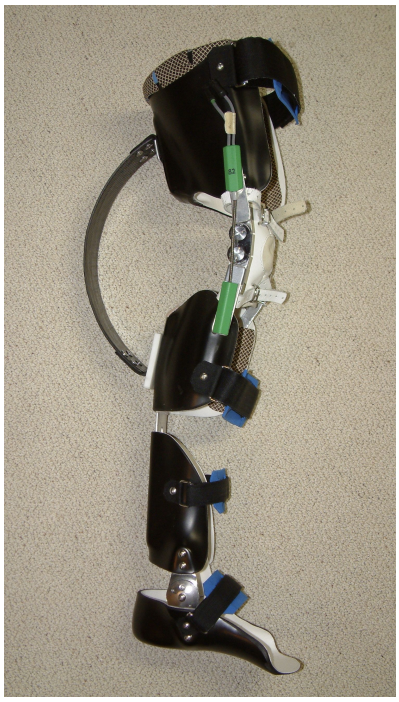

Figure 3.1 Photograph of the elastic knee-ankle-foot orthosis (eKAFO).

3.3.2 General procedure

Subjects hopped on their left legs at two frequencies (2.2 Hz and preferred frequency) under two orthosis conditions. In all conditions subjects wore the knee-ankle-foot orthosis (KAFO) shown in Figure 3.1. The design and construction of this orthosis was described in [Cherry 06] and [Cherry 07]. In one condition (Spring, or Spr), the subjects hopped with the custom-built light stiff composite leaf spring attached as shown. In the other condition (No Spring, or NoS) the spring was disconnected at the connection to the shank and taped to the thigh segment so as not to change the mass properties of the mechanism significantly. The stiffness of the spring was chosen to be about 30% of the knee stiffness for subjects as tested in pilot studies. This stiffness was comfortable for subjects while providing adequate stiffness for subjects to sense that the brace was providing a significant torque at the knee. The mean brace stiffness across all subjects was 5.6 N-m/°, which was effectively 31.5% of the total knee stiffness when hopping in the Spring condition.

Subjects followed the beat of a digital metronome when hopping at 2.2 Hz. Actual hopping frequency was measured at 2.2 Hz (SD 0.02) for both orthosis conditions. This frequency was chosen because it is greater than the preferred hopping frequencies found in previous studies [Ferris 06, Farley 91] and the leg is typically spring-like in this range [Farley 91]. In the preferred frequency trials subjects were instructed to hop at a self-selected

frequency with the metronome turned off. Subjects were told that the hopping motion should be continuous and that they should select the frequency they would choose if hopping for an extended period of time. The preferred hopping frequency was significantly different between orthosis conditions [$P = 0.017$, 1.93 Hz (SD 0.128) for NoS, 2.04 (SD 0.140) for Spr conditions].

Subjects were instructed not to use their arms for assisting their hopping motion but were allowed to extend them to the side while hopping to assist with balance. Four trials were conducted for each spring condition at each frequency (2.2 Hz and preferred). The order of the 16 trials was randomized and data was collected for five seconds of each trial after the subject reached a steady hopping motion. Rest was provided after each four trials and additional rest was provided if desired.

3.3.3 Knee-ankle-foot orthosis

The KAFO used for this study was constructed from polypropylene with steel reinforcement at the joints. This orthosis provided full range of motion in the sagittal plane at both the knee and ankle joints. The length of the shank segment was made such that it was adjustable for individuals with different leg lengths. Due to this and the use of polypropylene for the thigh and shank sections, the same brace was used for all subjects with only minor modification needed. Additionally, the angle of spring engagement was made to be adjustable to allow for variations between subjects. This angle was set after collecting and analyzing data from four trials at each frequency in the No Spring condition. The angle of spring engagement was then set to the average knee angle at ground contact. The orthosis was constructed such that when the knee was more extended than this angle no force was applied by the spring [Cherry 06]. The orthosis mass was 1.8 kg.

3.3.4 Data collection

Segment and joint kinematics were collected using a seven-camera motion analysis system (120 Hz, Motion Analysis, Santa Rosa, CA). Reflective markers were placed on the left foot, shank, thigh, ankle, knee and hip as well as the torso. We collected ground reaction forces using a force plate (1.2 kHz, Advanced Mechanical Technology, Watertown, MA) rigidly attached to concrete sub-flooring. We also independently measured the knee angle of the orthosis using an electrogoniometer (1.2 kHz, Biometrics, Ladysmith, VA).

We collected muscle activation (electromyography, or EMG) levels for eight major lower limb muscles: tibialis anterior, soleus, medial gastrocnemius, lateral gastrocnemius, vastus medialis, vastus lateralis, rectus femoris, and medial hamstrings (1.2 kHz, Konigsberg

Instruments, Pasadena, CA). We prepared subjects' legs by shaving and cleaning with alcohol before attaching bipolar surface electrodes (interelectrode distance: 3.5 cm). We taped electrodes and wires to the skin and used a mesh stocking to hold wires in place, reducing movement artifact in the EMG data. We also visually examined each electrode for noise and cross-talk before data collection.

3.3.5 Data analysis

We used commercial software (Visual3D, C-Motion, Rockville, MD) for data filtering and inverse dynamics calculations. We filtered motion and goniometer data with a low-pass zero-lag fourth-order Butterworth filter (cutoff frequency: 6 Hz). We filtered force plate data similarly but with a 50 Hz cutoff frequency. We calculated internal muscle moments about the lower limb joints using the kinematic marker and force plate data. Inertial properties of the limbs were estimated based on anthropometric measurements. Foot, shank, and thigh mass and inertia were modified to account for the orthosis whose mass properties were known.

3.3.6 Electromyography

We filtered the electromyography data using a high-pass zero-lag fourth-order Butterworth filter (cutoff frequency: 20 Hz) to attenuate movement artifacts and then performed full wave rectification. We used this data to calculate root-mean-squared (RMS) muscle activation levels during the stance phase of each hop in order to compare muscle activation levels across conditions. We also created linear envelopes of the EMG data for the entire hop cycle (ground contact (GC) to ground contact) by low-pass filtering (cutoff frequency: 6 Hz) the high-pass filtered and rectified EMG data. The RMS data were normalized by the mean value for each muscle on each subject in the No Spring condition at the preferred frequency. The linear envelopes for each subject were averaged for all hops and then normalized by the maximum value of the resulting linear envelope.

3.3.7 Joint angle definitions

All joints were defined in the sagittal plane. Ankle angle was defined as the complement to the angle between the shank and foot segments (angle increases with dorsiflexion). Knee angle was defined as the complement to the internal angle between the shank and thigh segments (angle increases with knee flexion). Hip angle was defined as the complement to the internal angle between the thigh and pelvis (angle increases with hip flexion).

3.3.8 Stiffness calculations

Using commercial software (Matlab, The MathWorks, Natick, MA) we calculated leg stiffness as the linear least squares fit of the vertical ground reaction force verses center of mass displacement, excluding data points whose force was below five percent of the maximum force during that hop. The center of mass displacement was found by dividing the vertical ground reaction force by the subject's mass, then integrating twice. The first integration constant was found by assuming that the mean center of mass velocity over one hop cycle was zero. The second integration constant was assumed to be zero since we are not interested in the absolute position of the center of mass but only the relative displacement over time. This process is demonstrated in Figure 3.2(a). Additionally, in order to double check that the center of mass displacements we calculated were reasonable, we plotted the calculated center of mass motion with the sacral marker motion as seen in Figure 3.2(b). This shows that the calculations are indeed correct.

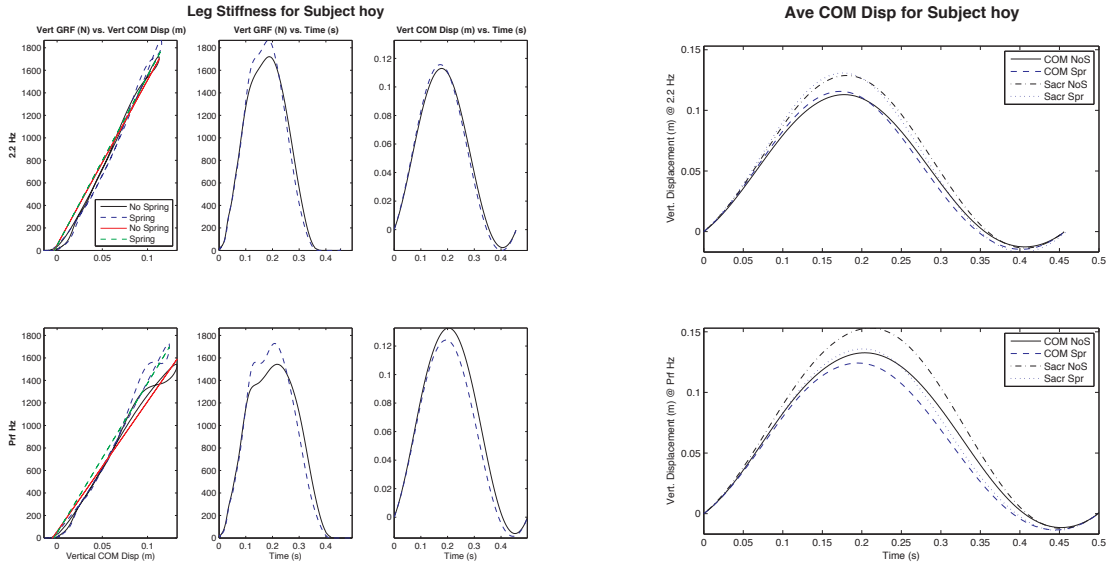

(a) (b)

Figure 3.2 Leg stiffness and center of mass displacement for an individual subject. (a) Leg stiffness is calculated using the least squares linear fit of the vertical ground reaction force versus the center of mass displacement. (b) Center of mass displacement was verified by plotting it with the sacral marker's vertical motion versus time.

Similarly, we calculated stiffness at each joint by finding the linear least squares fit of each joint's internal moment with respect to its rotation (Figure 3.3). Again we excluded data points whose moments were less than five percent of the maximum so as to obtain the linear behavior of each joint after the initial impact of ground contact has occurred.

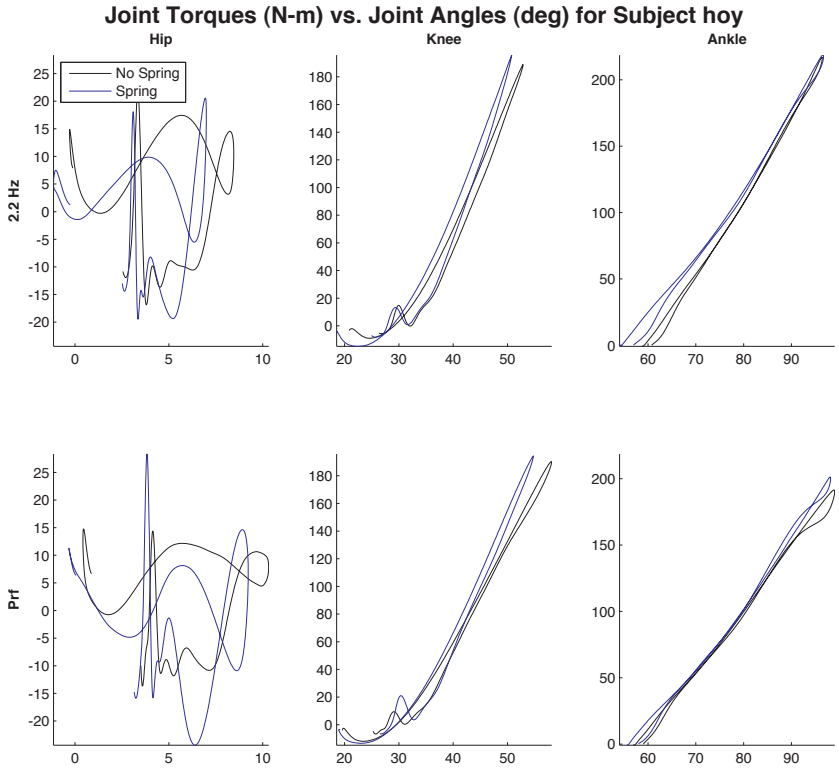

Figure 3.3 Stiffnesses for each joint were calculated from the linear least squares fit of the joint moment versus joint angle for each hop. Data shown here is the average for all 20 hops on an individual subject.

For the knee orthosis we used experimental measurements to validate the modeled stiffness of the system as described previously [Cherry 06]. We used an electrogoniometer to measure the absolute rotation of the orthosis knee joint while hopping. Due to the compliant nature of the leg there was significant relative rotation between the orthosis and the biological knee joint during the Spring condition. This will be addressed further in the following section (see Figure 3.4(a)).

The goniometer data was synchronized with the motion and force data using an analog-to-digital converter and the EVaRT software (Motion Analysis, Santa Rosa, CA). Knowing the stiffness of the brace and its angle of rotation we calculated the moment contributed by the orthosis to the knee as the difference between the knee internal moment as calculated by inverse dynamics and the orthosis moment as calculated from the orthosis stiffness and measured orthosis angle (Equation 3.1). We then calculated the biological knee stiffness using a linear least squares fit of the biological knee moment versus the knee angle as measured using the motion capture system. Finally, the effective orthosis stiffness was calculated by subtracting the biological knee stiffness from the total knee stiffness (Equation

3.2). The stiffnesses for a single subject's average data is shown in Figure 3.4(b) for demonstration.

$$Biological\ Knee\ Moment = Total\ Knee\ Moment - Orthosis\ Moment \tag{3.1}$$

$$Orthosis\ Stiffness = Total\ Knee\ Stiffness - Biological\ Knee\ Stiffness \tag{3.2}$$

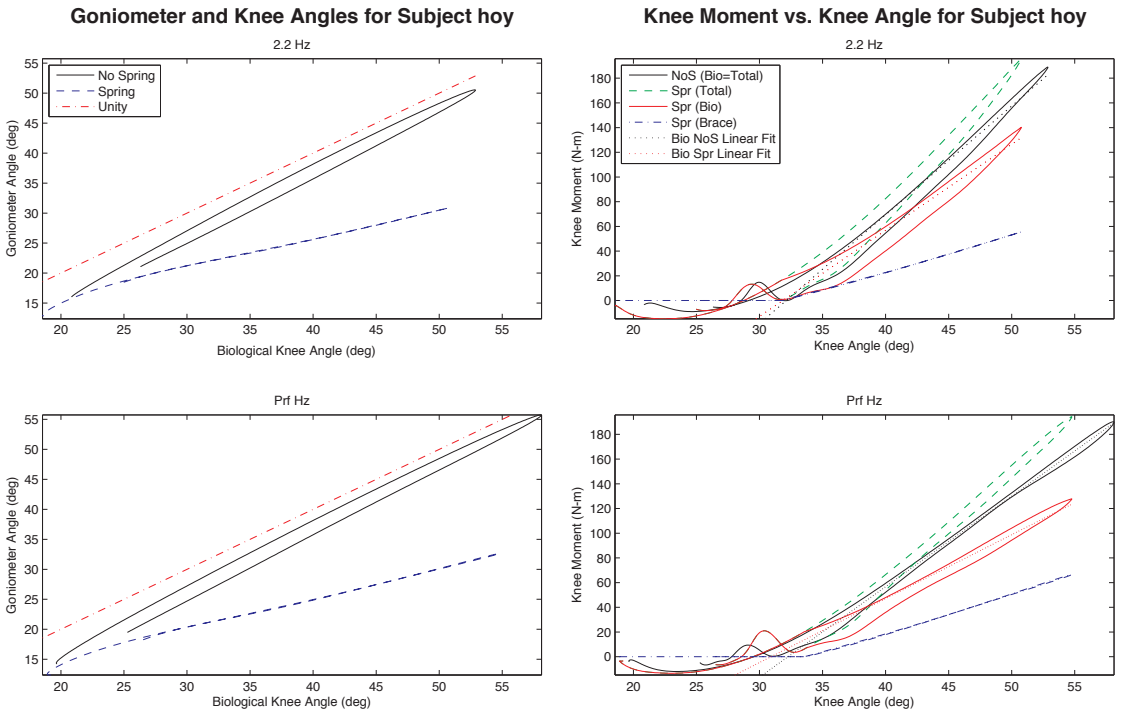

Figure 3.4 Knee angles and stiffness for an individual subject. (a) Angles for the biological knee joint and the knee joint on the orthosis were measured independently using motion capture and electrogoniometer data. Reduced range of motion in the Spring condition was due to soft tissue deformation on the upper leg. (b) Total knee stiffness was calculated using inverse dynamics for both conditions. In the Spring condition biological knee stiffness was found by subtracting the instantaneous moments provided by the orthosis from the total knee stiffness.

3.3.9 Statistical analyses

We used a three-way ANOVA (subject, frequency, spring condition) to determine significant differences in kinematic, kinetic, and electromyographic data between the Spring and No Spring conditions ($P < 0.05$ as significance level). Because our focus was on the effect between the two orthosis conditions we did not analyze differences related to inter-subject

variability (subject was treated as a random effect). To determine whether significant variations occurred between controlled frequency hopping and preferred frequency hopping we conducted additional analyses using separate ANOVAs for 2.2 Hz and the preferred frequency. Because there were significant differences between the two, the results of these two ANOVAs will be presented here. All statistical analyses were performed with the JMP software (Version 7, SAS Institute, Cary, NC).

3.4 Results & Discussion of Results

3.4.1 Stiffness Values

In both the controlled and preferred frequency trials the biological knee stiffness decreased significantly ($P = 0.038$ and $P = 0.025$ respectively). Unlike previous studies [Ferris 06] this decrease was not 100% accounted for by the stiffness of the orthosis. Total knee stiffness increased significantly for both frequencies in the Spring condition ($P = 0.001$ and $P < 0.001$ for 2.2 Hz and Prf Hz respectively). Additionally, in the controlled frequency trials the ankle stiffness decreased significantly while there was no change in the overall leg stiffness ($P =< 0.001$ and $P = 0.865$ respectively). This is contradictory to the results obtained by Farley and Morgenroth [Farley 99] in which they determined that leg stiffness is coupled to ankle stiffness while knee stiffness had little effect. For the preferred frequency trials subjects maintained a similar ankle stiffness ($P = 0.136$) while increasing leg stiffness significantly ($P = 0.015$). This increase in leg stiffness can be partially explained by the increase in preferred hop frequency since previous work has shown that leg stiffness increases with increased stride frequency [Farley 96, Arampatzis 99, Ferris 97, Kerdok 02]. The results for stiffness changes are shown in Figure 3.5(a). All data is summarized numerically in Table 3.1.

In looking at the plotted data it should be noticed that the error bars are quite large even though the results are significant statistically. This is due to the variation between subjects, not between conditions within a subject. To illustrate this point Figure 3.5(b) is provided. The trends from the averaged data across all subjects are consistent but now the error bars are much smaller since the standard deviation on particular stiffness values did not change dramatically between hops for a given subject.

It should also be noted that for the controlled frequency trials there were no significant changes in kinematic measures whereas for preferred frequency trials subjects landed with a more flexed knee but underwent less rotation (Table 3.1). This might be a result of trying to maximize usage of the elastic element in the orthosis by flexing the knee a greater amount

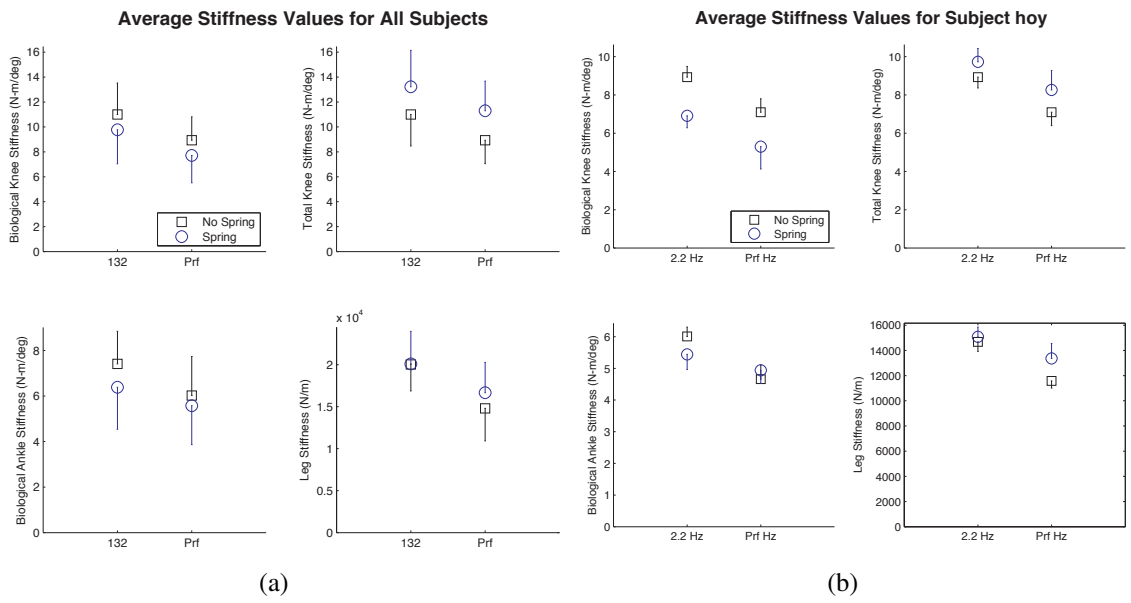

Figure 3.5 Stiffness values averaged for (a) all subjects and (b) a single subject. Error bars are two way and represent the standard deviation between subject mean stiffness values. The error bars are shown here one way only for clarity as they overlap significantly. (b) For a single subject, error bars are significantly smaller since they now represent the standard deviation between different hops for a single subject.

before ground contact. The increased stiffness of the orthosis and the total knee stiffness may explain the decrease in maximum rotation.

3.4.2 Muscle Activation Levels

During the stance phase of the hop cycle there was a significant decrease in the muscle activation levels for all three knee extensors included in the study for both frequencies in the Spring condition (Figure 3.6). Vastus Medialis decreased by 15 and 20% in the 2.2 Hz and Prf Hz trials respectively ($P = 0.007$ and $P < 0.001$). Vastus Lateralis was decreased by 16 and 27% in the 2.2 Hz and Prf Hz trials respectively ($P = 0.00239$ and $P < 0.001$). Rectus Femoris was decreased by 19 and 28% in the 2.2 Hz and Prf Hz trials respectively ($P = 0.006$ and $P < 0.001$). On average this means that for controlled frequency hopping, quadriceps muscle usage decreases by roughly 16% while it decreases 25% when subjects are allowed to choose their own posture and hop frequency. No other muscle groups experienced significant changes in activation levels.

The linear envelopes for the muscle activation confirm that the muscle activation levels for the quadriceps muscle group (VM, VL, RF) indeed appear lower during the stance phase

of the hop cycle. The hop cycle as shown begins with left ground contact and ends at left ground contact. The stance phase lasts about the first two thirds of the hop cycle.

3.5 Conclusions

This chapter has presented the results obtained for hopping with an elastic knee orthosis. It was shown that adding elastic energy storage in parallel with the knee while hopping enables subjects to decrease their muscle activation levels in the knee extensors both for controlled and preferred frequency hopping with the spring active. For the preferred frequency trials subjects chose to hop with a higher frequency and had an associated increase in leg stiffness. In the preferred frequency trials in the Spring condition subjects also landed with a more flexed knee but underwent less knee flexion during stance. This was associated with an increase in the total knee stiffness and a slight but significant decrease in biological knee stiffness in the Spring condition.

Table 3.1 Summarized values for all numerical data. NoS—No Spring condition, Spr—Spring condition, Prf—Preferred frequency, LTA—Left tibialis anterior, LSO—Left soleus, LMG—Left medial gastrocnemius, LLG—Left lateral gastrocnemius, LVM—Left vastus medialis, LVL—Left vastus lateralis, LRF—Left rectus femoris, LMH—Left medial hamstrings.

Frequency, Hz	2.2				Prf			
Spring Condition	NoS	Spr	% Change	ANOVA *P* Value	NoS	Spr	% Change	ANOVA *P* Value
Leg Stiffness, Mean(SD)								
Leg Stiffness, kN/m	20.03(3.149)	20.10(3.872)	0.3%	0.865	14.80(3.863)	16.67(3.610)	12.6%	0.015*
Hop Frequency, Mean(SD)								
Hop Frequency, Hz	2.19(0.020)	2.19(0.019)	0.0%	0.769	1.93(0.128)	2.04(0.140)	5.7%	0.017*
Knee Brace Stiffness over TOTAL Knee Stiffness in Spr Condition, Mean(SD)								
Pct Stiffness, %	0.00(0.000)	27.13(6.924)	N/A	N/A	0.00(0.000)	32.78(6.904)	N/A	N/A
Joint Stiffnesses, Mean(SD)								
Tot Knee, Nm/deg	11.00(2.525)	13.23(2.916)	20.3%	0.001*	8.94(1.875)	11.30(2.374)	26.4%	<0.001*
Bio Knee, Nm/deg	11.00(2.525)	9.77(2.731)	-11.2%	0.038*	8.94(1.875)	7.71(2.190)	-13.8%	0.025*
Ankle, Nm/deg	7.41(1.427)	6.38(1.845)	-13.9%	<0.001*	6.02(1.714)	5.57(1.705)	-7.5%	0.136
Correlation Coefficients, Mean(SD)								
Tot Knee, N/A	0.92(0.047)	0.93(0.045)	N/A	N/A	0.95(0.041)	0.95(0.034)	N/A	N/A
Bio Knee, N/A	0.92(0.047)	0.89(0.054)	N/A	N/A	0.95(0.041)	0.92(0.046)	N/A	N/A
Ankle, N/A	0.96(0.037)	0.92(0.080)	N/A	N/A	0.95(0.046)	0.92(0.077)	N/A	N/A
Joint Angle Data, Mean(SD)								
HipAngleAtGC, deg	5.25(9.565)	5.61(8.930)	6.9%	N/A	4.85(9.130)	5.89(9.365)	21.4%	N/A
KneeAngleAtGC, deg	23.86(10.562)	24.97(10.366)	4.7%	0.17	21.50(10.197)	23.78(10.451)	10.6%	<0.001*
AnkleAngleAtGC, deg	58.47(5.431)	59.75(4.984)	2.2%	0.361	56.34(6.162)	58.08(7.066)	3.1%	0.211
MaxHipBend, deg	4.14(1.646)	3.62(3.755)	-12.6%	N/A	7.19(1.691)	5.72(4.050)	-20.4%	N/A
MaxKneeBend, deg	20.33(3.790)	19.65(3.741)	-3.3%	0.544	28.73(4.536)	24.63(4.364)	-14.3%	0.007*
MaxAnkleBend, deg	30.19(5.385)	29.22(6.353)	-3.2%	0.413	34.71(6.355)	32.03(8.515)	-7.7%	0.075
RMS EMG Amplitudes during Stance, Mean(SD)								
LTA, mV/mV	1.12(0.261)	1.19(0.264)	6.2%	0.317	1.00(0.000)	1.10(0.160)	10.0%	0.091
LSO, mV/mV	0.99(0.073)	0.98(0.137)	-1.0%	0.926	1.00(0.000)	0.97(0.157)	-3.0%	0.54
LMG, mV/mV	1.00(0.059)	1.01(0.133)	1.0%	0.765	1.00(0.000)	0.97(0.147)	-3.0%	0.602
LLG, mV/mV	1.03(0.076)	1.01(0.165)	-1.9%	0.739	1.00(0.000)	0.99(0.163)	-1.0%	0.898
LVM, mV/mV	0.95(0.078)	0.81(0.099)	-14.7%	0.007*	1.00(0.000)	0.80(0.077)	-20.0%	<0.001*
LVL, mV/mV	0.90(0.072)	0.76(0.167)	-15.6%	0.0239*	1.00(0.000)	0.73(0.136)	-27.0%	<0.001*
LRF, mV/mV	0.92(0.079)	0.75(0.143)	-18.5%	0.006*	1.00(0.000)	0.72(0.145)	-28.0%	<0.001*
LMH, mV/mV	1.15(0.114)	1.17(0.172)	-1.7%	0.489	1.00(0.000)	1.05(0.110)	5.0%	0.177

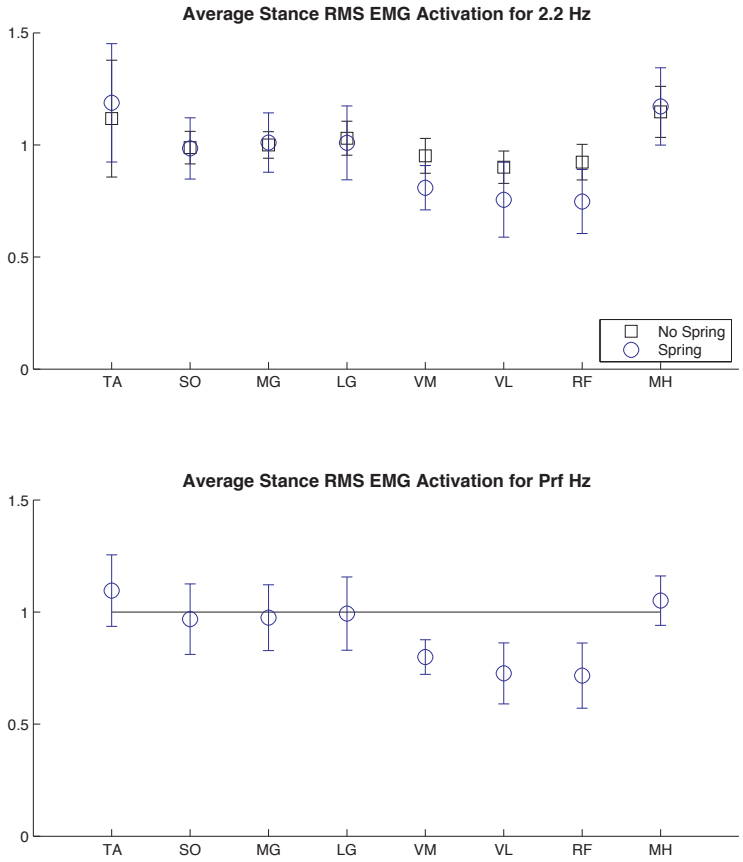

Figure 3.6 Stance phase RMS muscle activation levels averaged for all subjects. In both the controlled (132 bpm / 2.2 Hz) and preferred frequency trials there was a significant reduction in muscle activation of the quadriceps muscle group. No other muscle groups had a statistically significant change. LTA—Left tibialis anterior, LSO—Left soleus, LMG—Left medial gastrocnemius, LLG—Left lateral gastrocnemius, LVM—Left vastus medialis, LVL—Left vastus lateralis, LRF—Left rectus femoris, LMH—Left medial hamstrings. *—$P < 0.05$

In contrast, during controlled frequency hopping (2.2 Hz) subjects maintained constant leg stiffness and leg kinematics, but decreased their ankle stiffness in addition to increasing total knee stiffness and decreasing biological knee stiffness as in the preferred frequency trials. This shows that subjects choose to modulate stiffness levels of individual joints while hopping under controlled conditions without changing their leg stiffness. At both frequencies the biological knee stiffness decreases and knee extensor muscle activation levels decrease, indicating that elastic exoskeletons may be effective at reducing metabolic cost of locomotion in bouncing gaits.

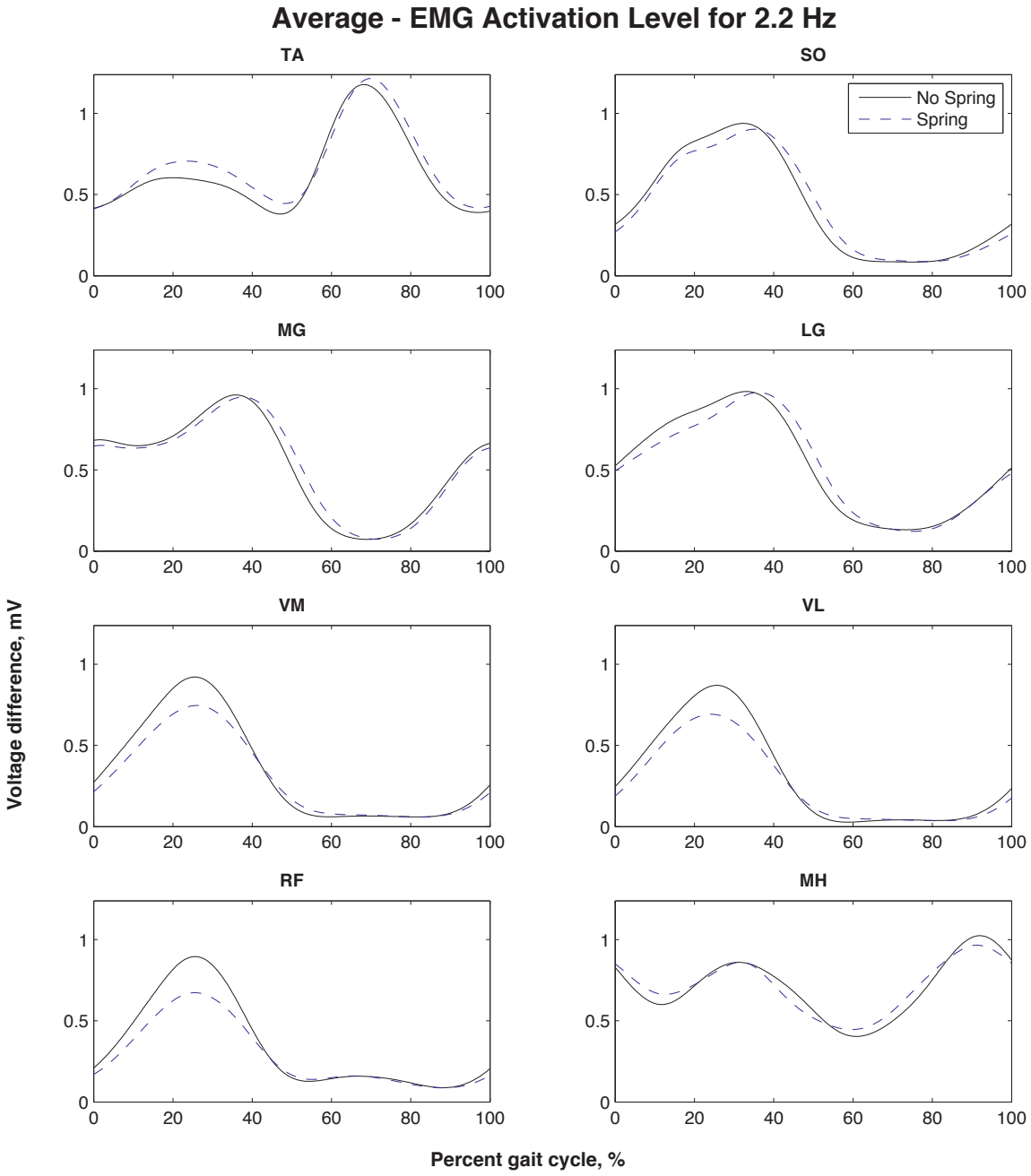

Figure 3.7 Fixed frequency muscle activation levels for eight superficial muscles on the lower leg. Curves shown are from hopping at the controlled frequency of 2.2 Hz or 132 bpm and represent the averaged curves for all subjects. Subject curves are the average of all hops normalized by the maximum value of that subject's average linear envelope.

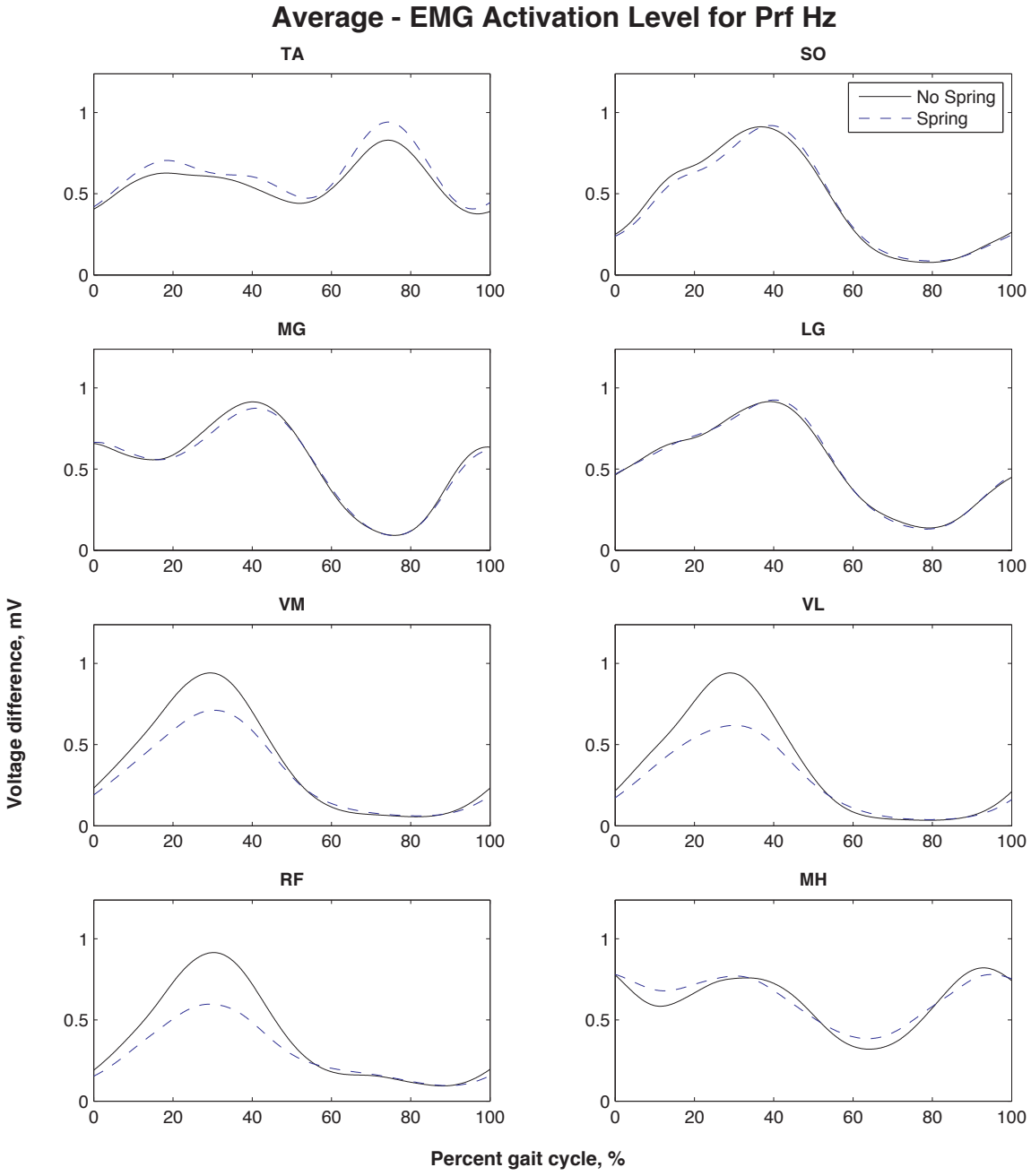

Figure 3.8 Preferred frequency muscle activation levels for eight superficial muscles on the lower leg. Curves shown are from hopping at the preferred frequency and represent the averaged curves for all subjects as in Figure 3.7.

3.6 Acknowledgments

The authors wish to acknowledge the assistance of Jacob Godak in fabrication and modification of the braces and leaf springs as well as Catherine Kinnaird for her assistance in data collections and Steven Emanuel for guidance in machining operations. This research was supported by NSF BES-0347479 and an NSF graduate research fellowship for the first author.

Chapter 4

Design of an Elastic Exoskeleton

This chapter was written by Michael S. Cherry, Sridhar Kota, and Daniel P. Ferris. It was published as a paper with the title "An elastic exoskeleton for assisting human running" in the proceedings of the ASME International Design Engineering Technical Conferences in August 2009 [Cherry 09].

4.1 Abstract

This paper presents the design and preliminary evaluation of an elastic lower-body exoskeleton (eExo). Human legs behave in a spring-like fashion while running. We selected a design that relied solely on material elasticity to store and release energy during the stance phase of running. The exoskeleton included a novel knee joint with a cam and a Bowden cable transferring energy to and from a waist-mounted extension spring. We used a friction-lock clutch controlled by hip angle via a pneumatic cylinder to release the cable during swing phase for free movement of the leg. The design also incorporated a composite leaf spring to store and release energy in the distal portion of the exoskeleton about the foot and ankle. Preliminary test data for our target subject showed that his typical leg deflection was 0.11 m with leg stiffness of 16 kN/m while running at 3.0 m/s. We used these values to set the desired stiffness (60$\pm$15% of the normal leg stiffness, or 9.6$\pm$2.4 kN/m) and deflection (0.11 m) of the exoskeleton. We created simplified multi-body and full finite element quasi-static models to achieve the desired system stiffness and validate our results, respectively. The final design model had an overall stiffness of 7.3 kN/m, which was within the desired range. We fabricated a single-leg prototype of the exoskeleton that weighed 7.1 kg. We tested the exoskeleton stiffness quasi-statically and found a stiffness of 3.6 kN/m. While running, the exoskeleton provided $\sim$30% of the total leg stiffness for two subjects. Although the stiffness was lower than desired, the fabricated prototype demonstrated the ability of a quasi-passive exoskeleton to provide a significant portion of an individual's leg stiffness while running.

4.2 Introduction & Background

Locomotion is central to people's ability to function independently in their daily lives. Able-bodied individuals take for granted their ability to move about as they perform daily tasks. Individuals with disabilities that affect their locomotive capacity are well aware of the challenges. In a way all individuals are limited in their locomotive capacity. For example we are all bounded by the speeds we can run and the distances we can walk while carrying heavy loads.

Our broad research aim is to develop wearable mechanisms (exoskeletons) for assisting human locomotion, benefitting both able-bodied and individuals with disabilities. For example, those who are able-bodied could run farther at the same speed before becoming fatigued with the addition of an exoskeleton. This would be highly beneficial in either military or search and rescue operations where it is critical to traverse large distances quickly and over rough terrain. An exoskeleton that reduced loads required by specific muscle groups in the leg could also benefit individuals with disabilities, such as muscle atrophy in the lower limb, restoring their locomotive ability. For example, an individual with an atrophied quadriceps muscle group could use an elastic exoskeleton to provide a knee extension (straightening) torque while walking and running, decreasing the demands on existing muscles and enabling locomotion at higher speeds and with greater comfort. Decreasing loads at specific joints in the lower limb may prove beneficial for individuals suffering from osteoarthritis. A leg exoskeleton capable of sustaining a portion of an individual's body weight would decrease the bone on bone forces at the joints and decrease pain while enabling locomotive ability. In this sense the elastic exoskeleton could take on the role of a body-weight support system that does not need to be used in a laboratory environment. Typical body-weight support systems are large, bulky and not suitable for daily use. Development of a lightweight low-profile wearable exoskeleton that supports a significant portion of body weight could be used for locomotion rehabilitation in the wearer's home and natural surroundings.

4.2.1 Literature Review

The most well-publicized exoskeletons in mass media are highly complicated and energy intensive wearable robots (Berkeley [Kazerooni 07], Cyberdyne [Kawamoto 05], and Sarcos [Jacobsen 04]). These robots are designed to augment human capability through active mechanical power generation via motors and actuators. In general, they do not make use of elastic components to store and release energy during locomotion. In contrast, humans make

excellent use of elastic energy storage and return during both human walking and running (see [Farley 98a], [Sawicki 09], and [Alexander 90]).

Only a handful of devices have been designed to incorporate elasticity, decreasing the demands on actuators while enabling simpler designs. One method for including elasticity is through series elastic actuators. The RoboWalker [Pratt 04b] and the powered exoskeleton developed by Low et al. [Low 06] use this method. Walsh et al. developed an alternate method of incorporating elasticity [Walsh 06] in which elastic elements were placed at the hip and ankle joints in an exoskeleton designed to carry heavy loads. A variable-damper was used at the knee in this design, resulting in small but significant power-consumption by the device. Carr and Newman implemented the same variable damper in a leaf-spring-based elastic leg exoskeleton to model and understand locomotion by astronauts in space suits [Carr 08]. Banala developed an entirely passive elastic exoskeleton [Banala 06] based on principles of gravity balancing [Herder 01]. Dollar and Herr designed a quasi-passive knee exoskeleton for use while running but have only published results from bench tests thus far [Dollar 08a]. The device by Dollar and Herr is the most similar to the work presented in this paper. A more complete review of exoskeletons and orthoses for assisting human locomotion can be found in [Dollar 08b].

4.2.2 Summary

The objective of the research presented in this paper was to simulate, design, fabricate, and test an elastic exoskeleton for assisting human running. The design we present in this paper depends solely upon material elasticity to store and release energy during locomotion while supporting the weight of the user. The only energy required to operate the device is used for controlling a friction-lock clutch. This clutch enables switching between stiff and compliant states for the stance and swing phases of running, respectively. The design also aims to be a low-profile exoskeleton, matching the motion of the legs without encumbering their mobility.

4.3 Design Procedure

The simplest model for running includes a spring representing the function of the legs and a point mass representing body mass (see Fig. 4.1, [Blickhan 89], [McMahon 90], and [McGeer 90]). Human walking dynamics can also be explained using a spring-mass model (see [Alexander 92] , [Geyer 06], [O'Connor 07], and [Whittington 09]). During walking, however, leg deflections are smaller and play a lesser role in the overall energetics of the

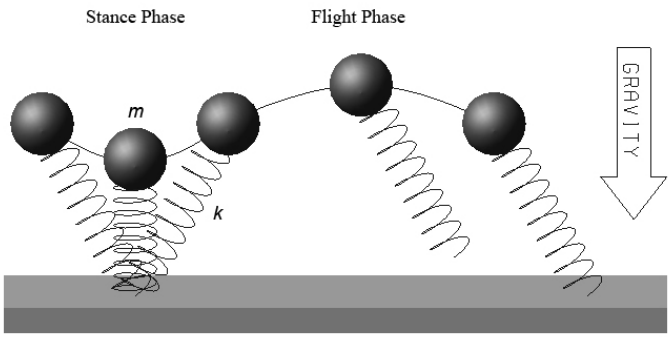

Figure 4.1 Spring-mass model for running. m—point mass, k—spring constant representing leg stiffness. This model accurately describes the center of mass motion and ground reaction forces for bouncing gaits. This dependence on energy storage via elastic mechanisms was the primary reason for selecting running as the application of our elastic exoskeleton. Adapted from [McMahon 90].

system compared to running. Consequently an elastic leg exoskeleton would likely be more effective for running, which will be the focus for our design.

4.3.1 Setting Design Requirements

We tested a single subject running on a force-plate mounted treadmill to collect information about design parameters for the exoskeleton. Visual markers were attached to the lower limbs and torso to record body motion. Trials were conducted at three different speeds (2.6, 3.0, and 3.4 m/s) and in two running conditions, running with heel-strike and running on the balls of the feet (toe running). Data was similar for all trials. The results presented and used for setting design requirements are taken from the 3.0 m/s toe-running trials.

We used two visual markers to define connection points of the exoskeleton to the subject near the lateral iliac crest (hips) and the fifth metatarsal head (foot). We calculated the desired length of the exoskeleton by taking the norm of the vector between these two markers. We calculated the portion of the ground reaction force that would be directed along the exoskeleton by taking the dot product of the direction vector with the ground reaction force vector during stance. These results are provided in Figs. 4.2 and 4.3 respectively.

We set length specifications from the length data and determined the desired stiffness by calculating the linear least squares fit through the mean force-deflection curve shown in Fig. 4.3. The desired exoskeleton stiffness was approximate because there was large variability in leg stiffness. Consequently it was not critical to have an exact value for the exoskeleton stiffness, but was sufficient to have it in a reasonable range. Previous designs of elastic orthoses for hopping (see [Ferris 06] and [Cherry 06]) demonstrated that an orthosis with

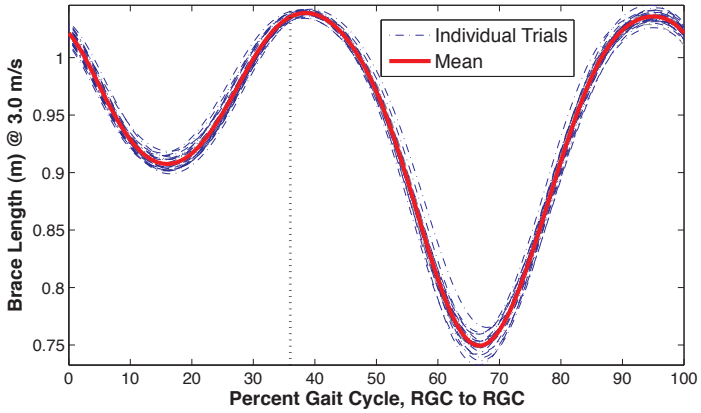

Figure 4.2 Length of vector between proposed attachment points near lateral iliac crest and fifth metatarsal head. The horizontal axis represents percent stride cycle, starting and ending at right ground contact (RGC). The vertical dotted line represents right take-off (RTO).

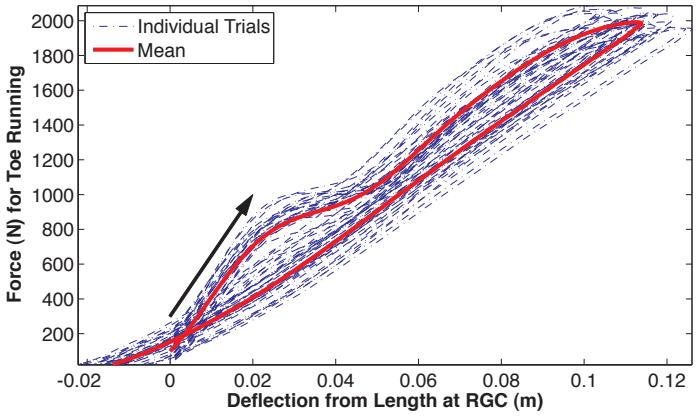

Figure 4.3 Portion of ground reaction force directed along proposed exoskeleton. The horizontal axis represents deflection of the proposed exoskeleton from the initial length at ground contact. The arrow indicates direction of force development.

30-50% of the relevant joint's stiffness allows for meaningful decreases in muscle activation without becoming uncomfortable or excessively perturbing the user's kinematics. In these designs it was also noted that much of the stiffness provided by the orthoses was lost at the interface between the orthoses and the human subjects (e.g. soft-tissue deformation). To compensate for this loss in stiffness the target stiffness should be increased by approximately 50%. Consequently, to achieve the desired 30-50% effective stiffness we set the design specification for exoskeleton stiffness at 45-75% leg stiffness, or 60$\pm$15%. The design specifications are summarized in Tab. 4.1.

4.3.2 Conceptual Design

During the concept generation phase over a dozen concepts were considered and evaluated. The desired attributes for the exoskeleton were as follows: lightweight, minimal moving mass on the legs, low-profile (closely matches the shape of the leg during all phases of the stride cycle), quasi-passive (relying solely on elastic mechanisms to store and release energy while running), and robust to variations in the users kinematics as well as adjustable to variations between users. The top five concepts were ranked according to these criteria using Pugh charts and a final concept was selected. Due to the space requirements these various concepts and their ranking are not presented in this paper. Rather, we focus on the design that was selected as the best candidate.

The Knee Disk

In this concept (see Fig. 4.4) the leg exoskeleton would attach to the hips of the wearer by a conventional spherical joint. A lightweight rigid structure (e.g. hollow tube) would extend from the hip joint to the general area of the knee. Although this segment would lie in close proximity to the thigh, it would not be attached so as not to constrain the motion of the leg. This rigid segment would connect with a revolute joint to the compliant segment that would extend from the end of this rigid link down to the ball of the foot near the fifth metatarsal head. The compliant segment would also rigidly attach to a pulley (knee disk, or cam) over which a cable would be routed.

This Bowden cable would remotely control the state of the leg exoskeleton. When the cable moves freely (MidSwing in Fig. 4.4) the leg sections would bend at the joint between the rigid upper and compliant lower segments. When the cable is held taut (MidStance in Fig. 4.4) the compliant segment would compress to store energy while the knee joint would also bend, storing energy in the extension spring attached to the other end of the cable. This energy would build up during the first half of stance and then release as the user progresses towards push-off. In essence, the knee disk in conjunction with the extension spring located on the back of the wearer would act as a torsion spring at the knee without having to place

Table 4.1 Design specifications for the elastic exoskeleton based on preliminary running data.

Description	Value
Initial exoskeleton length	1.02 m
Exoskeleton deflection under load	0.11 m
Approximate exoskeleton stiffness	9.6±2.4 kN/m

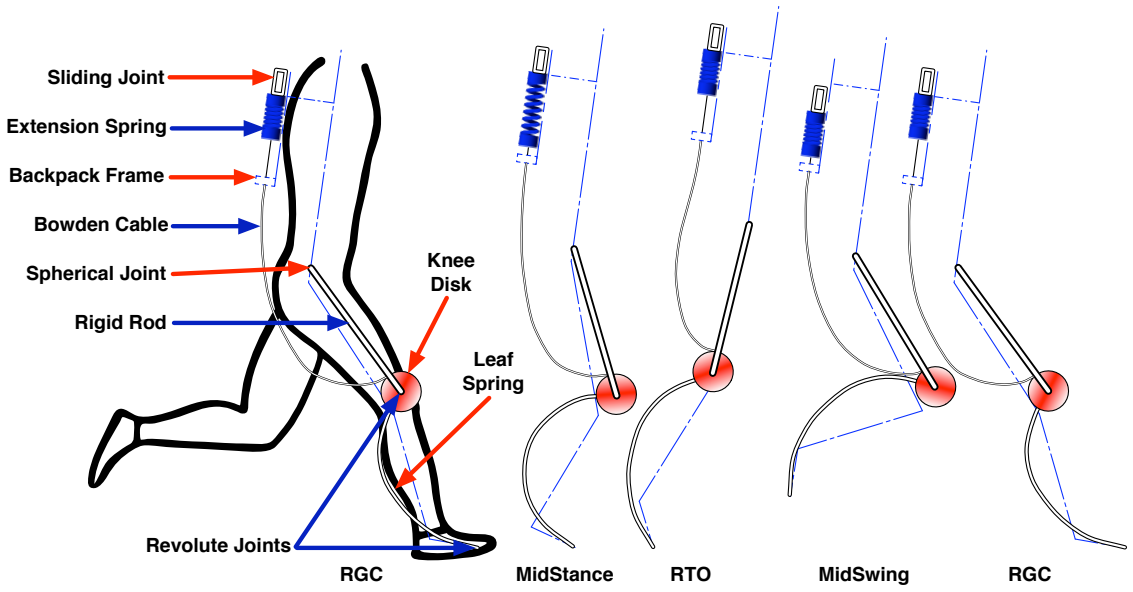

Figure 4.4 Conceptual design for an elastic leg exoskeleton extending from the hips to the foot. Compliance is included via the leaf spring extending from the knee region to the foot and at the exoskeleton knee by means of an extension spring and a bowden cable. This cable system is also the means whereby the system is allowed to move freely during swing phase and lock during stance phase to provide the desired stiffness. Components addressed in the detailed design stage are labeled.

the mass of a torsion spring there. As the foot leaves the ground the sliding joint on the back releases and the user could freely move their leg during the swing phase. The sliding joint could be controlled by a variety of means including a variable damper, ratchet-pawl mechanism, or friction lock clutch.

This concept would allow for relatively little mass on the legs and a robust method for transitioning the exoskeleton between stance and swing phase configurations. This design would also match the shape of the leg quite closely throughout the running stride cycle. The major disadvantage to this design was that the spring located on the back would increase the total mass of the device. The impact of this was acceptable since the weight would be attached to the trunk where it would be the least costly to carry from a metabolic perspective [Browning 07].

4.3.3 Detailed Design

The overarching goal of the detailed design phase was to select dimensions for all components such that the design would achieve a relatively low weight with acceptable exoskeleton stiffness and factors of safety. Of secondary importance we desired to keep the exoskeleton low profile throughout the stride cycle. To this end we attempted to minimize the diameter

of the knee disk and constrain the maximum knee disk rotation during stance. Preliminary testing indicated that the knee underwent 30 degrees of rotation during the stance phase of running. In order to keep the exoskeleton low profile during the stance phase we sought to have the exoskeleton knee joint undergo a similar rotation. However, the amount of rotation did not need to match exactly since the exoskeleton did not attach to the user's leg near the knee.

In this exoskeleton design the user does not feel the effects of the knee spring separately from the lower-leg leaf spring. Rather, the overall stiffness of the exoskeleton is felt by the user as a force on the joint connecting the rigid rod to the hip harness. The two elastic components combined provide the desired stiffness. Consequently, it was necessary to choose the diameter of the knee disk in conjunction with selecting the extension spring stiffness and the stiffness for the lower-leg leaf spring. This required a system model that captured the effects of all three values.

System Modeling

In the system model the leaf spring was modeled as a linear compression spring and the knee disk/extension spring combination was modeled as a torsion spring at the knee. A screenshot of this model is shown in Fig. 4.5. In the physical system, when the leaf spring compresses the top of the spring rotates unlike the top of the idealized compression spring. To compensate for this rotation a dummy body representing the knee disk was created and a coupler caused it to rotate relative to the compression spring as the spring compressed. The rate at which it rotated as well as the stiffness of the spring itself was extracted from a finite element model of the leaf spring (see Fig. 4.6). In the leaf spring model a 3.6 cm displacement directed along the line between the two revolute joints was imposed at the top while the joints at the bottom were pinned to ground.The reaction force required to cause the deflection and resulting knee joint rotation were measured. The resulting stiffness curve and coupling of rotation to compression are shown in Figs. 4.7 and 4.8 respectively.

Comparison of ADAMS System Model to Full Finite Element Model

In order to verify that the multi-body ADAMS system model was accurate we created the equivalent model in ANSYS. In this model the thigh rod was modeled as a solid steel rod such that it underwent negligible deformation. The leaf spring was the same as the one used in the previous section. The upper link and the leaf spring were connected with a revolute joint and a torsion spring as in the ADAMS model. The leaf spring was connected to ground with revolute joints as before. An 11 cm displacement was applied to the top of the upper

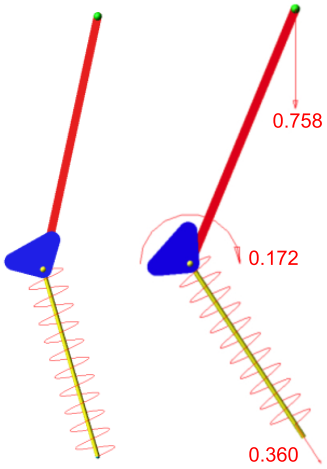

Figure 4.5 ADAMS model of the exoskeleton system. A torsion spring at the "knee" represents the stiffness of the extension spring on the user's back and knee disk combined. The lower-leg leaf spring was modeled as a compression spring. A coupler provided the correct knee disk rotation as the leaf spring compressed. Values for the compression spring stiffness and rotational coupler were calculated from a finite element model of the leaf spring (fig. 4.6). Forces (in kN) and torques (in kN-m) shown are for the maximum deflection of 11 cm.

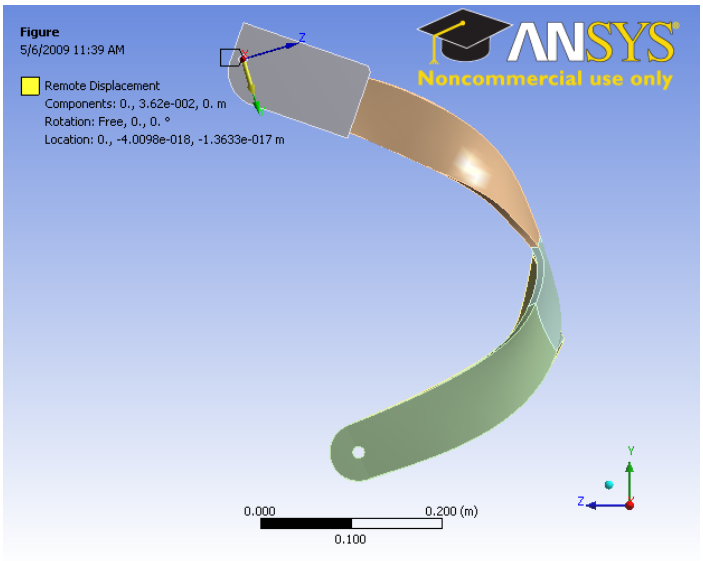

Figure 4.6 Finite element model of carbon composite lower-leg leaf spring. This model was used to calculate idealized values for the multi-body ADAMS model.

rod while it was able to rotate freely about the x-axis, the same axis as the other revolute joints. This model is shown in Fig. 4.9 while Fig. 4.10 shows the resulting ground reaction forces, knee disk rotations, and leaf spring deformations for both the simplified multi-body model and the full finite element model.

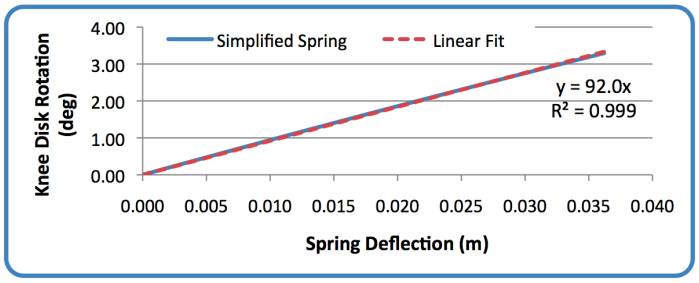

Figure 4.7 Rotation of the top of the leaf spring as it is compressed. Best-fit linear slope was used as a rotational coupler in the ADAMS model.

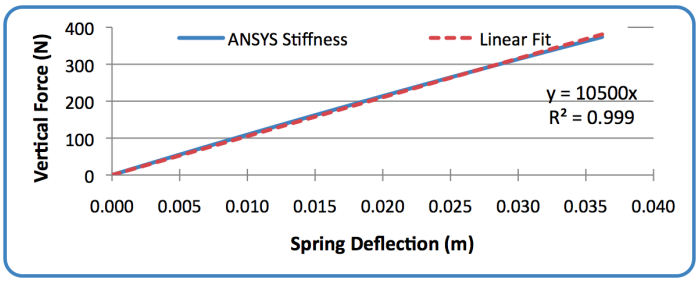

Figure 4.8 Reaction force required to compress spring through the applied deflection. Best-fit linear slope was used as the compression spring stiffness in the ADAMS model.

These plots show that the two models agreed with a relatively high degree of accuracy. There was some discrepancy between the two models that is easily explained by simplifications involved in the ADAMS model. Specifically, the finite element model of the leaf spring only had an applied displacement whereas the physical system and full finite element model have applied forces and torques at the knee joint. The applied displacement estimated the force accurately, but could not provide a torque. Although this discrepancy was significant, the error introduced by making this simplification was minimal (see Fig. 4.10). Consequently, we were confident that the model remained sufficiently accurate for design purposes.

Another reason for the discrepancy was out-of-plane effects present in the ANSYS model but neglected in the ADAMS model. The ADAMS model assumed that the leaf spring behaved as a simple compression spring that could not buckle out of plane due to revolute joints at both the top and bottom of the spring. In the finite element model the leaf spring was allowed to buckle and twist which provided some reaction torques to the upper and lower connections of the spring. The leaf spring had two revolute joints at its lower end and a revolute joint connecting the leaf spring to the thigh segment. Because of this the exoskeleton leg did not buckle out of plane even though it was given that degree

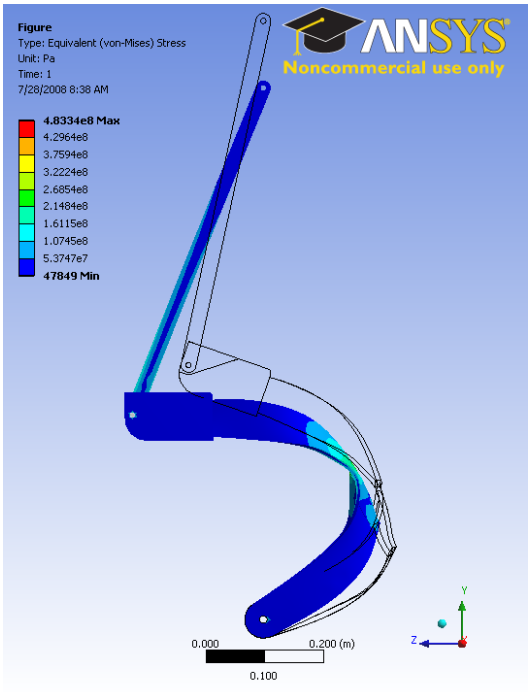

Figure 4.9 Finite element model of the exoskeleton leg system used to validate the simplified ADAMS model.

of freedom in the full finite element model. At the full 11 cm vertical hip deflection the maximum out-of-plane deflection at the knee joint was a negligible 0.14 cm.

All finite element models were constructed in ANSYS Workbench with Solid186 elements. These are 20-node elements and the vast majority of them were quadratic. A small number of tetrahedral and wedge elements were also used, e.g. to maintain proper shape of the elements in areas of large curvature or abnormal shape. The mesh density was chosen in order to guarantee at least two elements through the thickness of the smallest dimension in the parts. This provided adequate resolution of bending stresses throughout the model.

Elastic Elements

Using the ADAMS model, we first went about determining the desired values for the torsion spring and leaf spring stiffnesses. In order to simplify the selection of parameters for the lower-leg leaf spring only two design variables were used, the cross-sectional thickness and width. This constant cross-section was used throughout the leaf spring. The design variables for the torsion spring were the extension spring stiffness and the knee disk diameter. We varied these four values until a combination was achieved resulting in approximately 30

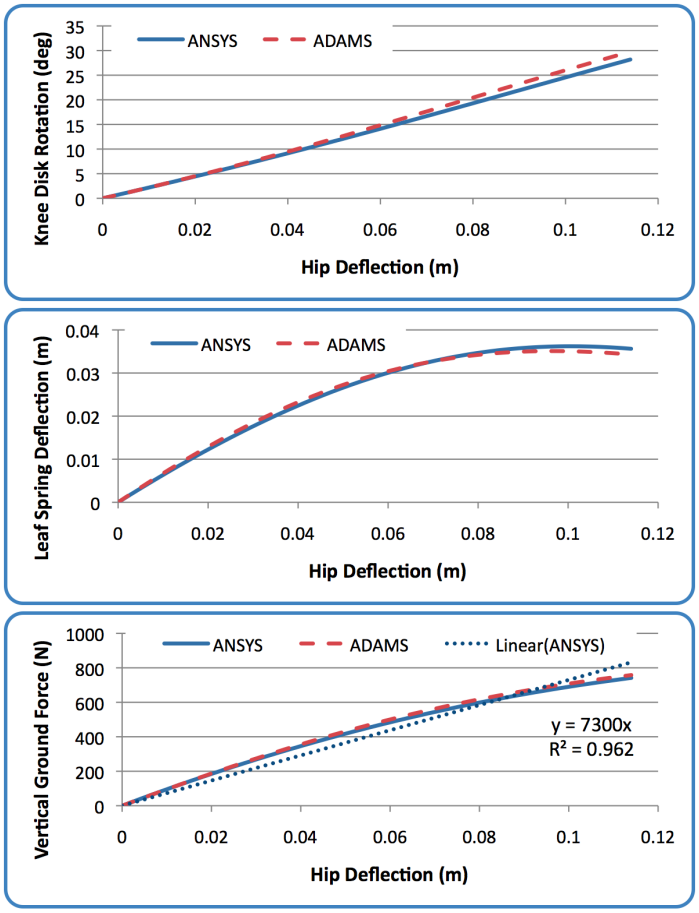

Figure 4.10 Plots of knee disk rotation, leaf spring deflection, and vertical ground reaction force for both the simplified ADAMS model and the full finite element model. The ANSYS model validates that the ADAMS model was reasonably accurate and could be used for design synthesis and iteration of system design variables.

degrees of knee disk rotation and overall exoskeleton stiffness in the range of 9.6±2.4 kN/m. The values of these variables and the resulting design objectives are provided in Tab. 4.2.

The results shown in the previous section on system modeling used these values. Consequently, the forces, deflections, and stresses shown in those figures are correct for the prototype that was fabricated. For the leaf spring, note that the maximum stress did not occur at the final time-step shown in Fig. 4.9; rather, it occurred just beforehand. This is easily seen in Fig. 4.10 where the leaf spring deformation decreases at the end of hip deflection. Physically this occurred because the vertical force from the applied displacement became less effective as the knee disk rotated according to cosine of the angle of rotation. The stress shown in Fig. 4.6 of just the leaf spring shows the true maximum stress for the leaf spring.

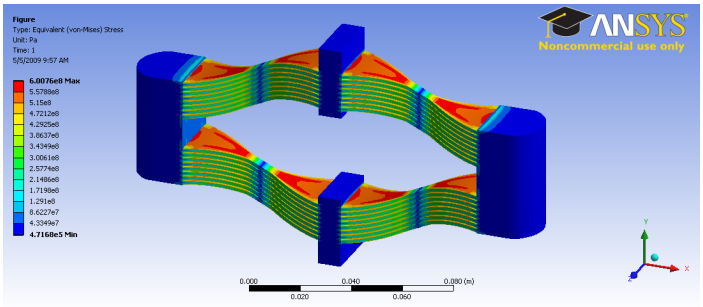

Figure 4.11 Finite element model of carbon composite extension spring for the backpack system. A tapered cross-section was used to evenly distribute stress and minimize mass.

The material used for the leaf spring was carbon composite in an epoxy matrix. Physical testing of this material showed that typical modulus and fracture strength are 35 GPa and 675 MPa respectively (unpublished results of in-house testing). The maximum stress as seen in Fig. 4.9 was 483 MPa, yielding a safety factor of 1.4, which is adequate for this application.

The extension spring was also fabricated from carbon composite sheets. Figure 4.10 above showed that the knee rotation for the ADAMS model underwent a maximum rotation of 30 deg. With the knee disk diameter of 0.053 m, this resulted in a maximum extension spring displacement of 0.029 m and maximum load of 3.32 kN (746 lbf). The purchased pre-fabricated sheets specified a modulus of 45 GPa with a failure stress of 760 MPa. We used closed-form equations to model the tapered cross-section extension spring and verified the results using a nonlinear finite element model (Fig. 4.11). Maximum stress in the failure analysis was 600 MPa, resulting in a safety factor of 1.3.

Table 4.2 Values for design variables of elastic elements. These values were obtained by iterating on their values using the ADAMS system model until the design objectives were satisfied.

Design Variables	Value
Extension spring stiffness (kN/m)	116
Knee disk diameter (m)	0.053
Resulting torsional stiffness (N-m/deg)	5.77
Spline cross-sectional thickness (mm)	7.62
Spline cross-sectional width (mm)	63.5
Design Objectives	**Value**
Knee disk rotation (deg)	29.8
Exoskeleton stiffness (kN/m)	7.3

Backpack Frame

The purpose of the backpack frame was to support the Bowden cable housing at the bottom and the friction-lock and sliding joint at the top. Before knowing the final topology of the frame, we modeled this overall setup quasi-statically in ADAMS as seen in Fig. 4.12. The loads for this simulation were taken from the system model presented in Sec. 4.3.3. The joints in this model were spring-like bushing elements with stiffness approximately matching the physical system. These elastic elements allowed the loads to be shared between redundant joints even though the system was statically indeterminate. The loads on the joints are shown as red vectors. These loads were extracted from the ADAMS model and applied as the loading condition in the ANSYS finite element model of the backpack frame as seen in Fig. 4.13.

The goal for backpack frame design was to minimize mass and maximize stiffness. In order to achieve this we used topology optimization with loads determined from the ADAMS analysis. The resulting design is shown in Fig. 4.13. Because failure due to buckling was a concern in this design, we also performed a buckling analysis. The load multiplier was 2.7 as seen in Fig. 4.13, meaning that if the load were increased by a factor of 2.7 the frame would buckle. We also performed a static failure analysis comparing the yield strength to the von Mises stress for the frame (Fig. 4.13 (b)). The minimum safety factor for this analysis was 2.1, indicating that the frame will yield before it buckles and that the device will not fail under the modeled loads.

All other components of the design were similarly analyzed and refined. For each part the goal was to minimize mass while maintaining safety from failure for the given load. Rather than perform detailed optimizations for each component, designs were refined manually. At this stage it was adequate to keep the weight of the device low and quickly design and build a prototype to test the concept of the exoskeleton. Future work will include further design refinement to truly minimize the system mass.

4.4 Prototype Fabrication & Evaluation

We fabricated a prototype for one leg of the exoskeleton in order to evaluate the design concept. Only one leg of the exoskeleton was fabricated at this point as the design was not entirely finalized. Table 4.3 provides weights for individual segments of the prototype and the total mass as calculated for the future two-leg system. Figures 4.14 and 4.15 show the prototype in approximately the mid-stance and mid-swing positions. The overall function of the prototype was described in Sec. 4.3.2 of this paper.

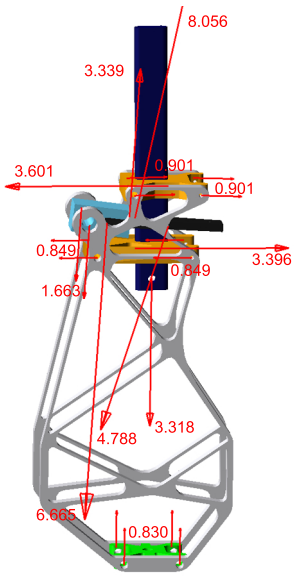

Figure 4.12 Quasi-static forces in backpack system. These forces occur at maximum knee deflection (30 deg) during stance and were used to design the backpack frame. The 3.32 kN force is the applied load from the Bowden cable and spring. The 0.83, 0.85, and 1.66 kN loads are reaction forces on the frame. The 8.06, 3.34, 4.79, and 6.67 kN loads are between components of the friction lock.

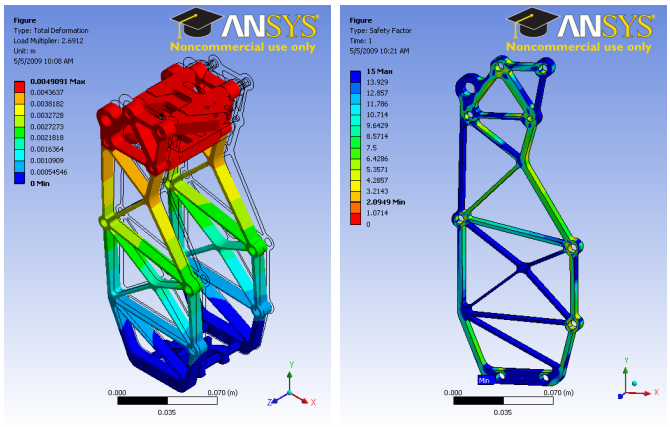

(a) (b)

Figure 4.13 Finite element model of the backpack frame used for failure analysis including (a) buckling and (b) stress analysis. This model was optimized through topology optimization and manual design refinement to minimize the mass while maintaining an adequate safety factor.

4.4.1 Quasi-Static Testing

A variety of preliminary tests were performed using this version of the prototype. First we measured the quasi-static performance of the exoskeleton for comparison with modeled behavior. Figure 4.16 shows the overall stiffness of the exoskeleton. The shallowest curves

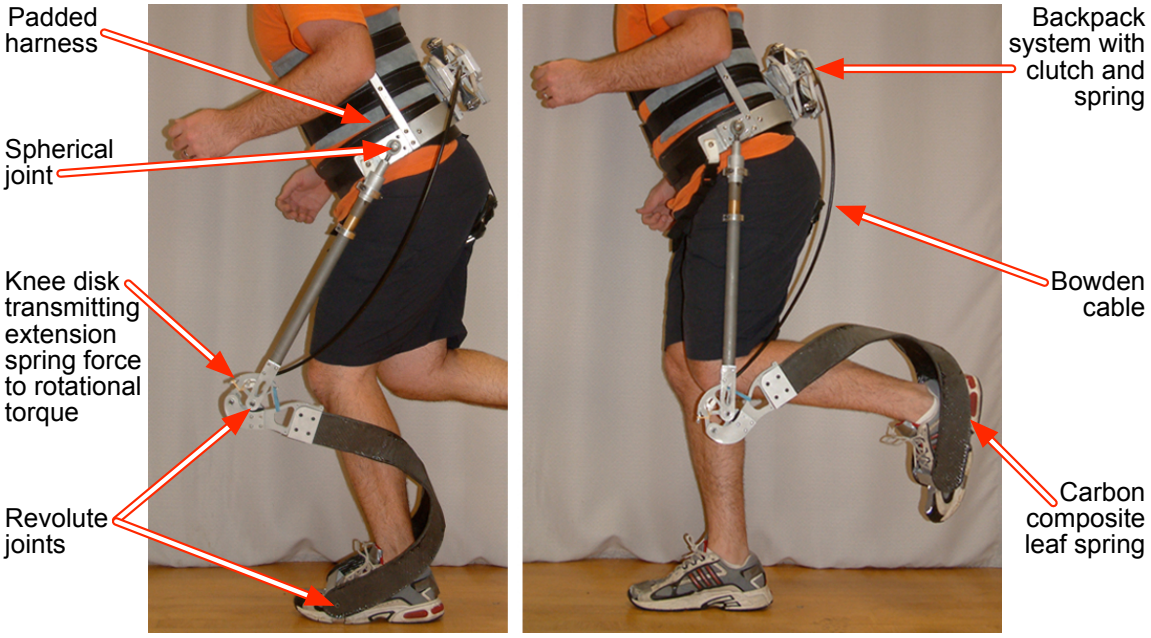

Figure 4.14 Lateral views of the elastic exoskeleton in approximately the (a) mid-stance and (b) mid-swing phases of running.

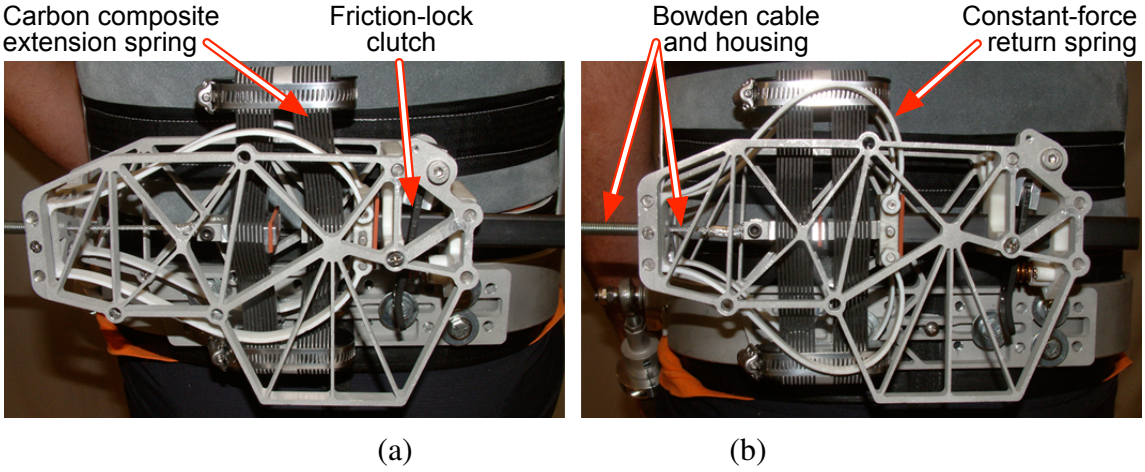

Figure 4.15 Backpack system at (a) mid-stance and (b) mid-swing phases of running. Note how the composite extension spring is deflected at mid-stance while the white plastic return spring is deflected at mid-swing.

(in red) are for the original spring as designed and discussed to this point in the paper. As presented in Tab. 4.4 the actual stiffness of the exoskeleton was much less than predicted. Specifically, the designed stiffness was 7.3 kN/m while the tested stiffness was 3.6 kN/m,

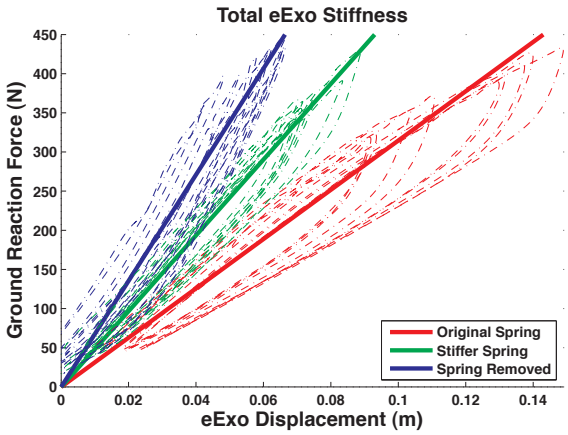

Figure 4.16 Quasi-static force-displacement test results for the exoskeleton. Individual curves for 10 trials are plotted. The mean linear best-fit stiffness for each condition is shown in bold. Tests were done with the original and a stiffer spring in the backpack as well as with the backpack spring removed.

roughly half of the predicted value. This discrepancy was due to the Bowden cable system and is discussed in conjunction with Fig. 4.17.

This testing also quantified the energy lost by the exoskeleton system as it was compressed and extended. An ideal spring loses no energy as it compresses and extends to its original length. The shapes of the curves seen in Fig. 4.16 indicate that there were significant negative work loops, and consequently significant energy loss. When the stiffer spring was used the curves more closely matched the linearized approximation, indicating that the energy loss decreased. When the spring in the backpack was removed entirely the energy loss decreased even further. These results are summarized in Tab. 4.4 along with stiffness values.

The energy loss in and decreased stiffness of the exoskeleton system can be attributed to the Bowden cable. In the quasi-static testing above we saw that as the backpack spring

Table 4.3 Masses for the preliminary prototype and its segments.

Prototype segment	Weight (lbf)	Mass (kg)
Harness	6.8	3.1
Left leg only	5.7	2.6
Backpack system	3.2	1.5
Total for one leg	15.6	7.1
Calculated total for two legs	24.5	11.1

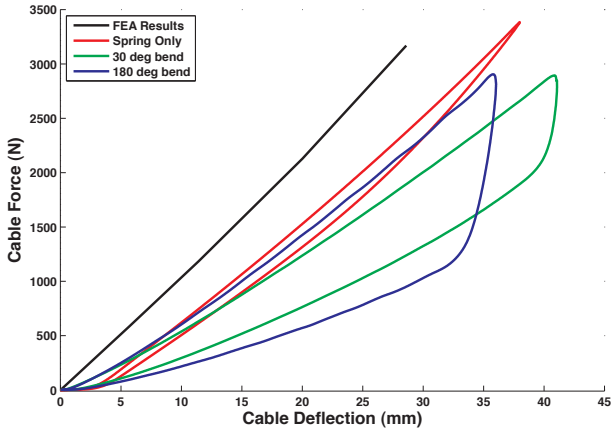

Figure 4.17 Force-deflection results for the backpack spring system. The Bowden cable significantly affects the energy-storage capacity of the backpack system.

Backpack spring	Spring Rate (kN/m)	eExo Stiffness (kN/m)	% Leg Stiffness	Energy Loss (%)
Original	111	3.6	22	29
Stiffer	174	4.8	30	21
Removed	N/A	7.6	47	15

Table 4.4 Experimentally tested exoskeleton stiffness and energy loss for three backpack spring stiffnesses.

stiffness was increased the energy loss decreased. With the stiffness increase came a decrease in cable movement within the housing. Recent research in robotics indicates that Bowden cables are extremely effective at decreasing moving mass but that the friction involved in them can be problematic (see [Schiele 08] and [Veneman 06]), as was the case in our elastic exoskeleton. Figure 4.17 shows the force-deflection behavior of the backpack system tested in isolation on an Instron load frame. When the spring was removed from the backpack and tested by itself, the behavior was fairly close to the FEA results and the energy loss was minimal. However, when the spring was placed in the backpack and the Bowden cable was attached the energy loss went up substantially. This effect became extremely dramatic as the bend in the cable increased (Tab. 4.5). These curves also demonstrate why the exoskeleton stiffness was significantly less than predicted. Although the slopes of the curves on the loading portion are similar to the FEA model, the cable deflection was substantially higher. This meant that for a given exoskeleton knee rotation the transmitted force was significantly less than desired. Essentially this loss of deflection resulted in an apparent decrease in torsion spring stiffness and explains the decreased stiffness of the exoskeleton system.

In order to ameliorate these losses minor modifications were made to the design. First, the stiffer spring was used rather than the original one. Second, a minor change was made to

the cable routing to decrease the total angle through which the Bowden cable was required to bend. As presented in Tab. 4.4 the stiffness for this modified system was 30% leg stiffness for the preliminary subject and the energy loss was 21%.

4.4.2 Control System

The control system for the exoskeleton clutch was very simple. A real-time control system (dSpace, dSPACE Inc., Wixom, MI, USA) received input from an electrogoniometer that measured the hip angle. This signal was filtered and differentiated to yield hip angular velocity. When the sign of the angular velocity changes from positive to negative the control system identified the peak in hip flexion. This event occured just before ($\sim$140 ms for our subject) heel strike. The lag induced by filtering at 6 Hz and the electromechanical delay for engaging the clutch occupy much of this time ($\sim$100 ms in preliminary testing). Consequently the clutch engaged just before heel strike so that the exoskeleton was stiff during the stance phase as it should be. After a fixed time (350 ms) the control signal was sent again. This time delay was chosen so that the actuator attempted to disengage the clutch while the subject was still in the stance phase and the clutch was still under significant load. Because the clutch being used was a friction lock and the actuator was a pneumatic piston that provided a relatively small force, the clutch was not able to release until the system was unloaded. This occurred naturally just before the end of stance phase due to the fact that the toe-hip distance was always shorter at heel-strike than at take-off (see Fig. 4.19). The clutch was released before the end of stance so that the exoskeleton would provide minimal resistance during leg swing. This behavior is summarized in Fig. 4.18.

4.4.3 Exoskeleton Running

The simple control system described in the previous section enabled individuals to run while wearing the exoskeleton. We successfully completed testing of the device on two subjects of

Table 4.5 Backpack system energy loss.

Backpack Setup	Energy Loss Percent (%)
FEA Analysis	0
Spring Only	9
30 deg Bend	34
180 deg Bend	55

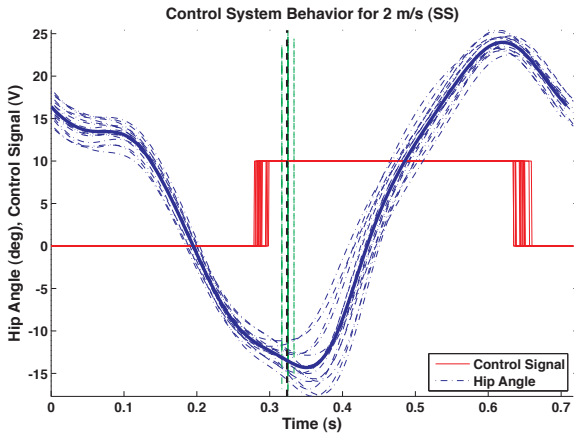

Figure 4.18 Behavior of the control system for the friction lock clutch. Individual curves are shown for 16 strides and the mean is provided in bold lines. Data is plotted from left heel strike to left heel strike. Peak hip flexion was detected using an electrogoniometer at which point the clutch was allowed to engage (control signal drops to zero) such that the exoskeleton was stiff during the stance phase. Before the end of stance (vertical dashed line) the pneumatic cylinder disengaged the clutch to enable leg swing.

similar stature. The results for both subjects were similar so only one set is presented here. The results shown in this section demonstrate the performance and areas for improvement of the elastic exoskeleton. This section is not intended to be an all-inclusive description of human performance while wearing the device. Rather, the focus of this paper is on the design of the device. The human biomechanical results will be presented in a future article. Consequently this section focuses on the high-level description of the exoskeleton's performance while running.

During the stride cycle the exoskeleton successfully modulated from the stiff to the soft behavior. Figure 4.19(a) shows the force in the exoskeleton as a function of the stride cycle (normalized from left heel strike to left heel strike). During the first half of the plot the force in the exoskeleton develops to a maximum mean value of about 700 N. Recall from Fig. 4.3 that the subject's leg typically provided $\sim$2000 N at mid-stance. This means that the exoskeleton provided roughly 35% of the peak force during stance phase. This was slightly higher than our quasi-static testing results indicating that the exoskeleton provides $\sim$30% of the total leg stiffness with the stiffer spring in the backpack.

Figure 4.19(b) shows the length of the exoskeleton while running. At heel-strike the exoskeleton was roughly 1.02 m long and at mid-stance it decreased to roughly 0.97 m, or about 5 cm. At toe-off the length was roughly 1.05 m, significantly longer than the length at heel-strike. The secondary joint at the exoskeleton knee allowed the knee to hyper-extend and enabled this increase in length. This also enabled the backpack spring and Bowden cable

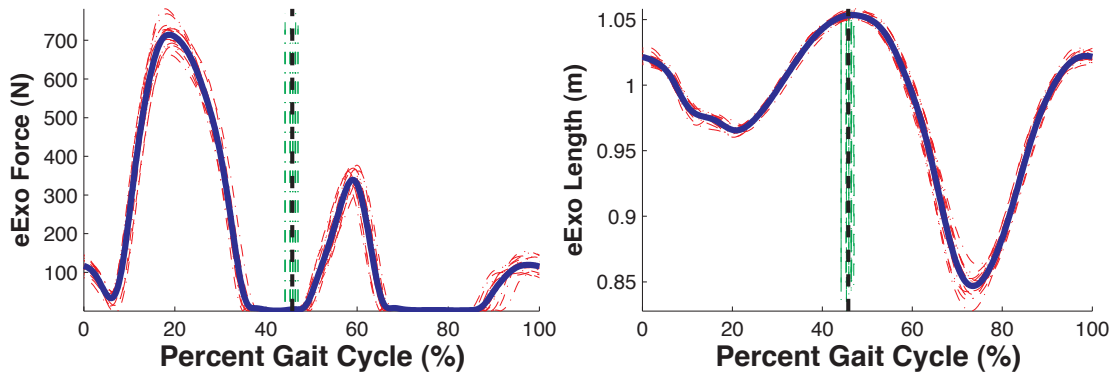

(a) (b)

Figure 4.19 Exoskeleton (a) force and (b) length during the stride cycle. Individual trials are shown for 16 strides and the mean is in bold. The plot begins and ends at left heel-strike; the vertical dashed line represents left toe-off, the end of stance phase.

to become unloaded so that the friction lock could release. During the swing phase, after the vertical dashed line representing toe-off, the exoskeleton length decreased significantly as the knee joint was allowed to bend with relatively small resistance. These lengths are slightly higher than those presented in Fig. 4.2 because the hip attachment point was slightly higher on the waist than assumed in the preliminary design phase.

The resistance provided by the exoskeleton at the beginning of swing phase was the major area for improvement of the device at this point. The resistance will not be zero because some force will always be required to fold up the exoskeleton, or cause it to bend at the knee. Let us refer briefly to this force as the bending force. In this prototype force transmitted at the foot through the shoe provided the bending force. This was quite costly and uncomfortable as the force is applied at the most distal part of the leg. We have since modified the exoskeleton so that a small force is applied on the thigh near the knee via an elastic strap. Applying a bending force proximally decreased the amount of force required and significantly diminished the force peak that occurred just after toe-off. The results of running with the modified system will be presented in a future publication.

This effect was not noticed in the system model because the system was only modeled quasi-statically. Inertial effects of swinging the leg were the major cause of this undesired resistance. When the stance leg swung backwards (hip extension) at the end of stance the exoskeleton thigh segment had a tendency to continue swinging (Newton's 1st Law). The subject's leg started to swing forward for the swing phase but the exoskeleton proceeded backwards towards the kinematic singularity where the hip, knee, and ankle joints were all in a line. As the exoskeleton approached that singularity the force required at the foot to fold

up the exoskeleton leg and swing it forward became quite large. This effect was exacerbated when subjects ran at 3.0 m/s.

The small bump in the force at the end of the swing phase just before heel-strike, on the other hand, is not a concern. We believe this force resulted from the exoskeleton leg and harness readjusting as the leg slowed its forward motion in preparation for ground contact. This force was imperceptible to the subjects and was present even while running with the Bowden cable completely disengaged.

4.5 Conclusion

The aim of this design project was to create an elastic exoskeleton to assist human running. Current exoskeletons are constrained by their need for large amounts of power. This is largely due to the inclusion of large motors and bulky structure on the legs. In contrast, the exoskeleton presented in this report is quasi-passive and has a minimal amount of mass on the legs. It relies solely on material deformation or elasticity to store and release energy during the stance phase of running, providing assistance for human running without the need for complex control systems or heavy actuators and power supplies.

A novel knee joint design was implemented in order to achieve a low-profile design with minimal moving mass. This design allowed an extension spring and clutch to be placed on the back where it was relatively inexpensive metabolically to carry. It also provided a torque and rotation at the knee in order to achieve the desired leg stiffness during stance and to more closely follow the shape of the leg both during stance and swing phases of running. Preliminary results while running with the exoskeleton showed that it successfully provided stiffness during stance phase. However, this version of the prototype suffered from significant resistance at the beginning of swing phase due to inertial effects and a kinematic singularity in the exoskeleton.

Future work will present a refined design in which the force at the beginning of leg swing is ameliorated. A second leg will also be included. We will use this device to study human interaction with an elastic exoskeleton while running. In specific we plan to study the effect of elasticity in parallel with the leg on the metabolic cost of running.

4.6 Acknowledgments

This work was supported in part by the National Science Foundation through grant number BES-0347479. Conceptual design and preliminary modeling was done with the assistance of Brandon Chan, Sean Mitera, Philip Dowhan, and Joe Cho. Youngseok Oh provided

initial guidance with finite element modeling, Anne Manier and Les Wontorcik assisted with fabrication of the harness and leaf spring, and Evelyn Anaka assisted with data collections.

Chapter 5

Neuromechanical Adaptation to Running with an Elastic Exoskeleton

This chapter was written by Michael S. Cherry, Daniel P. Ferris, and Sridhar Kota as a manuscript for publication as a journal article.

5.1 Abstract

Humans bounce along the ground when they hop and run, providing spring-like behavior with their muscles and tendons. Elastic mechanisms could conceivably assist this motion by contributing additional energy storage and return. We developed an elastic lower limb exoskeleton that adds stiffness in parallel with the entire leg [Cherry 09]. The objective of this paper was to determine how humans are affected by the parallel elasticity when they hop and run.

Six subjects ran with and without the exoskeleton at 2.3 m/s. While running in the exoskeleton there was a significant increase in metabolic cost ($P < .0001$). During the swing phase, hip flexor and extensor muscle activation levels also increased ($P < .0001$). Although the exoskeleton was designed to provide 30-50% of leg stiffness, while running, it provided only 23% and 25% of leg stiffness in two configurations. In addition, the exoskeleton supported only 7.0% and 7.2% of the peak vertical ground reaction force. The reasons the exoskeleton developed such low force levels during running were harness compliance and controller function. Our results provide concrete suggestions for improving future designs of exoskeletons for assisting human running.

5.2 Introduction & Background

The broad aim of this research is to develop wearable mechanisms (exoskeletons) for assisting human locomotion, benefitting both the able-bodied and individuals with disabilities. For

example, those who are able-bodied could run farther at the same speed before becoming fatigued with the addition of an exoskeleton. This would be highly beneficial in either military or search and rescue operations where it is critical to traverse large distances quickly and over rough terrain. An exoskeleton that reduces loads required by specific muscle groups in the leg could also benefit individuals with disabilities, such as muscle atrophy in the lower limb, restoring their locomotive ability. For example, an individual with an atrophied quadriceps muscle group could use an elastic exoskeleton to provide a knee extension (straightening) torque while walking and running, decreasing the demands on existing muscles and enabling locomotion at higher speeds and with greater comfort. Decreasing loads at specific joints in the lower limb may prove beneficial for individuals suffering from osteoarthritis. A leg exoskeleton capable of sustaining a portion of an individual's body weight would decrease the bone on bone forces at the joints and decrease pain while enabling locomotive ability. In this sense the elastic exoskeleton could take on the role of a body-weight support system that does not need to be used in a laboratory environment. Typical body-weight support systems are large, bulky and not suitable for daily use. Development of a lightweight low-profile wearable exoskeleton that supports a significant portion of body weight could be used for locomotion rehabilitation in the wearer's home and natural surroundings.

5.2.1 Literature Review

The most well-publicized exoskeletons in mass media are complicated and energy-intensive wearable robots [Kazerooni 07, Kawamoto 05, Jacobsen 04]. These robots are designed to augment human capability through active mechanical power generation (e.g. electric motors and hydraulic cylinders). In general, they do not make use of elastic components to store and release energy during locomotion. In contrast, humans make excellent use of elastic energy storage and return during both human walking and running [Farley 98a, Sawicki 09, Alexander 90].

Only a handful of devices have been designed to incorporate elasticity, decreasing the demands on actuators while enabling simpler designs. One method for including elasticity is through series elastic actuators. The RoboWalker [Pratt 04b] and the powered exoskeleton developed by Low et al. [Low 06] use this method. Walsh et al. developed an alternate method of incorporating elasticity [Walsh 06] in which elastic elements were placed at the hip and ankle joints in an exoskeleton designed to carry heavy loads. A variable-damper was used at the knee in this design, resulting in small but significant power-consumption by the device. Carr and Newman implemented the same variable damper in a leaf-spring-based elastic leg exoskeleton to model and understand locomotion by astronauts in space suits

[Carr 08]. Banala developed an entirely passive elastic exoskeleton [Banala 06] based on principles of gravity balancing [Herder 01]. Dollar and Herr designed a quasi-passive knee exoskeleton for use while running but have only published results from bench tests thus far [Dollar 08a]. Grabowski and Herr also designed a quasi-passive exoskeleton for use while running that extends from modified shoes to a waist harness [Grabowski 09]. This device has only been tested while hopping but is the most similar to the exoskeleton presented in this paper. A more complete review of exoskeletons and orthoses for assisting human locomotion can be found in [Dollar 08b].

5.2.2 Summary

The objective of the research presented in this paper was to evaluate an elastic exoskeleton for assisting human running. The design of this exoskeleton was presented previously in [Cherry 09]. A redesigned shank spring is included in this paper in order to eliminate attachment at the medial surface of the shoes. This was done to enable running safely with a narrow stance width. The stiffness of the new system decreased significantly while mass properties remained practically unchanged. The exoskeleton presented in this paper depends solely upon material elasticity to store and release energy during locomotion while supporting the weight of the user. The only energy required to operate the device is used for controlling a friction-lock clutch. This clutch enables switching between stiff and compliant states for the stance and swing phases of running, respectively. The design also aims to be a low-profile exoskeleton, matching the motion of the legs without encumbering their mobility.

5.3 Methods

5.3.1 Subjects

Six healthy subjects participated in this study [6 men, 0 women; age 23 yr (SD 4.1), mass 80 kg (SD 6.1), height 1.8 m (SD 0.02)]. Due to the difficulty of the task only trained runners were recruited. Subjects were sought who could comfortably wear the shoes that were built into the exoskeleton and were within the exoskeleton's range of height adjustability. The University of Michigan Institutional Review Board granted approval for this project and all participants gave informed, written consent.

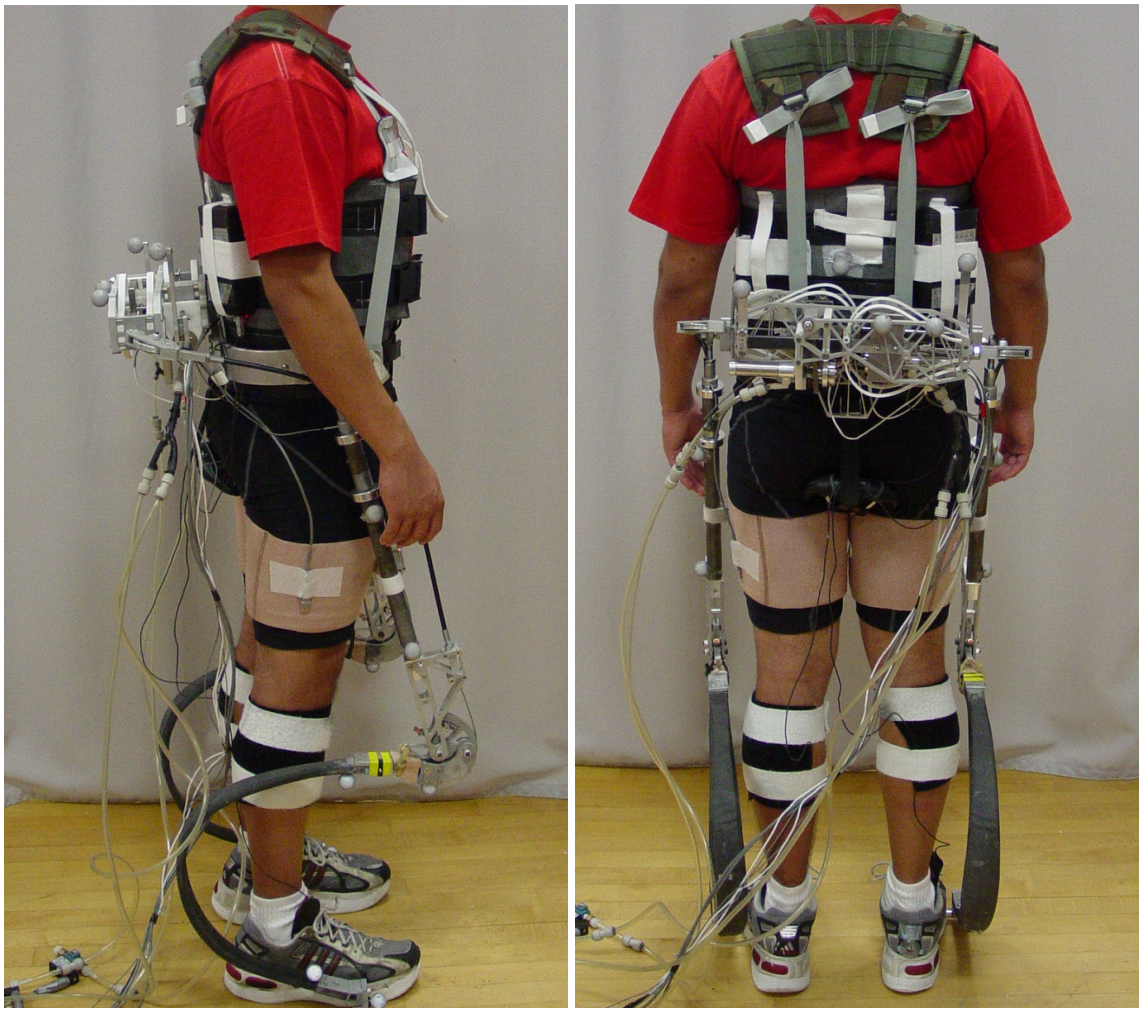

Figure 5.1 Photographs of the elastic exoskeleton (eExo).

5.3.2 General procedure

Subjects ran on a force plate-mounted treadmill at 2.3 m/s for 7 minutes in four conditions. The first condition was normal running in which no exoskeleton was used (NE). In the other three conditions subjects wore the exoskeleton shown in Figures 5.1 and 5.2. The design and construction of this exoskeleton was described in [Cherry 09] and Chapter 4 of this dissertation. In one of these conditions the exoskeleton was disengaged (Dis) such that the exoskeleton would provide minimal stiffness but would be primarily dead weight. In the other two conditions the exoskeleton was engaged such that the exoskeleton would provide stiffness during the stance phase of running but would provide minimal resistance during swing phase. The backpack system was modified between these two trials in order to provide different stiffness levels of the exoskeleton. In the softer of the two configurations a spring was used in the backpack system (Eng_Spr) such that the exoskeleton knee joint

behaved as a torsional spring during stance. In the stiffer of the two configurations the spring was removed from the backpack (Eng_NoS) and replaced with a rigid bracket.

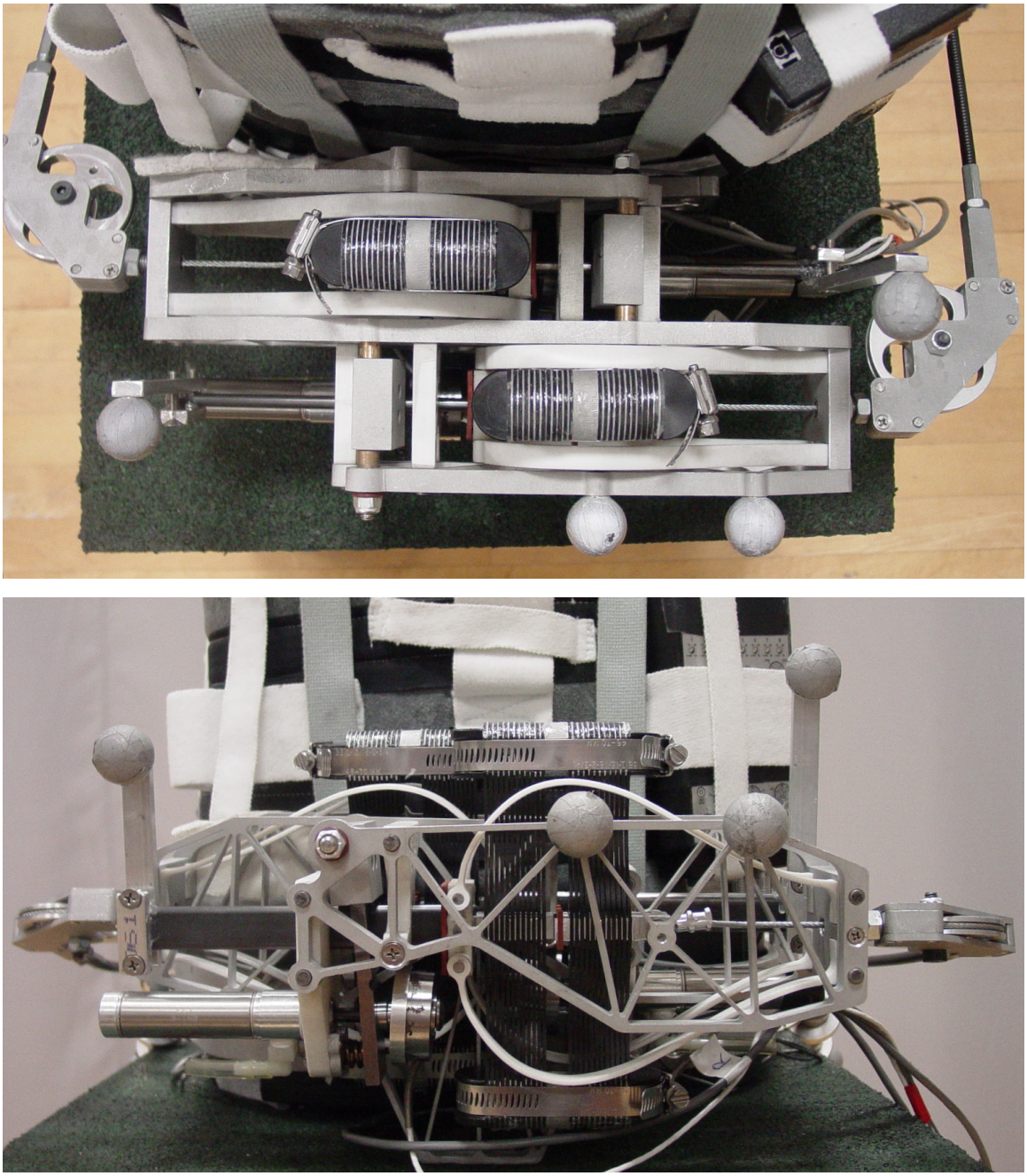

Figure 5.2 Photographs of the eExo backpack system.

We performed force-deflection testing of the isolated exoskeleton in order to determine the nominal stiffness values in the two configurations. This was done by placing the shoe from an individual eExo leg on the ground and bouncing up and down on the eExo harness. Motion of the eExo was recorded during these trials and used to determine the deflection

of the exoskeleton leg as well as the composite shank spring. Knowing the stiffness of the shank spring we calculated the force in the spring and then used that force to calculate the ground reaction force. The two stiffness levels tested had mean values of 2.2 kN/m and 5.4 kN/m which were effectively 18% and 44% of the mean leg stiffness measured while running with no exoskeleton (see Figure 5.3). Due to the methods used in calculating this stiffness, the values are approximate. Future testing could be done using a force-plate to measure the ground reaction force directly rather than use the shank spring to calculate its value. However, this is not necessary because we measured the stiffness of the exoskeleton while running using the shank spring deflection as discussed here. These stiffness values are presented in Section 5.4.1.

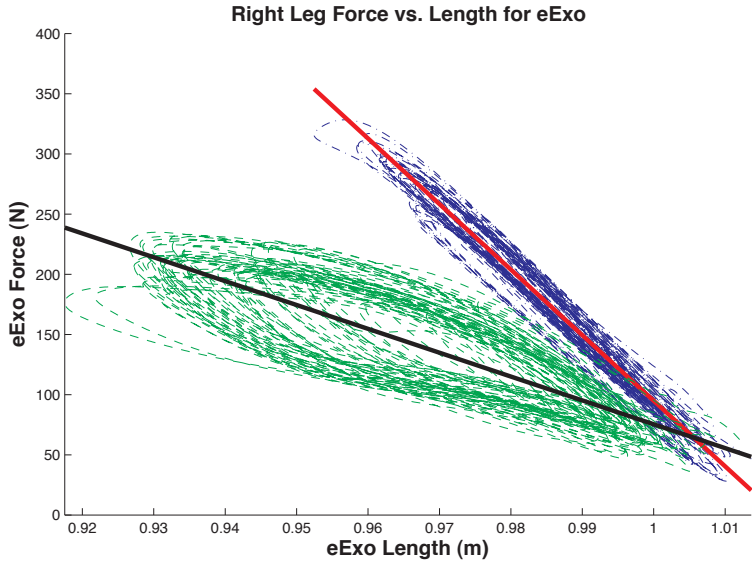

Figure 5.3 Isolated eExo force-deflection test results.

Subjects were allowed to choose their own stride frequency and stride width while running. Subjects were not given instruction on how they should use the device. They were, however, given time to practice running in the exoskeleton. Subjects ran in the exoskeleton on two separate days. On the first day, the exoskeleton was sized to fit the individual subject. Subjects then ran for at least 7 minutes in each of two conditions, with the exoskeleton engaged and disengaged. During this time the exoskeleton controller timing was tuned to the individual subject. This tuning consisted primarily of setting the time delay between peak hip flexion (which occurs just before heel strike) and when the exoskeleton clutch is engaged so that the elastic exoskeleton will be stiff during stance phase. On the second day, subjects ran in all four conditions as described previously. At least 3 minutes of rest was provided between all trials and additional rest was provided if desired.

5.3.3 The Elastic Exoskeleton

The exoskeleton used for this study was constructed primarily from carbon composite, machined aluminum, and steel tubing. This exoskeleton attached to the subjects at a waist harness and custom-modified running shoes. The exoskeleton hip joint provided full range of motion in all three axes (spherical joint). The exoskeleton ankle joint provided motion in only one axis (revolute joint). The length of the thigh segment was made such that it was adjustable for individuals with varying leg lengths. Due to this as well as an adjustable waist harness the same exoskeleton was used for all subjects with only minor modification needed. Additionally, we designed the exoskeleton knee joint such that the backpack spring would engage at a set angle of exoskeleton knee joint rotation. This angle was set in the standing position for each subject so that the exoskeleton would provide the desired stiffness when the exoskeleton length became shorter than the subjects' standing leg length. When the leg was more extended than this, the knee joint allowed extension with minimal restoring force from a secondary spring constructed of surgical tubing [Cherry 09]. The orthosis mass was 11.1 kg in all three exoskeleton conditions.

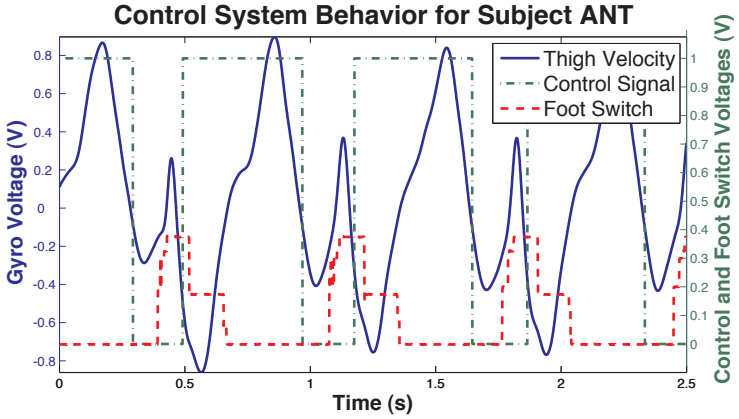

Figure 5.4 Control system behavior for subject ANT. The solid line represents the voltage from the gyro measuring thigh angular velocity. Positive values represent motion from extension to flexion (anterior direction). Peak hip extension occurs at the zero-crossing from positive to negative values. The dash-dot line represents the control signal. When this signal has a value of 1 the pneumatic cylinder is applying pressure to the friction lock which disengages the clutch when the exoskeleton leg is not under load. When the value is 0 there is no air pressure and the clutch is engaged. The dashed line represents foot switch voltage. Non-zero values indicate the stance phase of running.

We controlled the exoskeleton using a real-time control system (Control Desk, dSpace Inc., Wixom, MI, USA). For each leg the inputs to the controller were thigh angular velocity and a foot contact switch. The output was a control signal to a pneumatic cylinder that engaged and disengaged the backpack system clutch for that leg. We used the angular velocity signal to detect the point of peak hip flexion before ground contact. After a subject-

specific time delay the control signal was sent to engage the clutch such that the exoskeleton would be stiff during the stance phase of running. The foot switch detected the point at which the foot actually struck the ground and the duration of the stance phase. Due to the behavior of the friction-lock clutch, sending a control signal to disengage the clutch during stance would only release the clutch when it was no longer under load. Consequently we sent the control signal during the middle of stance phase as determined by the foot-switch signal. By doing this the clutch would disengage automatically as soon as the energy stored during leg compression was released. This always occurred before toe-off because humans consistently have a longer length between their toes and hips at heel-strike than at take-off (see [Muybridge 55] and Figure 4.2). The control system behavior for one subject running in the exoskeleton is shown in Figure 5.4.

5.3.4 Data collection

Segment and joint kinematics were collected using an eight-camera motion analysis system (120 Hz, Motion Analysis, Santa Rosa, CA). Reflective markers were placed on the left and right foot, shank, thigh, ankle, knee and hip as well as the torso. We collected ground reaction forces using a custom-built force plate-mounted treadmill [Collins 09] rigidly attached to concrete sub-flooring. We also independently measured the thigh angular velocities using MEMS gyros (1.2 kHz, STMicroelectronics, Geneva, Switzerland) for use in the controller as described previously.

We collected muscle activation (electromyography, or EMG) levels for eight major lower limb muscles on each leg: tibialis anterior, soleus, medial gastrocnemius, lateral gastrocnemius, vastus medialis, vastus lateralis, rectus femoris, and medial hamstrings (1.2 kHz, Konigsberg Instruments, Pasadena, CA). We prepared subjects' legs by shaving and cleaning with alcohol before attaching bipolar surface electrodes (interelectrode distance: 3.5 cm). We taped electrodes and wires to the skin and then applied pre-wrap to hold wires in place, reducing movement artifact in the EMG data. We also visually examined each electrode for noise and cross-talk before data collection.

We measured oxygen consumption and carbon dioxide production using a metabolic analysis system (Max-II, AEI Technologies, Naperville, IL, USA). Before each collection the metabolic system was calibrated using known gas mixtures and a 3-L syringe. We included minutes 3.5 to 6.5 in the average for each subject in each condition. The first three minutes were used to allow the subjects to reach steady state energy consumption. The last minute or so was discarded due to a delay between breath expiration and breath analysis. Metabolic cost (W) was calculated using the standard equation from Brockway

[Brockway 87]. We calculated net metabolic power by subtracting the metabolic rate while standing from the metabolic rate for each trial. Standing trials were performed at the beginning and end of the data collection for each subject. Data was not normalized in any way in order to allow for comparison with similar studies (e.g. [Grabowski 09]).

5.3.5 Data analysis

We used commercial software (Visual3D, C-Motion, Rockville, MD) for data filtering and inverse dynamics calculations. We filtered motion data with a low-pass zero-lag fourth-order Butterworth filter (cutoff frequency: 6 Hz). We filtered force plate data similarly but with a 10 Hz cutoff frequency. We calculated internal muscle moments about the lower limb joints using the kinematic marker and force plate data. Inertial properties of the limbs were estimated based on anthropometric measurements. Foot and pelvis mass and inertia were modified in the three exoskeleton conditions to account for the exoskeleton whose mass properties were known. Because the exoskeleton did not attach rigidly to the shank and thigh we did not modify their mass and inertial properties.

5.3.6 Electromyography

We filtered the electromyography data using a high-pass zero-lag fourth-order Butterworth filter (cutoff frequency: 40 Hz) to attenuate movement artifacts and then performed full wave rectification. We used this data to calculate root-mean-squared (RMS) muscle activation levels during both the stance and swing phases of each stride in order to compare muscle activation levels across conditions. We also created linear envelopes of the EMG data for the entire hop cycle (ground contact (GC) to ground contact) by low-pass filtering (cutoff frequency: 10 Hz) the high-pass filtered and rectified EMG data. The RMS data were normalized by the mean value for each muscle on each subject in the NE condition. The linear envelopes for each subject were averaged for all strides in each condition and then normalized by the maximum value of the resulting linear envelope from the NE condition. These average curves were then averaged for all subjects in order to evaluate the overall effects of the different conditions.

5.3.7 Joint angle definitions

All joints were defined in the sagittal plane. Ankle angle was defined as the complement to the angle between the shank and foot segments (angle increases with dorsiflexion). Knee angle was defined as the complement to the internal angle between the shank and thigh

segments (angle increases with knee flexion). Hip angle was defined as the complement to the internal angle between the thigh and pelvis (angle increases with hip flexion).

5.3.8 Stiffness calculations

Using commercial software (Matlab, The MathWorks, Natick, MA) we calculated leg stiffness as the linear least squares fit of the vertical ground reaction force verses center of mass displacement, excluding data points whose force was below five percent of the maximum force during that stride. The center of mass displacement was found by dividing the vertical ground reaction force by the subject's mass, then integrating twice [Cavagna 75]. The first integration constant was found by assuming that the mean center of mass velocity over one stride cycle was zero. The second integration constant was assumed to be zero since we are not interested in the absolute position of the center of mass but only the relative displacement over time. This process is demonstrated in Figure 5.5(a). Additionally, in order to double check that the center of mass displacements we calculated were reasonable, we plotted the calculated center of mass motion with the sacral marker motion as seen in Figure 5.5(b).

Similarly, we calculated stiffness at the knee and ankle joints by finding the linear least squares fit of the internal moments with respect to their rotation (Figure 5.6). Again we excluded data points whose moments were less than five percent of the maximum so as to obtain the linear behavior of each joint after the initial impact of ground contact has occurred. No stiffness values were calculated for the hip joint as it was not spring-like during the stance phase of running.

5.3.9 Exoskeleton forces

Forces in the exoskeleton legs were measured from the elastic segments in the shank section of the exoskeleton. Reflective markers were placed on the exoskeleton in order to measure the motion of the exoskeleton and compression of the shank spring while running. The stiffness of the shank springs were determined using finite element analysis and quasi-static force-deflection testing. Using the measured stiffness and deflection data we calculated the approximate forces applied by the exoskeleton to the waist harness. An angle correction factor was used to account for the difference in angle between the shank section and the overall leg of the exoskeleton.

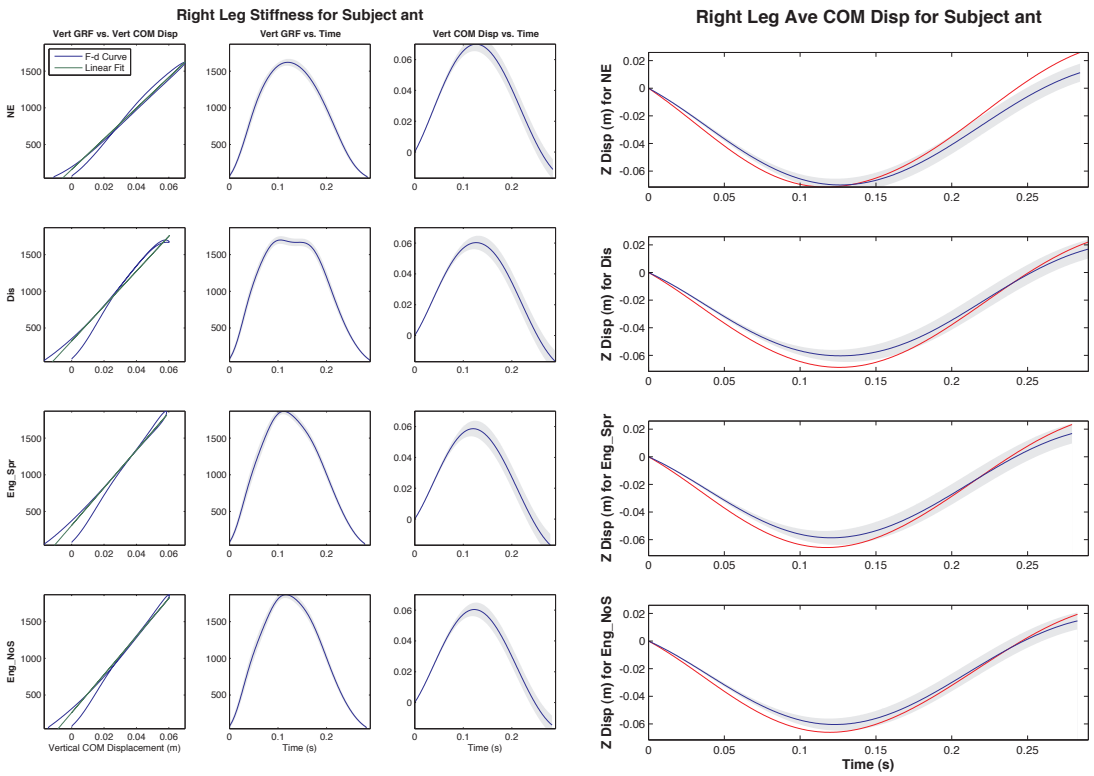

(a) (b)

Figure 5.5 Leg stiffness and center of mass displacement during stance phase of running. (a) Leg stiffness is calculated using the least squares linear fit of the vertical ground reaction force versus the center of mass displacement. The gray area represents the standard deviation of all trials at each point in the stance phase. (b) Center of mass displacement was verified by plotting it with the sacral marker's vertical motion versus time. The red solid line represents the average sacral deflection while the blue line with gray area surrounding it represent the average vertical center-of-mass deflection and its standard deviation.

5.3.10 Statistical analyses

We used a two-way ANOVA (subject, exoskeleton condition) to determine significant differences in kinematic, kinetic, and electromyographic data between the four conditions tested ($P < 0.05$ as significance level). Because our focus was on the effect between the exoskeleton conditions we did not analyze differences related to inter-subject variability (subject was treated as a random effect). Significant differences were detected using a post-hoc Tukey's Honestly Significant Difference (HSD) test. All statistical analyses were performed with the JMP software (Version 4, SAS Institute, Cary, NC).

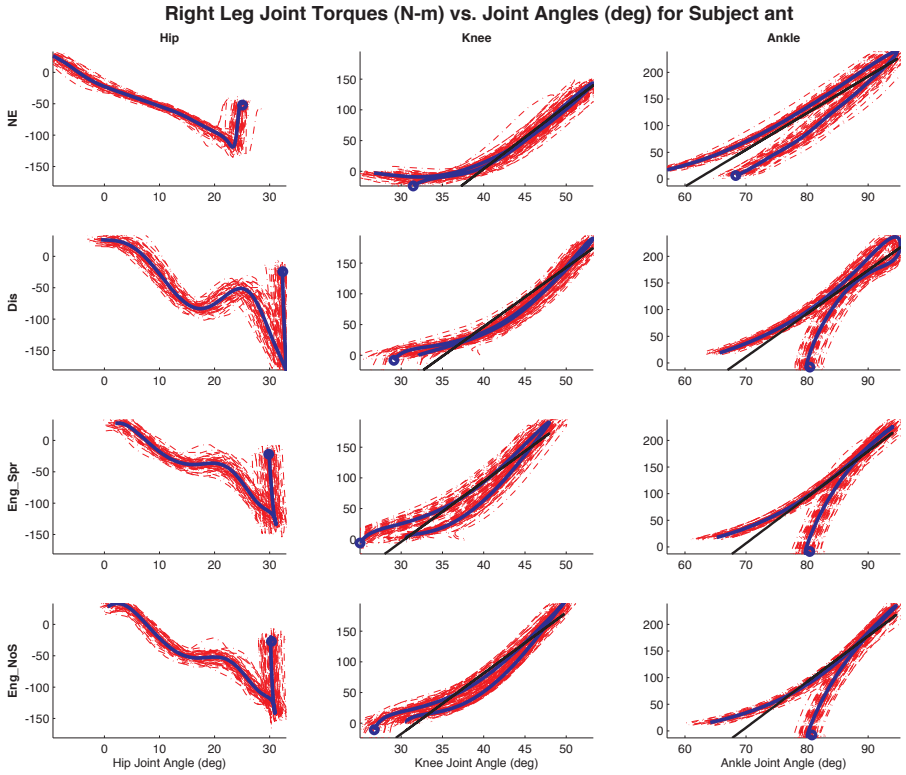

Figure 5.6 Stiffnesses for each joint were calculated from the linear least squares fit of the joint moment versus joint angle for each stride. Data shown here is the average for all strides on an individual subject. The curves begin at heel strike (denoted by the blue circles) and proceed to toe-off.

5.4 Results & Discussion of Results

5.4.1 Exoskeleton Performance

Although the exoskeleton was designed to provide 30-50% of the wearer's leg stiffness, the stiffness and forces provided by the exoskeleton were drastically less than this. Figure 5.7 shows the forces in the exoskeleton legs for an individual subject. Note that the right and left legs are quite symmetric, providing roughly the same forces. Also note that in the disengaged (Dis) condition the exoskeleton provides roughly 75 N peak force even though the clutch is entirely disengaged and providing negligible resistance to rotation at the exoskeleton knee joint. This is due to the passive effects of the design. Essentially the exoskeleton is a two-link mechanism with a revolute joint connecting them. As these two links become closer to in-line with each other the reaction force sustained when attempting to compress the exoskeleton increases. Because the shank section is a spring, the force in the system when attempting to compress the leg is oscillatory.

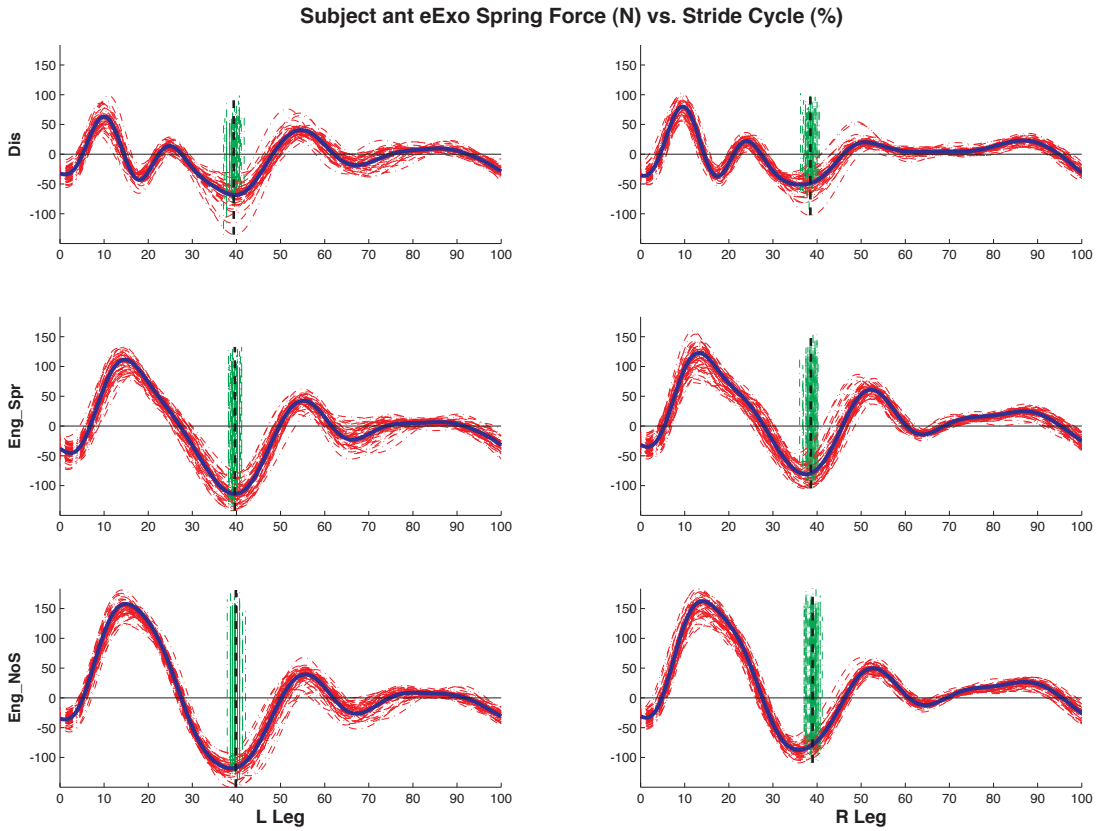

Figure 5.7 Force provided by the exoskeleton for an individual subject in all three exoskeleton conditions. Dashed lines represent individual trials and solid lines represent the average values. Vertical lines represent take-off and plots start and begin at ground contact. Plots are provided for both legs.

In the Eng_Spr and Eng_NoS conditions the force provided by the exoskeleton during stance phase increases noticeably, but not as much as expected. Peak ground reaction forces are on the order of 2000 N while in the stiffest condition (Eng_NoS) the exoskeleton force is about 150 N, or roughly 7% of the force in the human leg (see Tables 5.1 and 5.2). This low level of force will be discussed later but is believed to be a result of control timing and movement of the waist harness relative to the subject.

It should also be noted that at takeoff in the Dis condition, the resistive force is near 50 N. We believe this baseline resistance of roughly 50 N is a result of the secondary joint at the knee of the exoskeleton. As discussed earlier, the secondary knee joint enables extension of the leg beyond the standing leg length. An elastic band was used as a return spring to guarantee that the secondary joint returned to the original configuration rather than allowing the two-link leg to traverse through the change-point when the hip, knee, and ankle joints line up. If this were to happen the exoskeleton leg would no longer be able to provide stiffness during stance and the shank spring would contact the ground and become unsafe.

Consequently this elastic band is necessary to ensure safe function of the exoskeleton but causes undesired resistance to extension of the leg at toe-off.

In the two Eng trials the resistive force at toe-off is closer to 100 N. Recall that the exoskeleton force is calculated using the deflection of the shank spring. With this in mind we suspect that a portion of the resistive force is due to the rebound of the spring which occurs in late stance during the Eng conditions but near mid-stance in the Dis condition.

The exoskeleton length is shown in Figure 5.8 for the same individual subject as the force plot in Figure 5.7. Note that the length at ground contact was significantly shorter than at toe-off as discussed. During swing phase the distance from foot to hip attachments (exoskeleton leg length) was significantly shorter than during stance. This behavior mirrored the human leg length during running as desired.

Table 5.1 Average leg stiffness and force values for all subjects. Peak exoskeleton forces are also included, showing that the exoskeleton provided 7% of the peak vertical ground reaction force in both the Eng_Spr and Eng_NoS conditions. Values are shown as Mean (Standard Deviation) where appropriate.

Condition	NE	Dis	Eng_Spr	Eng_NoS
Total Leg Stiffness (kN/m)				
Left	12.4(0.96)	14.0(1.67)	15.4(1.74)	16.0(2.27)
Right	12.4(0.69)	14.6(1.66)	15.7(1.83)	16.3(2.42)
Average	12.4	14.3	15.6	16.1
Peak Vertical Ground Reaction Force (kN)				
Left	1.7(0.09)	1.8(0.09)	1.9(0.10)	1.9(0.10)
Right	1.7(0.09)	1.8(0.07)	1.9(0.06)	1.9(0.06)
Average	1.7	1.8	1.9	1.9

Eng_Spr	Eng_NoS
Peak Exoskeleton Force (N)	
134(60)	139(76)
128(52)	135(60)
131	137
Percent Peak Ground Force (%)	
7.1%	7.3%
6.9%	7.1%
7.0%	7.2%

Table 5.2 Exoskeleton leg stiffness values including percent total leg stiffness. The exoskeleton stiffness was roughly 25% of subjects' leg stiffness when running without the exoskeleton (NE condition). Despite this, the forces provided by the exoskeleton were drastically less (see Table 5.1). This discrepancy was the result of harness movement on the subjects.

Condition	Eng_Spr	Eng_NoS
Exoskeleton Leg Stiffness (kN/m)		
Left	2.9(1.60)	3.1(1.91)
Right	2.8(1.29)	3.1(1.51)
Average	2.9	3.1
Percent NE Leg Stiffness (%)		
Left	23.6%	25.0%
Right	22.4%	24.8%
Average	23.0%	24.9%
Percent Eng Leg Stiffness (%)		
Left	19.0%	19.5%
Right	17.7%	18.9%
Average	18.4%	19.2%

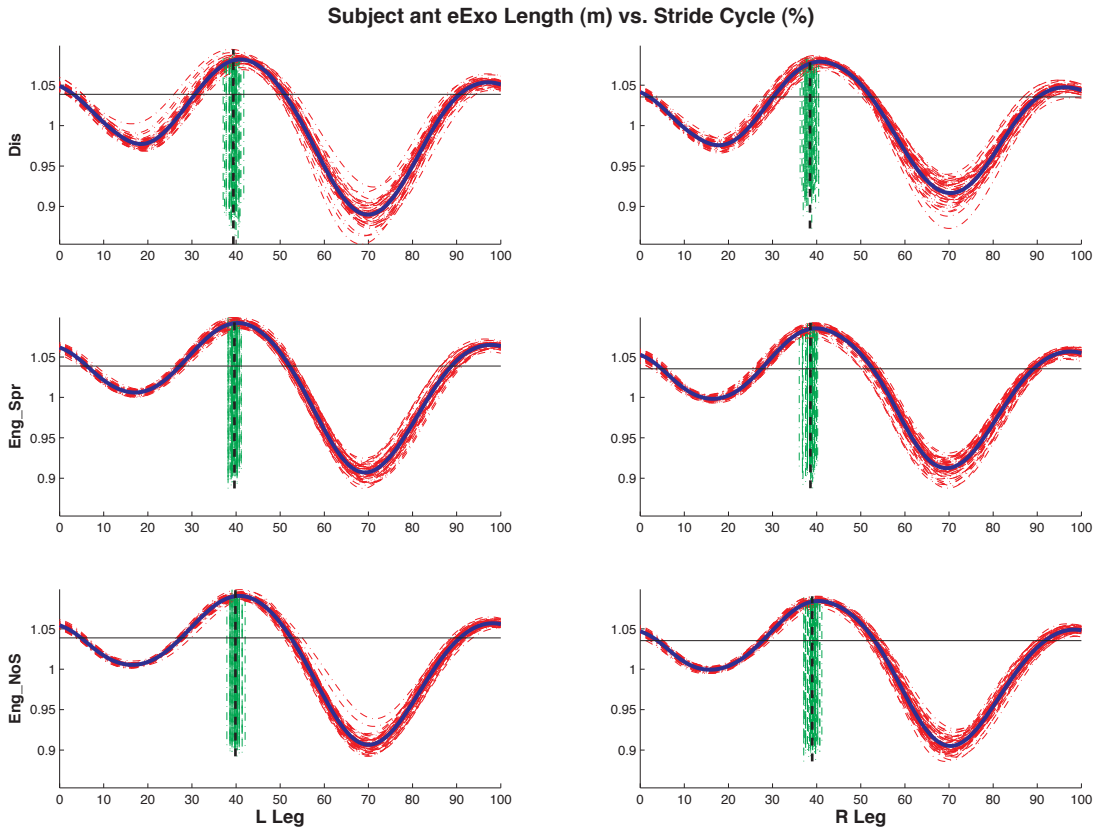

Figure 5.8 Exoskeleton length from hip to foot attachments for an individual subject in all three exoskeleton conditions. Dashed lines represent individual trials and the solid lines represent the average values. Vertical lines represent take-off and plots start and begin at ground contact. Plots are provided for both legs.

5.4.2 Stiffness Values

Ankle stiffness increased significantly in all three exoskeleton conditions when compared to normal running ($P < .0001$). Additionally, ankle stiffness was significantly lower in the Dis condition than in the Eng conditions ($P < .0001$). There was no significant difference in ankle stiffness between the two Eng conditions. No significant differences were detected in knee stiffness, even though the mean knee stiffness is higher when wearing the eExo. Total vertical stiffness and leg stiffness increased significantly for all exoskeleton conditions ($P < .0001$). These results may be explained by the increase in mass while wearing the exoskeleton. As shown in Figure 5.5(a) the vertical ground reaction forces increased when wearing the exoskeleton. There was also a slight decrease in center of mass displacement, probably due to the stiffness provided by the exoskeleton. As shown in Figure 5.6 the increased knee stiffness was primarily a result of increased torque at the knee joint rather than decreased range of motion. This increased torque was the result of increased ground

reaction forces with the added weight of the exoskeleton. The increased ankle stiffness may have been the result of a more pronounced heel strike when running with the exoskeleton.

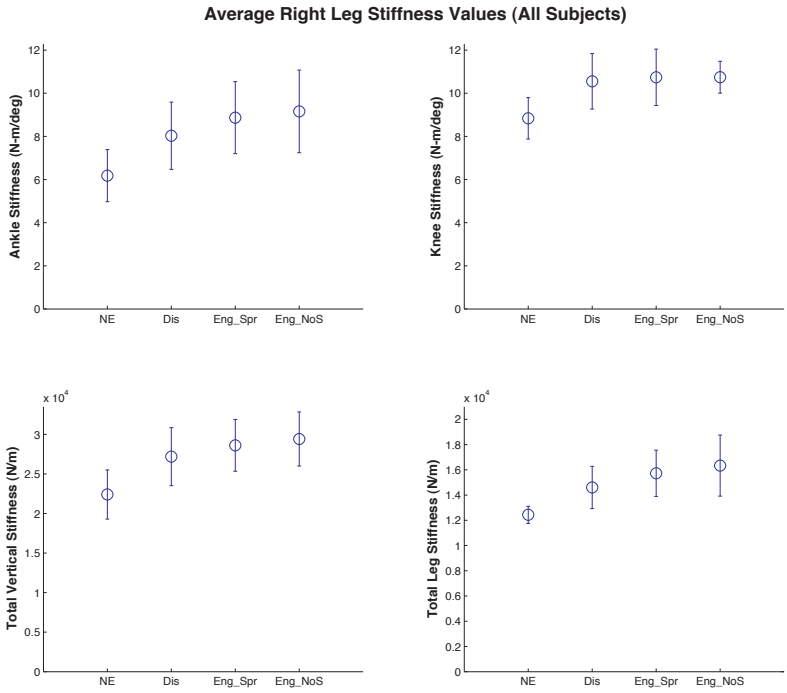

Figure 5.9 Stiffness values for the ankle and knee joints as well as the total vertical and leg stiffnesses.

The stiffness values for all conditions, averaged across all subjects is shown in Figure 5.9. The error bars in this plot are the standard deviation of the average stiffness values between subjects. No measure of within-subject variability is included in this plot. The variability within an individual subject can be seen in Figure 5.6 from the torque vs. rotation curves for each individual stride. It can also be seen in the leg stiffness data (Figure 5.5(a)) where the gray area represents the standard deviation of all trials for a given condition.

5.4.3 Muscle Activation Levels

Figure 5.10 shows the average EMG activation levels for all six subjects. RMS EMG activation levels for stance and swing are provided in Table 5.3. During the stance phase (initial portion of the plot) we see that there is a slight decrease (10-20%) in Vastus Medialis and Vastus Lateralis muscle activation levels as desired. This is most likely due to the stiffness provided by the exoskeleton to support the weight of the subject. The decrease is small and not statistically significant, corresponding to the small amount of force provided by the exoskeleton. It is expected that when more assistance is provided by the exoskeleton the decrease in VM and VL activation levels during stance will be more pronounced. During

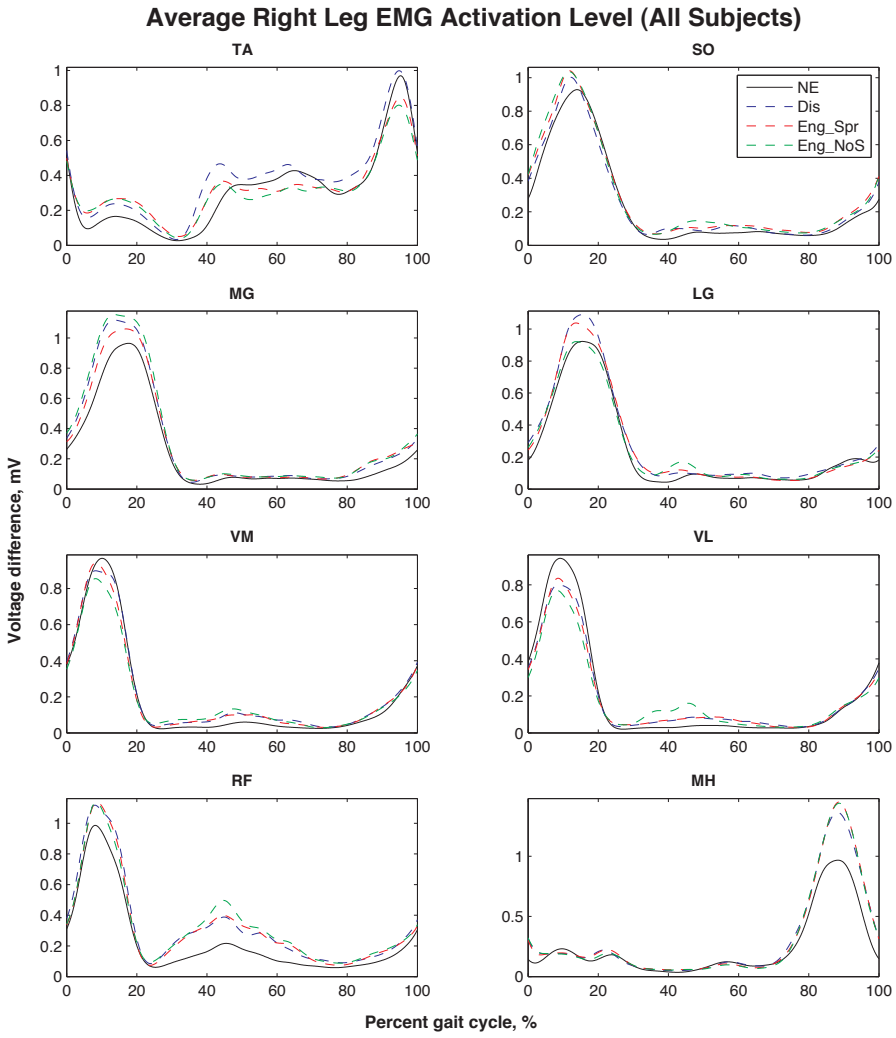

Figure 5.10 Muscle activation levels for eight superficial muscles on the right leg. Curves shown represent the averaged curves for all subjects. RTA—Right tibialis anterior, RSO—Right soleus, RMG—Right medial gastrocnemius, RLG—Right lateral gastrocnemius, RVM—Right vastus medialis, RVL—Right vastus lateralis, RRF—Right rectus femoris, RMH—Right medial hamstrings

Table 5.3 Summarized values for RMS EMG data, Mean(Standard Deviation). Data is normalized to mean RMS EMG for each muscle in the NE condition. ANOVA P values determined model significance for individual measures. Tukey's HSD test was used to determine significant differences between conditions. Asterisks in the Dis, Eng_Spr and Eng_NoS columns indicate values significantly different than NE condition at an alpha level of 0.05. No significant differences were detected between the Dis, Eng_Spr, and Eng_NoS conditions. L—Left leg, R—Right leg, TA—Tibialis anterior, SO—Soleus, MG—Medial gastrocnemius, LG—Lateral gastrocnemius, VM—Vastus medialis, VL—Vastus lateralis, RF—Rectus femoris, MH—Medial hamstrings.

Condition	Dis	Eng_Spr	Eng_NoS	ANOVA *P* Value
RMS EMG Amplitudes during Stance, Mean(SD)				
LTA, mV/mV	1.07(0.239)	1.16(0.312)	0.99(0.330)	0.584
LSO, mV/mV	0.93(0.186)	0.97(0.321)	0.88(0.312)	0.635
LMG, mV/mV	1.04(0.074)	1.06(0.112)	1.07(0.119)	0.346
LLG, mV/mV	1.11(0.495)	1.13(0.431)	1.10(0.498)	0.948
LVM, mV/mV	0.92(0.293)	0.92(0.308)	0.80(0.171)	0.076
LVL, mV/mV	1.02(0.052)	0.97(0.216)	0.85(0.197)	0.17
LRF, mV/mV	1.25(0.110)*	1.22(0.128)*	1.12(0.113)	0.002*
LMH, mV/mV	1.31(0.596)	1.56(0.953)	1.58(1.121)	0.162
RTA, mV/mV	1.49(0.715)	1.45(0.612)	1.43(0.586)	0.585
RSO, mV/mV	1.02(0.141)	1.08(0.165)	1.10(0.156)	0.183
RMG, mV/mV	1.18(0.267)	1.12(0.190)	1.23(0.285)	0.146
RLG, mV/mV	1.13(0.398)	1.09(0.206)	0.99(0.437)	0.553
RVM, mV/mV	0.97(0.250)	0.95(0.253)	0.87(0.267)	0.31
RVL, mV/mV	0.87(0.146)	0.85(0.178)	0.79(0.325)	0.065
RRF, mV/mV	1.22(0.138)*	1.19(0.117)*	1.18(0.116)*	<0.001*
RMH, mV/mV	1.34(0.886)	1.34(0.826)	1.29(0.729)	0.635
RMS EMG Amplitudes during Swing, Mean(SD)				
LTA, mV/mV	0.80(0.247)	0.78(0.117)	0.70(0.283)*	0.017*
LSO, mV/mV	0.95(0.355)	0.98(0.410)	0.91(0.395)	0.798
LMG, mV/mV	1.47(0.510)	1.63(0.503)*	1.68(0.590)*	0.004*
LLG, mV/mV	1.34(0.537)	1.58(0.732)	1.34(0.453)	0.076
LVM, mV/mV	1.06(0.274)	1.18(0.322)	1.30(0.700)	0.637
LVL, mV/mV	1.03(0.142)	1.08(0.284)	1.01(0.218)	0.835
LRF, mV/mV	1.32(0.249)*	1.52(0.356)*	1.46(0.316)*	<0.001*
LMH, mV/mV	1.31(0.137)*	1.36(0.175)*	1.32(0.181)*	<0.001*
RTA, mV/mV	1.13(0.697)	0.95(0.510)	0.90(0.491)	0.463
RSO, mV/mV	1.40(0.629)	1.62(0.730)*	1.59(0.623)	0.033*
RMG, mV/mV	1.54(0.548)	1.66(0.452)*	1.74(0.598)*	0.006*
RLG, mV/mV	1.21(0.432)	1.12(0.348)	1.20(0.371)	0.586
RVM, mV/mV	1.24(0.456)	1.14(0.294)	1.14(0.377)	0.559
RVL, mV/mV	1.09(0.220)	1.06(0.267)	1.11(0.361)	0.994
RRF, mV/mV	1.79(0.632)*	1.93(0.714)*	2.10(0.629)*	<0.001*
RMH, mV/mV	1.38(0.337)*	1.41(0.242)*	1.40(0.231)*	<0.001*

the stance phase there are increases in Medial and Lateral Gastrocnemius (MG and LG) muscle activation levels as well as for the Soleus (SO), Tibialis Anterior (TA), and Rectus Femoris (RF). Of these increases only RF is statistically significant for both legs. We suspect that increases in RF activation could have been used to stabilize the hip joint while the exoskeleton applied a vertical force laterally to the subject's torso.

During swing phase the hip flexors and extensors (RF and MH respectively) for both legs are significantly lower in the NE condition than all of the exoskeleton conditions. This is most likely a result of having to swing extra weight on the legs. Adding over 2 kg of exoskeleton mass to each leg substantially increases the effort required to swing the legs. Additional effort is also required to overcome the resistive force provided by the exoskeleton as discussed in Section 5.4.1. We expect that future efforts to decrease the mass of the exoskeleton, especially the mass that moves with the legs, will decrease the additional cost required to swing the legs while running.

5.4.4 Metabolic Cost

Metabolic cost increased significantly in all three exoskeleton conditions relative to the NE condition ($P < .001$). There were, however, no differences detected between exoskeleton conditions according to the Tukey's HSD test. This large increase in metabolic cost correlates well with the increases in hip flexor and extensor activation levels during the swing phase. The lack of decrease in metabolic cost in the engaged conditions relative to the disengaged condition is also not surprising given the small amount of force provided by the exoskeleton while running. Results for individual subjects and averaged values for all subjects are provided in Table 5.4.

Table 5.4 Metabolic cost for each subject and averaged data for all subjects. Two-way ANOVA model was significant with a P value $< .001$ for the Condition effect. Tukey's HSD test was used to determine significant differences between conditions. Superscripted numerals indicate NE significantly different than [1]—Dis, [2]—Eng_Spr, [3]—Eng_NoS. No significant differences were found between the three exoskeleton conditions.

Condition	NE	Dis	Eng_Spr	Eng_NoS
Net metabolic power consumption for each subject				
ANT	654	1014	1077	1052
APC	827	1296	1368	1424
CSG	686	1222	1291	1316
EBM	848	1245	1310	1292
EKJ	894	1187	1190	1233
OMT	735	1041	1066	1067
Mean (W)	774[1,2,3]	1168	1217	1231
SD (W)	96	114	127	146
% Change	N/A	50.8%	57.2%	59.0%

5.4.5 Stride Width

Another possible explanation for the increase in metabolic cost in the exoskeleton conditions is increased stride width. Although with the current designs subjects were not required to run with a wider stride width subjects consistently chose to do so ($P < .001$, Figure 5.11). In walking, increased stance width requires increased metabolic cost [Donelan 01] and could explain a portion of the increased metabolic cost in our study.

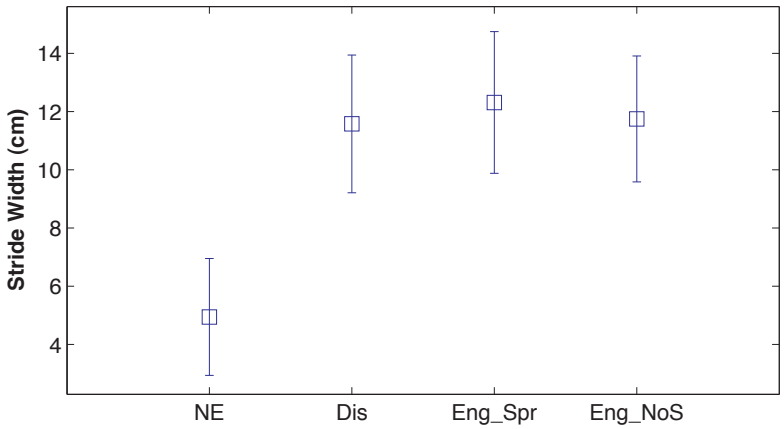

Figure 5.11 Stride width for an individual subject. Stride width increased significantly when subjects ran while wearing the exoskeleton ($P < .001$) but was not significantly different between exoskeleton conditions.

5.5 Follow-up Studies

5.5.1 Varied Stride Width

Because of the increased stride width used while running in the exoskeleton a post-testing pilot study was performed in which five subjects [5 men, 0 women; age 23 yr (SD 4.7), mass 78 kg (SD 8.2), height 1.8 m (SD 0.03)] ran with no exoskeleton but with varied stance width while we measured metabolic cost. Stance width was enforced by instructing subjects to run with their heels in line with a laser line. Live video from a camera placed posterior to the subject was streamed to a monitor in front of the subject. This allowed subjects to self-evaluate and correct in order to run at the desired widths. A picture of this setup is shown in Figure 5.12. No attempt was made at evaluating the subjects' desired stride width; rather, set values were chosen to encompass the range of stride widths used in the exoskeleton study. The actual widths as measured by the medio-lateral location of the heel markers at ground contact are shown in Table 5.5 along with the associated metabolic costs.

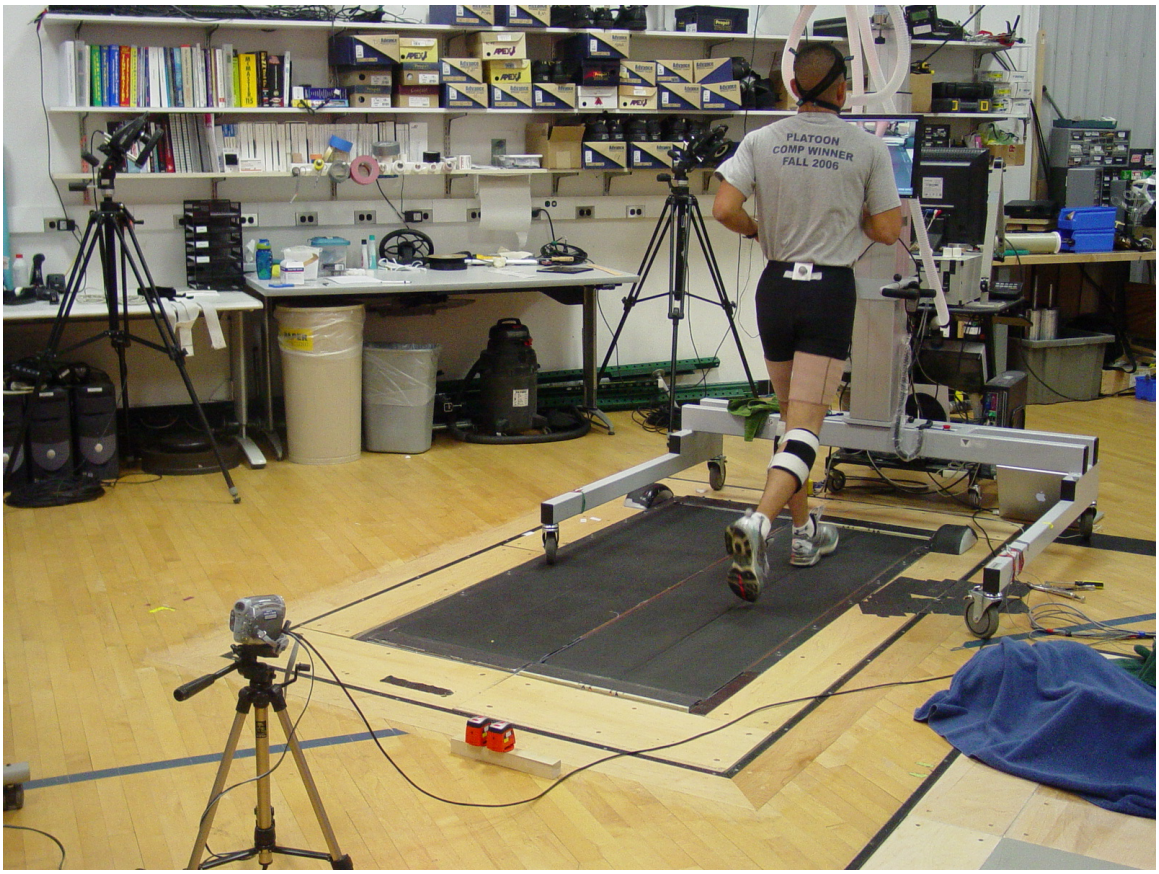

Figure 5.12 Setup for follow-up pilot study to determine the metabolic cost change due to running with an increased stride width. Laser level lines were projected onto the posterior of the subject and a video camera streamed a live image to a monitor placed in front of the subject.

Although the stride width increased significantly between all three running width conditions ($P < .0001$), the metabolic cost changes were not significant ($P = .090$). The stride widths chosen by subjects in this study are in the same range as the stride widths chosen in the exoskeleton study. As a result, we concluded that the increases in metabolic cost observed while subjects ran with the exoskeleton are not a direct consequence of the increased stride width chosen. We acknowledge that only five subjects were used and that with more subjects included in the study our results may become significant. However, even if significant the effect would still not be meaningful. Practically doubling the stride width only resulted in a 3% increase in metabolic cost.

5.5.2 Exoskeleton Hopping

In response to data recently published by Grabowski and Herr [Grabowski 09] we also performed a pilot study with subjects hopping while wearing the exoskeleton (Exo condition)

and while hopping normally (no exoskeleton, NE condition). Rather than sweep a variety of hop frequencies and test multiple exoskeletons over the course of multiple days, we chose to have subjects hop with the exoskeleton in the stiffest (Eng_NoS) condition at 2.2 Hz. Hop frequency was enforced with a digital metronome. Because we only tested one frequency we were able to have subjects hop with and without the exoskeleton on the same day.

Subjects [4 men, 0 women; age 23 yr (SD 5.4), mass 80 kg (SD 8.6), height 1.8 m (SD 0.03)] were instructed to hop for five minutes on both legs and that their feet needed to leave the ground between each hop. Oxygen consumption and carbon dioxide expiration were measured as previously, as were ground reaction forces and the motion of the exoskeleton. Unlike running, the exoskeleton knee joint was locked in place for this pilot study. For each subject the length of the exoskeleton was set such that it would provide assistance from the moment their toes hit the ground while hopping. This experimental setup is shown in Figure 5.13.

The exoskeleton provided significantly higher forces in this hopping study than in running. This was partly due to the adjustment of the exoskeleton such that it would engage at maximum leg length rather than at the leg length while standing. We were able to do this while hopping and not while running because when hopping we were able to lock the knee in place throughout the trial. When running the clutch in the backpack was required to engage and release with each stride in order to allow free motion during the swing phase. Additionally, when running it was necessary to avoid the change point where the hip, knee, and ankle joints line up because it makes the exoskeleton very stiff at the beginning of swing

Table 5.5 Stride width and metabolic cost for each subject and averaged data for all subjects. While the stride width was significantly different between conditions ($P < .0001$) there were no significant differences in net metabolic power ($P = .090$).

Condition	Narrow	Medium	Wide
Stride Width (cm)			
HCM	7.53	11.19	14.11
ESC	6.85	8.38	10.1
ELD	4.34	6.49	9.85
ES2	5.58	6.32	9.66
CSW	6.4	9.19	14.13
Mean (cm)	6.1	8.3	11.6
SD (cm)	1.23	2.02	2.33
% Change	N/A	35.4%	88.4%
Metabolic Power Consumption (W)			
HCM	804	814	829
ESC	847	838	826
ELD	718	759	780
ES2	771	782	791
CSW	723	738	766
Mean (W)	773	786	798
SD (W)	55	40	28
% Change	N/A	1.8%	3.3%

Figure 5.13 Setup for follow-up pilot study to determine the metabolic cost of two-legged hopping with and without the exoskeleton, similar to [Grabowski 09].

phase. With hopping there is no swing phase and consequently we were able to utilize this increased stiffness and lock the exoskeleton knee joint in an orientation near the change point. As a result, the exoskeleton was much stiffer in this pilot study than in running. The average stiffness of each leg of the exoskeleton was about 7 kN/m. The combined stiffness of the exoskeleton legs was 14 kN/m, or two-thirds of the total leg stiffness when hopping in the Exo condition (see Table 5.6 (b) and (c)).

Total leg stiffness was calculated from the ground reaction forces measured by the force-measuring treadmill. The force in the vertical direction was divided by the subject mass and then twice integrated to define the center of mass displacement. This was done according to the method presented in Section 5.3.8. Again the center of mass displacement was compared to the z-displacement of a marker on the subject's torso in order to validate

that our method was working properly. As seen in Table 5.6 (b) the total leg stiffness increased significantly when hopping in the Exo condition. Although this is in contrast to the results of Grabowski and Herr [Grabowski 09] the percent change is small and consistent with the results presented in Chapter 3 of this document.

Table 5.6 Tabulated data for hopping with (Exo) and without (NE) the exoskeleton. (a) Metabolic cost of hopping. Three of the four subjects did have small decreases in metabolic cost but no significant difference in metabolic cost was achieved. (b) Total leg stiffness. Stiffness increased significantly when hopping in the exoskeleton ($P < .05$). (c) Stiffness of the exoskeleton. The combined stiffness of both legs of the exoskeleton was 14.1 kN/m. This was 68% of total leg stiffness while hopping in the exoskeleton, or 73% of leg stiffness while hopping with no exoskeleton.

Condition	NE	Exo	% Change
Metabolic Power Consumption (W)			
HCM	668	625	-6.44%
ESC	769	757	-1.56%
ELD	639	592	-7.36%
ES2	633	733	15.80%
Mean (W)	677	677	0.11%
SD (W)	63.0	80.5	10.76%

(a)

NE	Exo	% Change
Total Leg Stiffness (kN/m)		
17.9	19.8	10.61%
22.9	24.0	4.80%
17.9	19.1	6.70%
18.0	20.3	12.78%
19.2	20.8	8.72%*
2.48	2.19	3.63%

(b)

Left Leg	Right Leg	Combined
Exoskeleton Leg Stiffness (kN/m)		
6.9	6.9	13.8
7.2	6.7	13.9
7.3	7.0	14.3
7.3	7.1	14.4
7.2	6.9	14.10
0.19	0.17	0.29

(c)

Metabolic cost was measured in an identical fashion to that of Section 5.3.4 with one exception. Instead of running for 7 minutes, subjects only hopped for 5 minutes. This was done to match the procedures of Grabowski and Herr [Grabowski 09]. We calculated the metabolic rate for each subject by averaging oxygen consumption and carbon dioxide expiration for minutes 2.5 to 4.5 as did they. Unlike their study, our metabolic cost did not decrease significantly. Three of the four subjects tested had small decreases in metabolic cost, but the fourth subject had a significant increase, resulting in an average increase in metabolic cost by 0.1%.

Discussion

There are a number of factors that could be the cause for the discrepancy between our results and those published by Grabowski and Herr [Grabowski 09]. First, our exoskeleton had a different stiffness value. When hopping at 2.2 Hz their stiffest exoskeleton was roughly 87% of leg stiffness while hopping with no exoskeleton. They stated that their softer exoskeleton was roughly half that stiffness, or about 44% of leg stiffness. Our exoskeleton was 73% of leg stiffness while hopping at 2.2 Hz with no exoskeleton. Their exoskeleton was 13.6 kN/m on average while ours was 14.1 kN/m as stated previously. This puts our exoskeleton in the correct range of stiffness values from a percentage standpoint, but with a higher absolute stiffness. In their paper they stated that the exoskeleton is harder to control when

the stiffness is large [Grabowski 09]. This could explain the inconsistency of our results for metabolic power consumption.

Second, the harness used on our exoskeleton is much different than the one they used. They incorporated a stunt harness into a large aluminum frame whereas we incorporated a bike seat and chest harness into a lower-profile aluminum waist band. Quite possibly their harness holds the aluminum frame more firmly to the pelvis and as a result is more comfortable. Although the bike seat does an excellent job at maintaining correct positioning of the waist band vertically on the subject, the waist band does not fit as firmly to the subject as desired and allows shifting of the waist harness on the subject. The chest harness is also not as effective as we would like. Specifically, when the chest harness is tightened such that it does not move on the subject the subjects are not able to breath freely. As a result the chest harness is never fully tightened and also allows substantial movement of the waist band on the subject. This is particularly problematic when running with the exoskeleton, but may have been an issue while hopping as well.

Third, Grabowski and Herr stated that their exoskeleton mass was approximately 10% of their subjects' mass, or roughly 7.2 kg as calculated from their mean subject mass of 71.6 kg. Our exoskeleton on the other hand had a mass of 11.1 kg, an increase of about 54%. Hopping with the additional weight almost surely increases the metabolic cost even though this weight is supported by the exoskeleton itself.

These differences suggest two significant areas for improvement of the exoskeleton. Specifically, the quality and comfort of the harness attaching the exoskeleton to the subject needs to be improved and the weight of the exoskeleton needs to be decreased. It may also be worth testing the exoskeleton again with the exoskeleton knee slightly more bent. This would decrease the stiffness of the exoskeleton without requiring any major modifications. With these changes we suspect that we would also achieve the 12-28% decrease in metabolic cost observed by Grabowski and Herr at 2.2 Hz.

5.6 Conclusions & Future Work

This paper presented the results obtained for running and hopping with an elastic exoskeleton. Although the device did not work as well as expected, valuable insight was gained from this study into how future devices can be designed to further improve performance of the exoskeleton. The comfort and quality of fit of the waist harness is critical to the success of the exoskeleton and merits additional attention and modification. As expected, further decreases in the weight of the exoskeleton are also expected to improve performance.

5.7 Acknowledgments

This work was supported in part by the National Science Foundation through grant number BES-0347479. Youngseok Oh, Kevin Lapprich, Brandon Chan, Sean Mitera, Philip Dowhan, and Joe Cho assisted with design and fabrication of the exoskeleton. Anne Manier and Les Wontorcik assisted with fabrication of the harness and leaf spring. Alberto Alfaro, Evelyn Anaka, Cara Lewis, Amy Sipp and Monica Majcher assisted with data collections.

Chapter 6

Conclusion

6.1 Summary & Contributions

The human leg behaves in a spring-like manner when hopping and running and has been shown to adapt remarkably fast to interactions with springy surfaces and orthoses [Farley 98b, Ferris 97, Ferris 98, Ferris 99, Ferris 06]. When hopping and running on elastic surfaces, humans modify their leg stiffness so that the overall surface-leg stiffness remains constant. When hopping with an elastic ankle orthosis, humans decrease ankle joint stiffness to compensate for the stiffness added in parallel to the joint. This is accomplished primarily through decreases in ankle plantar-flexor muscle activation levels. These results suggest that humans could similarly adapt to elastic exoskeletons and reduce the metabolic cost of locomotion, specifically the energy required for running and hopping. The work presented in this dissertation discussed two elastic exoskeletons to further understand human adaptation to spring-like devices. It also advances the field of human locomotion assistance towards developing a device that decreases the metabolic cost of human running.

Chapters 2 and 3 presented the design and evaluation of an elastic knee-ankle-foot orthosis (eKAFO) that assisted human hopping on one leg. The eKAFO provided about 30% knee stiffness during hopping, while allowing subjects to freely extend their knee beyond the spring set point, the initial uncompressed length of the spring. This enabled the brace to provide consistent stiffness during stance without preventing leg extension beyond the length at ground contact, or the time at which the foot hits the ground. Allowing subjects to extend their legs freely while providing the desired stiffness once the knee was flexed by the desired amount made the eKAFO both comfortable and effective. At both fixed and subject-chosen hop frequencies subjects decreased quadriceps muscle activations significantly. This suggested that an elastic exoskeleton that provides stiffness in parallel with the knee joint could be effective at reducing metabolic cost while running. Metabolic cost was not measured in this experiment due to the difficulty of sustaining one-legged hopping for a long enough time to measure a steady-state metabolic rate. In future work

with this device, time to fatigue could be measured as a corollary to metabolic cost. Subjects would be asked to hop on one leg with and without the eKAFO spring being attached and the times would be compared. Based on the decreased muscle activation levels in hopping with the spring engaged, we suspect that subjects would hop longer in that condition.

After completing the study involving the eKAFO, we decided to pursue an exoskeleton design that was in parallel with the entire leg rather than modify the eKAFO into a device for running. This was done for a variety of reasons. First, when running, knee stiffness is the primary determinant of overall leg stiffness [Arampatzis 99]. Augmenting the entire leg with parallel stiffness should allow subjects to decrease knee stiffness as a result. Second, in the eKAFO study the effects of soft tissue deformation at the posterior thigh were significant. Much of the energy that could be stored in the knee brace was lost due to this soft tissue deformation. In running the knee typically does not bend more than 25-30° [Arampatzis 99]. Typical leg deflections however are on the order of 10-15 cm [Farley 96, Ferris 99] and include effects from both knee flexion and ankle dorsiflexion in the first half of stance. As a result, pursuing parallel leg elasticity would allow the soft tissue deformation to have a lesser effect than parallel knee elasticity, while allowing the same potential benefits.

Chapters 4 and 5 presented the design and evaluation of the elastic exoskeleton (eExo) used in human running. This bilateral device extended from a waist harness down to custom-modified shoes with an elastic strap at the thigh. There were no rigid attachments to the shank or thigh so as not to constrain the motion of the wearer. When humans run, their legs behave in a remarkably spring-like manner during the stance phase when the foot is on the ground. Providing this spring-like function to support body-weight is viewed as the primary determinant in the metabolic cost of running[Kram 90, Farley 92]. We hypothesized that providing stiffness in parallel with the leg using the eExo would enable subjects to decrease their leg stiffness while running which would result in decreased metabolic cost for running.

The basic function of the eExo was to be stiff during the stance phase of running but provided relatively little resistance during the swing phase. This was accomplished by means of a friction-lock clutch mounted on the wearer's back. This clutch held and released a cable that was routed over a cam at the exoskeleton knee. When the cable was held taut the exoskeleton was stiff and the exoskeleton provided stiffness in parallel with the leg. When the cable was released, the knee joint could bend freely and the exoskeleton provided minimal resistance. If the exoskeleton were to remain stiff during the swing phase subjects would not be able to maintain foot clearance and they would trip and fall.

The exoskeleton was designed to provide two stiffness levels, 30% and 50% leg stiffness, in two exoskeleton conditions. The first prototype constructed (Chapter 4) provided the desired stiffness (4.8 and 7.6 kN/m). The second prototype used for running provided

significantly less stiffness when tested in isolation (2.2 and 5.4 kN/m). In a follow-up two-legged hopping test, this same exoskeleton provided 7 kN/m from each leg, combining to provide 14.1 kN/m, or 68% of total leg stiffness when hopping at 2.2 Hz with the exoskeleton. When hopping on two legs the total leg stiffness for both legs is roughly equivalent to leg stiffness while hopping on one leg. Consequently, with a practically identical exoskeleton leg stiffness, the percentage of total leg stiffness goes up dramatically. These test results demonstrate that the exoskeleton was capable of providing the desired stiffness and should be effective for assisting human running.

While running, however, the exoskeleton only provided 18% and 19% of total leg stiffness and 7.0% and 7.2% of maximum vertical ground reaction force in the Eng_Spr and Eng_NoS conditions. The decrease in force developed when running was primarily due to motion of the waist harness on the wearer. The decrease in stiffness was primarily due to controller behavior. Specifically, the motion of the waist harness did not allow the exoskeleton to compress as much as expected during stance. The controller problem refers to the fact that force did not begin to develop in the exoskeleton until a few tens of milliseconds after heel-strike, further decreasing the ability of the exoskeleton to store and release energy during stance. As a result, the exoskeleton provided minimal assistance while running and there was no decrease in metabolic cost. Rather, metabolic cost increased by 50-60% and hip flexor and extensor muscle activation levels increased significantly during swing phase. Although contrary to our hypothesized results and desired outcome, these results demonstrate the difficulty of implementing an exoskeleton that assists human running. It also provides guidance on future efforts in exoskeleton development.

6.2 Future Work

The comfort and firmness of exoskeleton waist harness fit is critical to the success of assisting human running. The design presented in this dissertation included a bike seat for maintaining consistent vertical positioning of the exoskeleton, a rigid aluminum waist band, and a chest harness which minimized rotation of the brace on the subjects. Rotation of the brace on the subject refers specifically to vertical motion of the lateral aspects of the brace, or up-and-down movement of the exoskeleton hip joints. The waist and chest harness also attempted to prevent rotation of the harness around the subjects, or about a vertical axis through the middle of their torso. This harness was adjustable for various subjects but custom-built for one individual originally. In addition, in order to allow subjects to breathe unconstrained the chest harness couldn't be tightened. The aluminum bands up the side of the chest harness provided resistance to rotation of the brace on the subjects, but because

the chest straps remained loose it did not secure the chest section as desired. It is suggested that to compensate for this the waist section be improved significantly in its fit. If the waist harness could be made to be more comfortable, perhaps it could be tightened further which would prevent the harness from rotating around the body and minimize rotation on the body as well.

A number of options exist to improve the performance of the controller and its timing. The most recent version of the exoskeleton incorporated a MEMS gyro for measuring thigh angular velocity. When the thigh angle reached maximum flexion just before heel strike, the angular velocity switched from positive to negative. This zero crossing was detected by the exoskeleton control system at which point the control signal was sent to engage the clutch in preparation for stance. Even though there was typically a 120 ms time span between peak hip flexion and heel strike for subjects, the exoskeleton was not able to begin developing force at heel strike. Delays in the system were a time delay from a low-pass filter on the gyro angular velocity, an electrical delay in sending the control signal across the room to the control valves, a pneumatic delay for developing adequate pressure in the pneumatic cylinder, and a mechanical delay to move the clutch into the engaged position where the cable was held taut.

Two approaches to improve the timing are to increase the cut-off frequency of the low-pass filter, or shorten the length of hosing between the control valves and the pneumatic cylinder. These would most likely yield only minor improvements in the timing though. Another approach to consider is to detect the maximum angular velocity at mid-stance rather than the zero-crossing at peak hip flexion. This would advance the timing of the controller by over 100 ms, giving more than adequate time to engage the clutch before heel-strike. The danger with pursuing this route is that if the clutch engages too early during swing phase the leg will not have fully extended and energy storage capacity would be decreased further. Maximum energy storage capacity is achieved when the clutch engages at the point of maximum leg length just before heel-strike.

Perhaps another approach entirely to this timing problem would be to measure the displacement of the cable in the Bowden cable housing directly, and when its motion stops, engage the clutch. This could even be done mechanically by means of a ratchet-pawl mechanism. This clutch type was considered previously but was not pursued because a friction-lock clutch is continuously variable instead of having discrete engagement points. In order to get the desired level of precision out of a ratchet-pawl mechanism, the teeth need to be very small and then it is unable to sustain the required loads. If a ratchet-pawl could be designed to sustain the desired loads and have adequate resolution, however, the pawl could be left in contact with the ratchet during the second half of swing as the exoskeleton

leg is extending. Just after the point of maximum extension the pawl would engage with a tooth on the ratchet and provide the desired stiffness during stance.

Even further in the future, improvements to the elastic exoskeleton could include integration of an elastic or powered hip orthosis that aids with leg swing. The results presented in Chapter 5 clearly show that swinging the weight of the exoskeleton legs increases muscle activation at the hips. Including leg swing assistance could mitigate these effects. In addition, the exoskeleton could be redesigned for carrying additional loads beyond body weight. This most likely would not improve the performance of the exoskeleton compared to normal running, but may provide a decrease in metabolic cost compared to running while carrying the load. With the exoskeleton in parallel with the leg as a whole, loads from a backpack could be transferred directly to the ground. This should decrease the metabolic cost as the exoskeleton could redirect the mass in the backpack during the stance phase rather than requiring the wearer's legs to do so.

Lastly, future work for a design of this nature would not be complete without discussing ways to decrease the mass of the device. Although each component of the exoskeleton was designed in CAD in order to do failure analysis, the components were not optimized for minimum possible weight. Topology optimization was performed for a few select components that would have been bulky had some effort at optimization not been done, but many more parts remain to be optimized. The easiest place to reduce weight on the exoskeleton at this point would be to remove the load cells from the thigh sections of the exoskeleton. These were implemented to measure the loads transmitted to the waist harness by the exoskeleton. In the end the shank section springs provided a more reliable measurement of the force in the exoskeleton though, making the load cells unnecessary. One of the major differences between the exoskeleton developed by Grabowski and Herr [Grabowski 09] and the one presented here is the weight of the device. This is most likely the reason why subject metabolic rate did not decrease significantly for all subjects included in our testing as theirs did.

With these recommendations, the exoskeleton performance should improve dramatically. Even if the metabolic cost of running is not decreased beyond baseline running levels the device could still be quite useful. Specifically, the exoskeleton could be useful at carrying loads as mentioned earlier. This application is of particular interest in military or search and rescue applications. In this application it is a major benefit that this device is quasi-passive. The exoskeleton uses drastically less energy than a powered exoskeleton such as those developed by Jacobsen and Kazerooni. This is particularly important for dismounted marching or insertion operations where light weight and low power are critical.

It could also decrease the loads on the joints of the leg. This would be beneficial for individuals suffering from knee osteoarthritis or recovering from a knee or ankle surgery. It could also be used as a rehabilitation device to enable individuals to begin recovery from leg joint surgeries earlier without placing undue loads on the affected joint. In short, elastic exoskeletons have the capacity to assist human locomotion for individuals who are either healthy or with disabilities. The work presented in this dissertation advances the field of locomotion assistance one step further in this effort.

Appendices

Appendix A

eExo Conceptual Design

This appendix contains a portion of the final report created by a team of senior-level undergraduates in Mechanical Engineering at the University of Michigan. I advised this group and worked extremely closely with them during the course of the semester (Winter 2008) in which this work was accomplished. Working with a team of engineers was invaluable in executing a successful conceptual design phase for creation of a whole-limb exoskeleton.

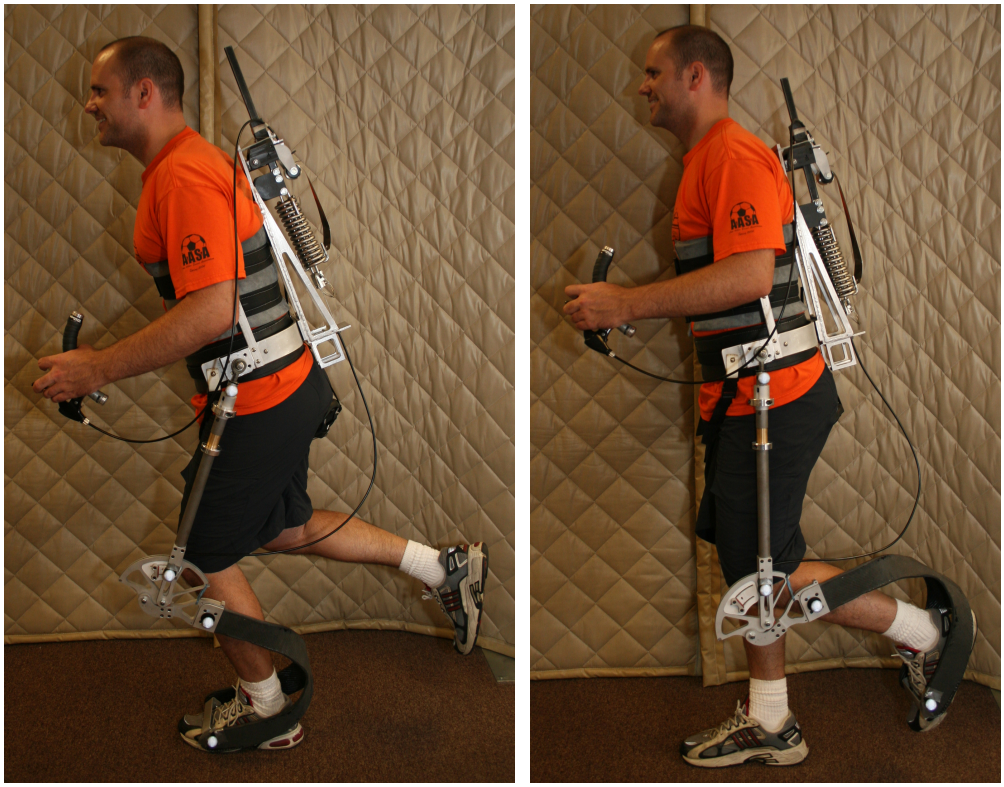

(a) (b)

Figure A.1 Original prototype of the elastic exoskeleton. This version of the prototype was designed and fabricated with the assistance of a team of senior-level undergraduates in Mechanical Engineering at the University of Michigan.

I had begun working on the project before this semester started and used my preliminary data and concepts to guide the team in our efforts to finalize the conceptual design of the exoskeleton. As a team we went on to build the first prototype of the elastic exoskeleton as shown in Figure A.1 before the semester ended. Significant changes were made to the exoskeleton before it was functional, but the basic working principles of the device were finalized at this stage in the research project.

A.1 Concept Generation

In order to generate the proposed concepts, we used several engineering methods including brainstorming, functional decomposition, and several group meetings involving functionality arguments. After the first set of designs was formed, the strong points of each design concept were evaluated in a working principal creation chart to funnel down our concepts to get the top designs. All of the design concepts considered are shown in Figures A.2 and A.3.

Pugh charts were used to select the top three designs from the generated concepts. The two main functions focused on were the method of energy storage and the mechanism for system actuation (simply, the locking or on/off mechanism). The specific concepts considered for these two main functions are provided in Figures A.4 and A.5 and the Pugh charts are provided in Tables A.1 and A.2.

Noticeable differences from the energy storage concepts are the number of pieces each concept incorporates. Using less energy storing components can be beneficial during the manufacturing process because of a reduction in the number of parts; however, disadvantages such as loss of energy in the system would benefit use of a one-piece system. The link-cam system (A.4 e)) has large energy storage benefits; however, the bulky system could potentially fail the low weight requirements of the customer.

Providing an actuation mechanism is crucial to the success of this design. As mentioned earlier, the trouble with attaching leaf springs to the leg is that the legs motion through the gait cycle must be free of resistance except during the heel-strike to toe-off phase. During this phase, the system must be engaged. The disadvantage of the bump stop is that the mechanism is not robust to variations in the user's gait. If the joint does not engage in the closed position no energy will be stored. The benefit of using the bump stop is the ease of manufacturing and the low part count. Ease of manufacturing is also true for the elastic knee joint. This piece can be incorporated to the whole elastic brace; however, the energy storage only provides torque through the swinging motion and does not support any body weight. The last three concepts: the ratchet pawl and the two brake systems (one with torsion spring) are concepts which allow for design of a sensor to activate these systems. The benefit of

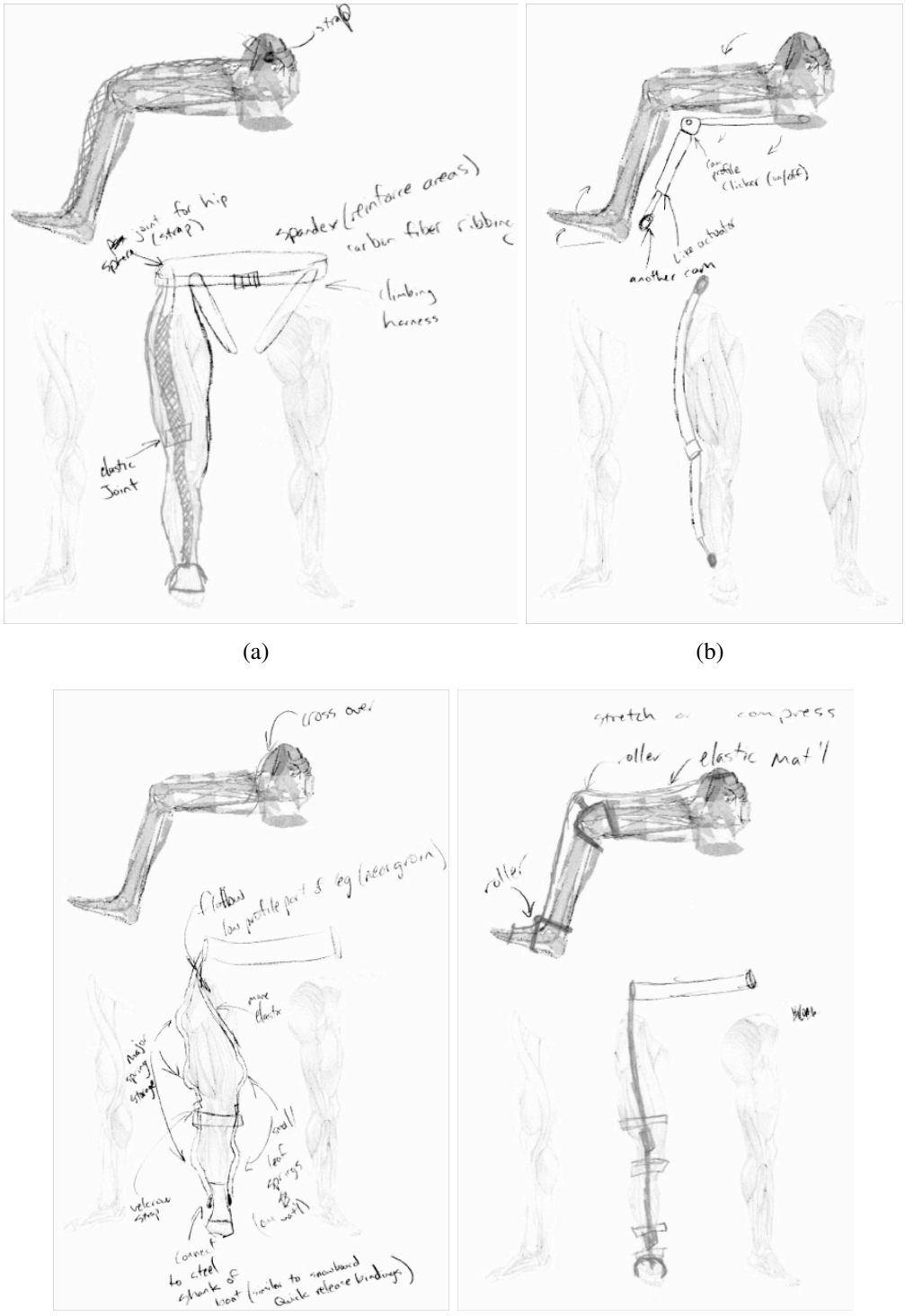

(a) (b)

(c) (d)

Figure A.2 Exoskeleton design concepts, part 1. a) Elastic ribbed pants, b) Cam and rods, c) Dual leaf spring, d) Elastic exotendon.

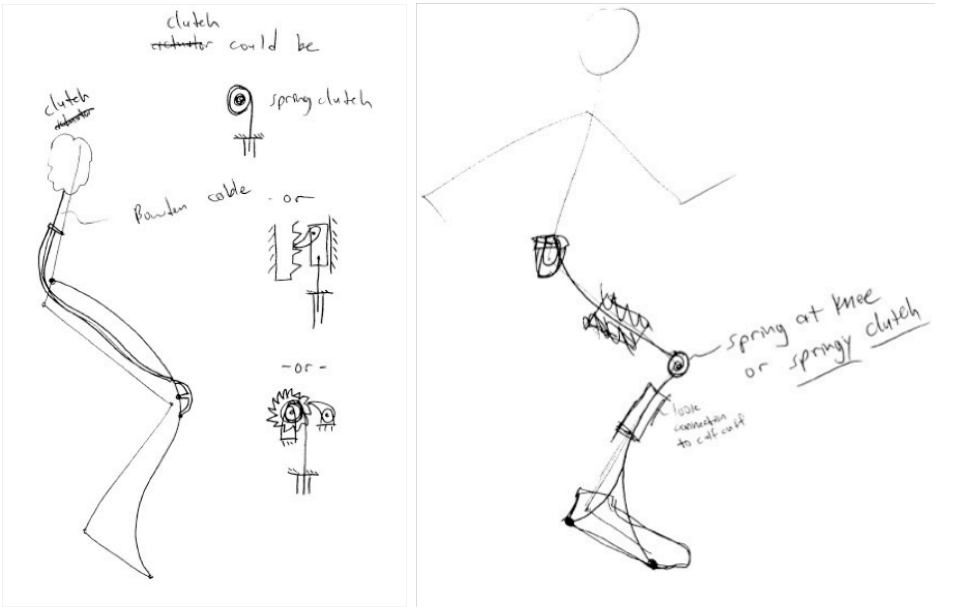

(a) (b)

(c) (d)

Figure A.3 Exoskeleton design concepts, part 2. a) Backpack/knee actuation, b) Spring/clutch at knee, c) Ratchet-pawl knee lock, d) Linear ratchet pawl backpack.

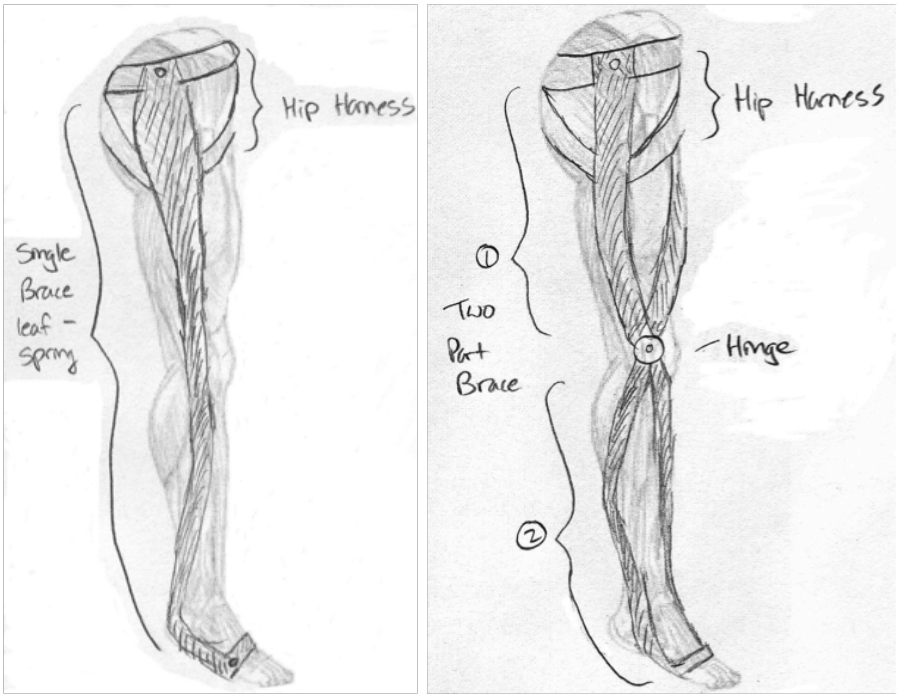

(a) (b)

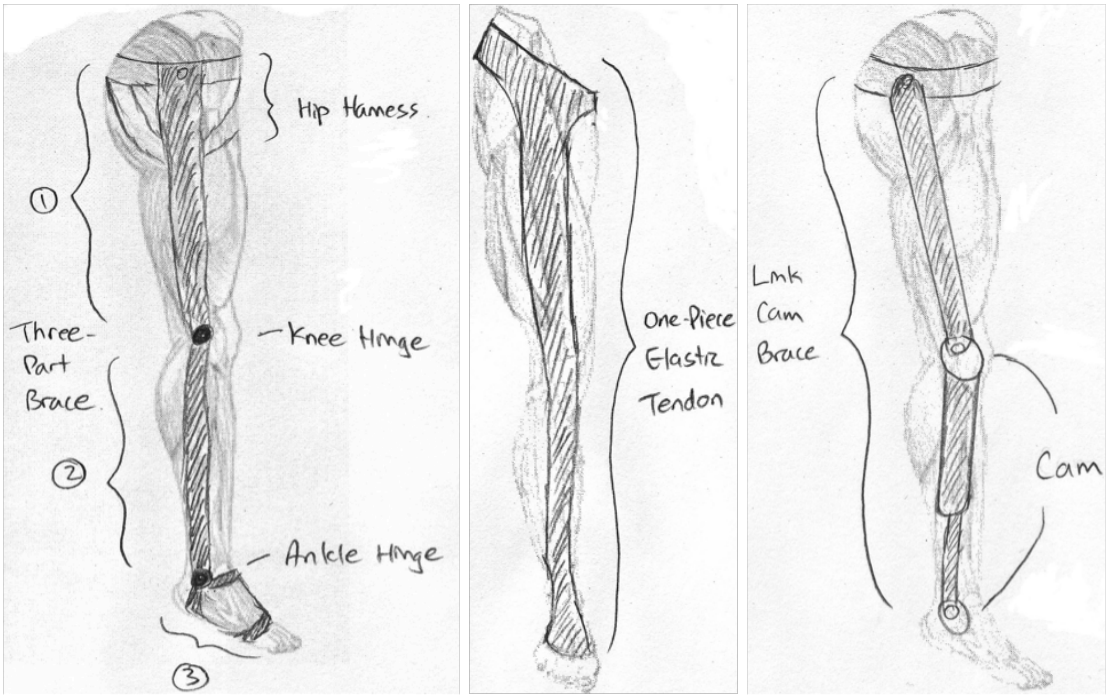

(c) (d) (e)

Figure A.4 Energy storage sub-function concepts. a) Single brace, b) Two-part brace (leaf spring with knee hinge, c) Three-part brace (leaf spring with knee and ankle hinges, d) One-piece elastic tendon, e) Link and cam brace.

	Sub-function: Energy Storage					
	Concept Variants					
Selection Criteria	A	B	C	D	E	REF
Low Weight	0	-	-	+	-	0
Low Profile	-	0	0	+	-	0
Safety	-	0	0	0	-	0
Body Support	+	+	+	-	+	0
Quick Release	+	+	+	-	-	0
Manufacturability	+	+	+	+	-	0
PLUSES	3	3	3	3	1	
SAMES	1	2	2	1	0	
MINUSES	2	1	1	2	5	
NET	1	2	2	1	-4	
RANK	2	1	1	2	5	
CONTINUE?	YES	YES	YES	YES	NO	

		Sub-Function: Energy Storage									
		Concept Variants									
		A		B		C		D		E	
Selection Criteria	Weight	Rating	Score	Rating	Score	Rating	Score	Rating	Score	Rating	Score
Low Weight	25%	2	0.5	2	0.5	2	0.5	1	0.25	4	1
Low Profile	25%	2	0.5	2	0.5	2	0.5	1	0.25	4	1
Safety	15%	2	0.3	2	0.3	2	0.3	2	0.3	4	0.6
Body Support	15%	1	0.15	1	0.15	1	0.15	4	0.6	1	0.15
Quick Release	10%	4	0.4	1	0.1	2	0.2	5	0.5	4	0.4
Manufacturability	10%	2	0.2	3	0.3	4	0.4	2	0.2	5	0.5
	Total	2.05		1.85		2.05		2.1		3.65	
	Rank	2		1		2		4		5	
	Continue?	YES		YES		YES		NO		NO	

Table A.1 Energy storage sub-function Pugh charts.

	Sub-function: Energy On/Off					
	Concept Variants					
Selection Criteria	A	B	C	D	E	REF
Low Weight	0	-	0	0	+	0
Low Profile	0	0	0	0	0	0
Safety	-	+	0	0	+	0
Body Support	+	+	+	+	-	0
Quick Release	+	+	0	+	-	0
Manufacturability	+	0	-	0	+	0
PLUSES	3	3	1	2	3	
SAMES	2	2	4	4	1	
MINUSES	1	1	1	0	2	
NET	2	2	0	2	1	
RANK	1	1	5	1	2	
CONTINUE?	YES	YES	NO	YES	YES	

		Sub-Function: Energy On/Off									
		Concept Variants									
		A		B		C		D		E	
Selection Criteria	Weight	Rating	Score	Rating	Score	Rating	Score	Rating	Score	Rating	Score
Low Weight	25%	1	0.25	2	0.5	2	0.5	2	0.5	1	0.25
Low Profile	25%	2	0.5	2	0.5	3	0.75	2	0.5	1	0.25
Safety	15%	3	0.45	3	0.45	3	0.45	2	0.3	2	0.3
Body Support	15%	2	0.3	1	0.15	1	0.15	1	0.15	6	0.8
Quick Release	10%	2	0.2	1	0.1	3	0.3	1	0.1	6	0.6
Manufacturability	10%	2	0.2	4	0.4	4	0.4	5	0.5	2	0.2
	Total	1.9		2.1		2.1		1.6		2.4	
	Rank	2		3		3		1		5	
	Continue?	YES		YES		YES		YES		NO	

Table A.2 Energy on/off sub-function Pugh charts.

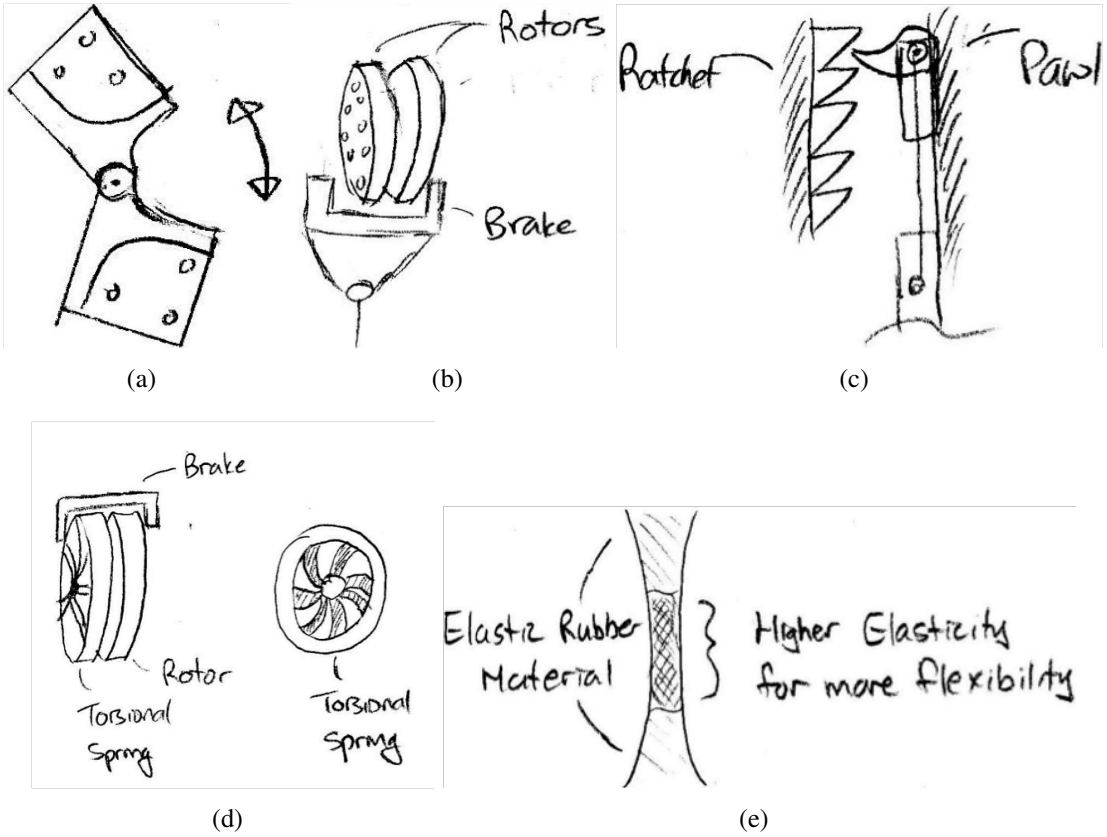

Figure A.5 Energy on/off sub-function concepts. a) Knee bump-stop, b) Clutching knee-brake system, c) Rathcet-pawl hip system, d) Torsion spring knee-clutch-brake system, e) Elastic knee joint.

the ratchet pawl at the hip is that it does not add weight to the lower rotating body parts. The only downside of using a ratchet pawl is the increased number of parts. The two brake systems are very similar, the torsion spring being the only real difference between the two. The added benefit of the torsion spring is the addition of potential energy storage to provide storage throughout the entire system and potential to maintain a low profile throughout the gait cycle. However, the added weight of the two systems on the rotating body parts can increase metabolic cost, which is the opposite of the goal sought to achieve.

Evaluation of both sub-functions will be difficult because each concept is fundamentally sound but also has its drawbacks. Consequently evaluation was not done for the two sub-functions combined. The next section will further evaluate the generated concepts considered for use.

A.2 Concept Selection

The selection of the final design must achieve three goals: be a passive system, which means there is no external power source; have low mass; and achieve a low-profile design. The ability to support body weight is very important - achieving this goal will reduce the amount of energy spent while running, resulting in decreased metabolic cost.

From the Pugh charts presented in the previous section, the following top design concepts were derived (see Figures A.6, A.7, and A.8).

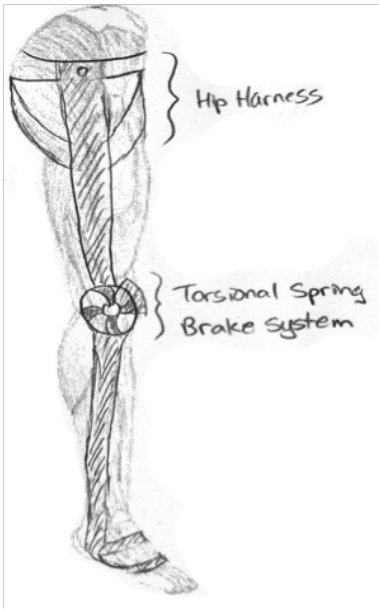

Figure A.6 System concept A.

Concept A features a two piece brace with a torsion spring and clutched brake system on a knee hinge that will store energy via the spring and add to the energy stored by the compliant brace. This design is unique, but the number of components has the potential of being high.

Concept B features a one-piece brace attached to a Ratchet Pawl system mounted on the back of the hip harness. This system would toggle the spring storage system on and off. The one-piece brace will be difficult to maintain a low profile and conform to the leg. The locking actuation mechanism makes this concept unique.

Concept C features a three-piece brace system that incorporates a bump-stop hinge at the knee which serves as the on/off mechanism. This design would be simple to manufacture, lightweight, and use fewer components than the other concepts. However, the design has a limited range of motion in the swing through phase of the gait cycle; this may present problems with the three-piece design.

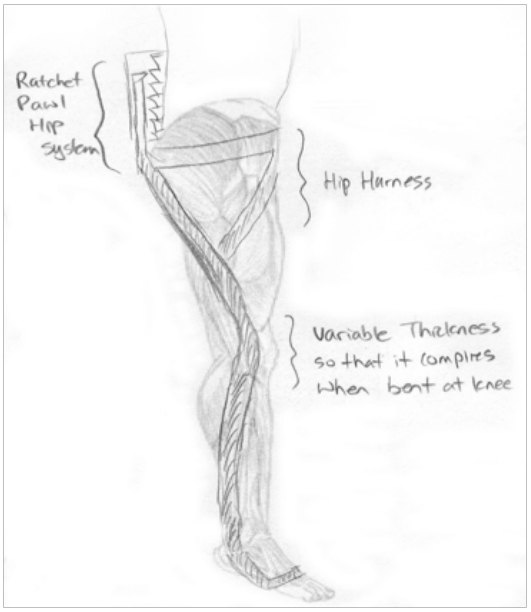

Figure A.7 System concept B.

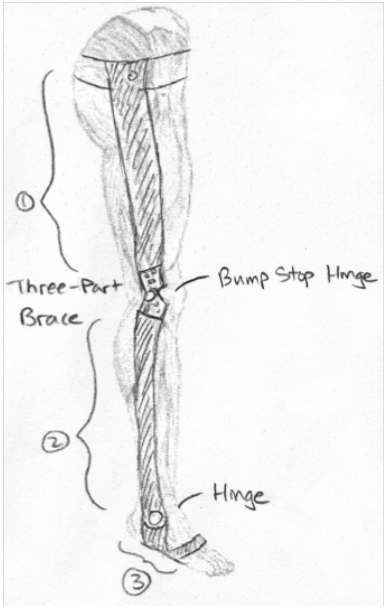

Figure A.8 System concept C.

Other concepts for interfacing the exoskeleton with the body, activating the system, and attaching methods were discussed in detail in team design meetings. These concepts were based on the current design model created by Michael Cherry.

The hip harness will wrap around the waist and under the groin to make a support that reacts to and balances the forces at heel strike that the energy storage mechanism will undergo. The attachment method between the hip and upper leg link will consist of a rod end mounted on the hip harness. The interface between the system and the foot/shoe is a difficult solution because no shoes are the same; however, the targeted application of this system is military use. Therefore, further research on the boots that soldiers use during combat must be conducted and development of a binding system should be undergone. This binding system would allow the soldier the ability to step into a foot slot and have his boot lock into the exoskeleton, much like a ski boot can snap onto a ski. Finally, for activation of the mechanism to turn the spring on and off during the appropriate time in the gait cycle, a foot sensor activation system should be used. This system would sense when the foot is in contact with the ground, turning the system on and storing energy; while the foot leaves the ground, the stored energy is released and the system will disengage.

		SYSTEMS					
		Concept Variants					
		A		**B**		**C**	
Selection Criteria	Weight	Rating	Weighted Score	Rating	Weighted Score	Rating	Weighted Score
# of Components	20%	3	0.6	2	0.4	3	0.6
Energy Storage	25%	1	0.25	3	0.75	2	0.5
Safety	15%	2	0.3	2	0.3	3	0.45
Manufacturability	10%	3	0.3	2	0.2	2	0.2
Degree of Motion	20%	2	0.4	2	0.4	3	0.6
Quick Release	10%	2	0.2	2	0.2	1	0.1
	Total	2.05		2.25		2.45	
	Rank	1		2		3	
	Continue?	YES		NO		NO	

Table A.3 System-level Pugh chart.

These three concepts were evaluated in a system-level Pugh chart. As seen in Table A.3, Concept A is implied as the best concept of the three evaluated. We agree with the Pugh chart selection and decided to use Concept A as the final design. The pros and cons for Concept A are listed below.

Pros:

- Continuous energy storage from hip to foot
- System independent of stride length

- Close proximity to leg through duration of swing and stance phase
- Supports body weight with opportunity to support additional weight
- Simple clutch mechanism for on/off switch

Cons:

- Additional weight on the rotating section of body
- Additional wear due to moving parts
- Complex parts and complex assembly

Overall, concept A will provide a challenge in its creation, but this concept is the idea to use for this project while incorporating compliant systems.

A.3 Concept Description

The final concept selected for this project combines a series of leaf springs with a linearized torsion spring at the knee. This linearized torsion spring will be implemented using a throttle cable guided around the radius of the knee disk attached to a linear coil spring. This coil spring is housed in a locking backpack mechanism which is to be attached to the hip harness. This system stores energy in the lower leg leaf spring and coil spring while maintaining a low profile during the entire swing and stance phases of the gait cycle. A rigid spline will attach to a custom hip harness by a spherical joint rod end. This upper leg spline will conform closely with the side and front of the thigh until it reaches the knee joint. The upper leg spline will be attached to a clevis which constrains the throttle cable along the edge of the disk. The knee joint will be a rigid disk that will allow for the throttle cable to arch around the outside of the disk. During knee rotation, the cable force will be transmitted to the coil spring, therefore acting as a torsion spring. The lower leaf spring will attach to the knee disk and follow the lower leg to the ankle joint and foot. The lower leaf spring will attach to the shoe of the user through a quick release system similar to the bindings on a snowboard. Optimizing this design will provide the most energy storage while maintaining a low profile.

Figure A.9 shows what the splines in the final design would look like. The main focus of the design is the incorporation of a linear spring at the back coupled to the knee disk via throttle cable to act as a torsion spring at the knee joint. This torsion spring allows for added energy storage and constrains the system to remain low profile. The splines of the leaf spring braces will be optimized to conform to the leg of Mike Cherry for whom this design will be created for further testing.

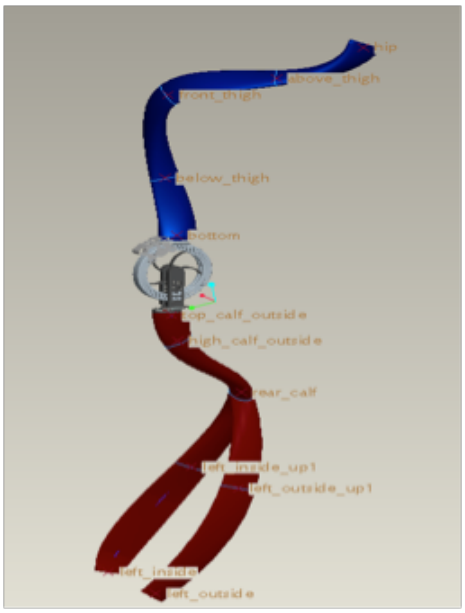

Figure A.9 Prototype alpha design.

The main idea for this concept is that the lower leaf spring stores energy in deformation, and the linear spring acting as a torsion spring at the knee disk keeps the system conforming to the users leg.

Appendix B

Customer Requirements

This appendix was also extracted from the senior design report referenced in Appendix A. The contents were not modified for inclusion in this dissertation but are provided to clarify the goals of the student team during their design process.

B.1 List of Requirements

This section presents the customer requirements with a detailed description. Primary goals for this design project are marked with an asterisk (*).

Low Profile*—The system should be low profile by nature, following within close proximity of the contours of the human leg during all positions of the gait cycle. It should safely store and release its energy while still conforming closely to the full range of motion of the hip, knee, and ankle joints. The system should not irritate or intrude the body at any time during the gait cycle.

Lightweight*—Since the overall goal of this product is to reduce metabolic cost during the running cycle, the system has to store and release at least as much energy as required to bypass its inherent weight. Therefore, the lighter the system, the greater the returns can be when the product is used in its full function.

Passive System*—A passive system is desired because it can simply be used and the number of parts can be significantly reduced, therefore creating a lighter product that will be cheaper to produce.

Adjustable Height—Having a system that can accept a group of users with a wide range of heights is ideal, but currently in the early stages of design this is a secondary goal. A select group of individuals that fits the specifications of the initial prototype can be chosen for its use. A long term goal in a later iteration of this design could be to make three or four different height systems (such as S, M, L, and XL for T-shirts or pants) that together can cover the height range of the pool of users.

Variable Stiffness—A system that has a variable stiffness is ideal because then additional loads can be added without the need of a new system. Also, if an adjustable height system is designed, this feature will be required because in general taller people are heavier than shorter people.

Defined Load—A secondary goal of this project is to design the system so that it can aid the user when a load, as simple as a soldiers pack, is being carried. This goal is addressed by creating a system with a variable stiffness.

Low Cost—Being able to produce a product with as little costs as possible is a goal of any engineering design. To help achieve this goal, it will be important to keep the number of parts to a minimum and to keep the design of the parts as simple as possible while still delivering the desired output. Choosing the best materials that are a balance of desired properties and costs will also be an important factor.

Quick Release—When designed for a military application, the system must be able to be removed easily if at any instance the user needs to perform a task that is beyond the designs limitations. A simple example of this would be if the user needs to crouch behind a wall without springing back up shortly after.

Simple Attachment Method—Being able to quickly attach and remove the exoskeleton many times during the day, maybe even within a few hours, makes this design functional for the customer. The attachment method must never be intrusive, nor should it cause excessive irritation to the user at its points of attachment.

Bibliography

[Alexander 90] R. McNeill Alexander. *Three uses for springs in legged locomotion*. The International Journal of Robotics Research, vol. 9, no. 2, pages 53–61, April 1990.

[Alexander 92] R. McNeill Alexander. *A model of bipedal locomotion on compliant legs.* Philosophical transactions of the Royal Society of London. Series B: Biological sciences, vol. 338, no. 1284, pages 189–198, 1992.

[Amundson 06] Kurt Amundson, Justin Raade, Nathan Harding & H. Kazerooni. *Development of hybrid hydraulic-electric power units for field and service robots*. Advanced Robotics, vol. 20, no. 9, pages 1015–1034, 2006.

[Ananthasuresh 94] Suresh G.K. Ananthasuresh, Sridhar Kota & Yogesh Gianchandani. *A methodical approach to the design of compliant micromechanisms*. Technical Digest. Solid-State Sensor and Actuator Workshop, pages 189 – 92, 1994.

[Arampatzis 99] Adamantios Arampatzis, Gert-Peter Bruggemann & Verena Metzler. *The effect of speed on leg stiffness and joint kinetics in human running*. Journal of Biomechanics, vol. 32, no. 12, pages 1349–1353, December 1999.

[Awtar 07] Shorya Awtar & Alexander H. Slocum. *Constraint-based design of parallel kinematic XY flexure mechanisms*. Journal of Mechanical Design, Transactions Of the ASME, vol. 129, no. 8, pages 816–830, 2007. Compilation and indexing terms, Copyright 2008 Elsevier Inc.

[Banala 06] Sai K. Banala, Sunil K. Agrawal, Abbas Fattah, Vijaya Krishnamoorthy, Wei-Li Hsu, John Scholz & Katherine Rudolph. *Gravity-balancing leg orthosis and its performance evaluation*. IEEE Transactions on Robotics, vol. 22, no. 6, pages 1228–1239, December 2006.

[Biewener 98] Andrew A. Biewener. *Muscle-tendon stresses and elastic energy storage during locomotion in the horse*. Comparative Biochemistry and Physiology, vol. B, no. 120, pages 73–87, 1998.

[Blaya 04] Joaquin A. Blaya & Hugh Herr. *Adaptive control of a variable-impedance ankle-foot orthosis to assist drop-foot gait*. IEEE Transactions on Neural Systems and Rehabilitation Engineering, vol. 12, no. 1, pages 24–32, March 2004.

[Blickhan 89] Reinhard Blickhan. *The spring-mass model for running and hopping*. Journal of Biomechanics, vol. 22, no. 11/12, pages 1217–1227, 1989.

[Bock 04] Alexander Bock. *U.S. Patent Number 6,719,671*, April 2004.

[Brockway 87] J. M. Brockway. *Derivation of formulae used to calculate energy expenditure in man*. Human Nutrition. Clinical Nutrition, vol. 41, no. 6, pages 463–471, Nov 1987.

[Browning 07] Raymond C. Browning, Jesse Modica, Rodger Kram & Ambarish Goswami. *The effects of adding mass to the legs on the energetics and biomechanics of walking*. Medicine & Science in Sports & Exercise, vol. 39, no. 3, pages 515–525, 2007.

[Carr 08] Christopher E. Carr & Dava J. Newman. *Characterization of a lower-body exoskeleton for simulation of space-suited locomotion*. Acta Astronautica, vol. 62, no. 4-5, pages 308–323, 2008.

[Cavagna 75] G. A. Cavagna. *Force platforms as ergometers*. Journal of Applied Physiology, vol. 39, no. 1, pages 174–179, Jul 1975.

[Cavagna 77] G.A. Cavagna & M. Kaneko. *Mechanical work and efficiency in level walking and running*. Journal of Physiology, vol. 268, no. 268, pages 467–481, June 1977.

[CDC 06] Centers for Disease Control and Prevention CDC. URL http://www.cdc.gov, Accessed May 2006.

[Cherry 06] Michael S. Cherry, Dave J. Choi, Kevin J. Deng, Sridhar Kota & Daniel P. Ferris. *Design and fabrication of an elastic knee orthosis — preliminary results*. In International Design Engineering Technical Conferences, numéro 2006-99622 in Proceedings. ASME, September 2006.

[Cherry 07] Michael S. Cherry, Sridhar Kota & Daniel P. Ferris. *Effects of an elastic knee orthosis on unilateral hopping*. In American Society of Biomechanics Annual Conference, Proceedings, August 2007.

[Cherry 09] Michael S. Cherry, Sridhar Kota & Daniel P. Ferris. *An elastic exoskeleton for assisting human running*. In International Design Engineering Technical Conferences, numéro 2009-87355 in Proceedings. ASME, August 2009.

[Chu 05] Andrew Chu, H. Kazerooni & Adam Zoss. *On the biomimetic design of the Berkeley Lower Extremity Exoskeleton (BLEEX)*. In 2005 IEEE International Conference on Robotics and Automation, volume 2005, pages 4345–4352, Apr 18-22 2005 2005.

[Collins 09] S. H. Collins, P. G. Adamczyk, D. P. Ferris & A. D. Kuo. *A simple method for calibrating force plates and force treadmills using an instrumented pole*. Gait and Posture, vol. 29, no. 1, pages 59–64, January 2009.

[Deharde 04] Mark Deharde, Kenneth A. Patchel & Thomas Watters. *U.S. Patent Application 2004/0049291 A1*, March 2004.

[Dick 91] G. John Dick & Eric A. Edwards. *U.S. Patent Number 5,016,869*, May 1991.

[Dollar 08a] Aaron M. Dollar & Hugh Herr. *Design of a quasi-passive knee exoskeleton to assist running*. In IEEE International Conference on Intelligent Robots and Systems, pages 747–754, 2008.

[Dollar 08b] Aaron M. Dollar & Hugh Herr. *Lower Extremity Exoskeletons and Active Orthoses: Challenges and State-of-the-Art*. IEEE Transactions on Robotics, vol. 24, no. 1, pages 144–158, 2008.

[Donelan 01] J. Maxwell Donelan, Rodger Kram & Arthur D. Kuo. *Mechanical and metabolic determinants of the preferred step width in human walking*. Proceedings of the Royal Society of London, vol. B, no. 268, pages 1985–1992, 2001.

[Earl 04] Jennifer E. Earl, Stephen J. Piazza & Jay Hertel. *The Protonics knee brace unloads the quadriceps muscles in healthy subjects*. Journal of Athletic Training, vol. 39, no. 1, pages 44–49, 2004.

[Empi 08] Empi Canada, Vaudreuil, Quebec Empi. *[Online] Protonics® elastic knee orthosis*, Accessed March 2008.

[Erdman 01] Arthur G. Erdman, George N. Sandor & Sridhar Kota. Mechanism design, analysis and synthesis. Prentice Hall, Upper Saddle River, NJ, 2001.

[Farley 91] C. T. Farley, R. Blickhan, J. Saito & C. R. Taylor. *Hopping frequency in humans: A test of how springs set stride frequency in bouncing gaits*. Journal of Applied Physiology, vol. 71, no. 6, pages 2127–2132, 1991.

[Farley 92] C. T. Farley & T. A. McMahon. *Energetics of walking and running: insights from simulated reduced-gravity experiments*. Journal of applied physiology (Bethesda, Md.: 1985), vol. 73, no. 6, pages 2709–2712, Dec 1992. LR: 20071114; PUBM: Print; GR: R01 AR 18140/AR/United States NIAMS; JID: 8502536; ppublish.

[Farley 93] Claire T. Farley, James Glasheen & Thomas A. McMahon. *Running springs: speed and animal size*. Journal of Experimental Biology, vol. 185, pages 71–86, 1993.

[Farley 96] Claire T. Farley & Octavio Gonzalez. *Leg stiffness and stride frequency in human running*. Journal of Biomechanics, vol. 29, no. 2, pages 181–186, 1996.

[Farley 98a] Claire T. Farley & Daniel P. Ferris. *Biomechanics of walking and running: center of mass movements to muscle action*. Exercise and Sport Sciences Reviews, vol. 26, no. 1, pages 253–285, January 1998.

[Farley 98b] Claire T. Farley, Han H. P. Houdijk, Ciska van Strien & Micky Louie. *Mechanism of leg stiffness adjustment for hopping on surfaces of*

different stiffnesses. Journal of Applied Physiology, vol. 85, no. 3, pages 1044–1055, 1998.

[Farley 99] Claire T. Farley & David C. Morgenroth. *Leg stiffness primarily depends on ankle stiffness during human hopping*. Journal of Biomechanics, vol. 32, pages 267–273, 1999.

[Ferris 97] Daniel P. Ferris & Claire T. Farley. *Interaction of leg stiffness and surface stiffness during human hopping*. Journal of Applied Physiology, vol. 82, no. 1, pages 15–22, 1997.

[Ferris 98] Daniel P. Ferris, Micky Louie & Claire T. Farley. *Running in the real world: adjusting leg stiffness for different surfaces*. Proceedings of the Royal Society of London, vol. B, no. 265, pages 989–994, 1998.

[Ferris 99] Daniel P. Ferris, Kailine Liang & Claire T. Farley. *Runners adjust leg stiffness for their first step on a new running surface*. Journal of Biomechanics, vol. 32, no. 8, pages 787–794, August 1999.

[Ferris 06] Daniel P. Ferris, Zaineb A. Bohra, Jamie R. Lukos & Catherine R. Kinnaird. *Neuromechanical adaptation to hopping with an elastic ankle-foot orthosis*. Journal of Applied Physiology, vol. 100, no. 1, pages 163–170, January 2006.

[Fukunaga 01] T. Fukunaga, K. Kubo, Y. Kawakami, S. Fukashiro, H. Kanehisa & C. N. Maganaris. *In vivo behaviour of human muscle tendon during walking*. Proceedings of the Royal Society of London B, vol. 268, no. 1464, pages 229–233, Feb 7 2001. LR: 20061115; PUBM: Print; JID: 101245157; ppublish.

[Geyer 05] Hartmut Geyer, Andre Seyfarth & Reinhard Blickhan. *Spring-mass running: simple approximate solution and application to gait stability*. Journal of Theoretical Biology, vol. 232, pages 315–328, 2005.

[Geyer 06] Hartmut Geyer, Andre Seyfarth & Reinhard Blickhan. *Compliant leg behaviour explains basic dynamics of walking and running.* Proceedings of the Royal Society of London B, vol. 273, no. 1603, pages 2861–2867, November 2006.

[Ghan 06] J. Ghan, R. Steger & H. Kazerooni. *Control and system identification for the Berkeley lower extremity exoskeleton (BLEEX)*. Advanced Robotics, vol. 20, no. 9, pages 989–1014, 2006. M1: Copyright 2007, The Institution of Engineering and Technology.

[Grabowski 09] Alena M. Grabowski & Hugh M. Herr. *Leg exoskeleton reduces the metabolic cost of human hopping*. Journal of Applied Physiology, May 2009.

[Guizzo 05] Erico Guizzo & Harry Goldstein. *The rise of the body bots*. IEEE Spectrum, pages 50–56, October 2005.

[Herder 01] J.L. Herder. Energy-free systems. theory, conception and design of statically balanced spring mechanisms. ISBN 90-370-0192-0, 2001.

[Herr 03] Hugh Herr & Ari Wilkenfeld. *User-adaptive control of a magnetorheological prosthetic knee*. Industrial Robot: An International Journal, vol. 30, no. 1, pages 42–55, 2003.

[Hollander 04] Kevin W. Hollander & Thomas G. Sugar. *Concepts for compliant actuation in wearable robotic systems*. Proceedings of the US-Korea Conference on Science, Technology and Entrepreneurship, August 2004.

[Hollander 05a] Kevin W. Hollander, Thomas G. Sugar & Donald E. Herring. *Adjustable robotic tendon using a 'Jack Spring'^{TM}*. Proceedings of the Design of Medical Devices Conference, June 2005.

[Hollander 05b] Kevin W. Hollander, Thomas G. Sugar & Donald E. Herring. *A robotic 'Jack Spring'^{TM} for ankle gait assistance*. Proceedings of the DETC, vol. DETC2005-84492, September 2005.

[Hollander 06] Kevin W. Hollander & Thomas G. Sugar. *Design of lightweight lead screw actuators for wearable robotic applications*. Journal of Mechanical Design, vol. 128, no. 3, pages 644–648, May 2006.

[Howell 01] Larry L. Howell. Compliant mechanisms. Wiley and Sons, August 2001.

[Hurst 04] Jonathan W. Hurst, Joel E. Chestnutt & Alfred A. Rizzi. *An actuator with physically variable stiffness for highly dynamic legged locomotion*. In International Conference on Robotics & Automation, Proceedings, pages 4662–4668. IEEE, April 2004.

[Ishikawa 05] M. Ishikawa, P. V. Komi, M. J. Grey, V. Lepola & G. P. Bruggemann. *Muscle-tendon interaction and elastic energy usage in human walking*. Journal of applied physiology (Bethesda, Md.: 1985), vol. 99, no. 2, pages 603–608, Aug 2005.

[Jacobsen 04] S. C. Jacobsen, M. Olivier, F. M. Smith, D. F. Knutti, R. T. Johnson, G. E. Colvin & W. B. Scroggin. *Research robots for applications in artificial intelligence, teleoperation and entertainment*. International Journal of Robotics Research, vol. 23, no. 4-5, pages 319–330, 2004.

[Kawamoto 02] H. Kawamoto & Y. Sankai. *Comfortable power assist control method for walking aid by HAL-3*. In International Conference on Systems, Man and Cybernetics, volume 4 of *Proceedings*, pages 6–11. IEEE, October 2002.

[Kawamoto 05] Hiroaki Kawamoto & Yoshiyuki Sankai. *Power assist method based on Phase Sequence and muscle force condition for HAL.* Advanced Robotics, vol. 19, no. 7, pages 717–734, 2005.

[Kazerooni 05] Homayoon Kazerooni. *Exoskeletons for human power augmentation*. In International Conference on Intelligent Robots and Systems, Proceedings, pages 3459–64, Edmonton, Alta., Canada, 2-6 Aug. 2005 2005. Dept. of Mech. Eng., California Univ., Berkeley, CA, USA, IEEE. M1: Copyright 2006, IEE; T3: 2005 IEEE/RSJ International Conference on Intelligent Robots and Systems.

[Kazerooni 07] Homayoon Kazerooni, Andrew Chu & Ryan Steger. *That which does not stabilize, will only make us stronger*. International Journal of Robotics Research, vol. 26, no. 1, pages 75–89, 2007.

[Kerdok 02] Amy E. Kerdok, Andrew A. Biewener, Thomas A. McMahon, Peter G. Weyand & Hugh M. Herr. *Energetics and mechanics of human running on surfaces of different stiffnesses*. Journal of Applied Physiology, vol. 92, pages 469–478, 2002.

[Kim 06] Charles J. Kim, Sridhar Kota & Yong-Mo Moon. *An instant center approach toward the conceptual design of compliant mechanisms*. Journal of Mechanical Design, vol. 128, no. 3, pages 542–550, May 2006.

[Kota 00] Sridhar Kota, Joel Hetrick, Zhe Li, Steve Rodgers & Thomas Krygowski. *Synthesizing high-performance compliant stroke amplification systems for MEMS*. Proceedings of the IEEE Micro Electro Mechanical Systems (MEMS), pages 164–169, 2000. Compilation and indexing terms, Copyright 2008 Elsevier Inc.

[Kota 01] Sridhar Kota. *U.S. Patent Number 6,301,742*, October 2001.

[Kram 90] Rodger Kram & C. Richard Taylor. *Energetics of running: a new perspective*. Nature, vol. 346, pages 265–267, July 1990.

[Kuitenen 02] Sami Kuitenen, Paavo V. Komi & Heikki Kyrolainen. *Knee and ankle joint stiffness in sprint running*. Med. Sci. Sports Exerc., vol. 34, no. 1, pages 166–173, 2002.

[Kuo 05] Arthur D. Kuo, J. Maxwell Donelan & Andy Ruina. *Energetic consequences of walking like an inverted pendulum: step-to-step transitions*. Exercise and Sport Sciences Reviews, vol. 33, no. 2, pages 88–97, 2005.

[Low 04] K. H. Low, Xiaopeng Liu, Hao Y. Yu & H. S. Kasim. *Development of a lower extremity exoskeleton - preliminary study for dynamic walking*. In 2004 8th International Conference on Control, Automation,

Robotics and Vision (ICARCV), volume 3, pages 2088–93, 6-9 Dec. 2004 2004.

[Low 05] K. H. Low. *Initial experiments on a leg mechanism with a flexible geared joint and footpad*. Advanced Robotics, vol. 19, no. 4, pages 373–99, 2005. M1: Copyright 2005, IEE.

[Low 06] K. H. Low, X. Liu & H. Yu. *Design and implementation of NTU wearable exoskeleton as an enhancement and assistive device*. Applied Bionics and Biomechanics, vol. 3, no. 3, pages 209–25, 2006.

[Lu 06] Kerr-Jia Lu & Sridhar Kota. *Topology and dimensional synthesis of compliant mechanisms using discrete optimization*. Transactions of the ASME.Journal of Mechanical Design, vol. 128, no. 5, pages 1080–91, 2006. M1: Copyright 2006, The Institution of Engineering and Technology.

[McGeer 90] Tad McGeer. *Passive bipedal running*. Proceedings of the Royal Society of London B, vol. 240, no. 1297, pages 107–134, 1990.

[McMahon 79] Thomas A. McMahon & Peter R. Greene. *The influence of track compliance on running*. Journal of Biomechanics, vol. 12, no. 12, pages 893–904, December 1979.

[McMahon 90] Thomas A. McMahon & George C. Cheng. *The mechanics of running: how does stiffness couple with speed?* Journal of Biomechanics, vol. 23, no. Suppl. 1, pages 65–78, 1990.

[Mochon 80] Simon Mochon & Thomas A. McMahon. *Ballistic walking*. Journal of Biomechanics, vol. 13, pages 49–57, 1980.

[Muybridge 55] Eadweard Muybridge. The human figure in motion. Dover Publications Inc., 1955.

[Myers 85] M. J. Myers & K. Steudel. *Effect of limb mass and its distribution on the energetic cost of running*. The Journal of Experimental Biology, vol. 116, pages 363–373, May 1985.

[NCOPE 06] National Commission on Orthotic & Prosthetic Education NCOPE. URL http://www.ncope.org/, Accessed May 2006.

[Novacheck 98] Tom F. Novacheck. *The biomechanics of running*. Gait and Posture, vol. 7, pages 77–95, 1998.

[O'Connor 07] Shawn M. O'Connor & Arthur D. Kuo. *Walking, Skipping, and Running Produced From a Single Bipedal Model*. In American Society of Biomechanics Annual Conference, Proceedings, 2007.

[Ossur 06a] Ossur hf., Iceland Ossur. *[Online] The Flex-Foot® Prosthesis*, Accessed May 2006.

[Ossur 06b] Ossur hf., Iceland Ossur. *[Online] The Rheo Knee® Prosthesis*, Accessed May 2006.

[Ossur 08] Ossur hf., Iceland Ossur. *[Online] AFO Dynamic*, Accessed March 2008.

[Pratt 04a] J. E. Pratt & B. T. Krupp. *Series elastic actuators for legged robots*. In Unmanned Ground Vehicle Technology VI, volume 5422, pages 135–44, Orlando, FL, USA, 13-15 April 2004 2004. SPIE-Int. Soc. Opt. Eng.

[Pratt 04b] Jerry E. Pratt, Benjamin T. Krupp & Steven H. Collins. *The RoboKnee: an exoskeleton for enhancing strength and endurance during walking*. In International Conference on Robotics & Automation, Proceedings, pages 2430–2435, New Orleans, LA, April 2004. IEEE.

[RDM 06] RDM sarl, Switzerland RDM. *[Online] Kangoo Jumps Rebound Exercise Jumping Shoes*, Accessed February 2006.

[Sawicki 09] Gregory S. Sawicki, Cara L. Lewis & Daniel P. Ferris. *It pays to have a spring in your step*. Exercise and Sport Sciences Reviews, no. In press, 2009.

[Schiele 08] Andre Schiele. *Performance difference of Bowden Cable relocated and non-relocated master actuators in virtual environment applications*. In International Conference on Intelligent Robots & Systems, Proceedings, pages 3507–3512. IEEE, 2008.

[UCSF 06] UCSF Disability Statistics Center UCSF. URL http://dsc.ucsf.edu, Accessed May 2006.

[van den Bogert 03] Antonie J. van den Bogert. *Exotendons for assistance of human locomotion*. BioMedical Engineering OnLine, vol. 2, no. 17, October 2003.

[Vehar 06] Christine M. Vehar & Sridhar Kota. *Generalized synthesis of nonlinear springs for prescribed load-displacement functions*. Proceedings of the DETC, vol. DETC2006-99657, 2006.

[Veneman 06] J. F. Veneman, Ralf Ekkelenkamp, R. Kruidhof, Frans C. T. van der Helm & Herman van der Kooij. *A Series Elastic- and Bowden-Cable-Based Actuation System for Use as Torque Actuator in Exoskeleton-Type Robots*. International Journal of Robotics Research, vol. 25, no. 3, pages 261–281, 2006.

[Vogel 98] Steven Vogel. Cats' paws and catapults: mechanical worlds of nature and people. Norton, New York, 1998.

[Walsh 06] C. J. Walsh, D. Paluska, K. Pasch, W. Grand, A. Valiente & H. Herr. *Development of a lightweight, underactuated exoskeleton for load-carrying augmentation*. In International Conference on Robotics & Automation, Proceedings, pages 3485–91, Orlando, FL, USA, 15-19 May 2006 2006. IEEE.

[Whittington 09] Ben R Whittington & Darryl G Thelen. *A simple mass-spring model with roller feet can induce the ground reactions observed in human walking.* Journal of Biomechanical Engineering, vol. 131, no. 1, page 011013, February 2009.

[Wittwer 02] Jonathan W. Wittwer, Troy Gomm & Larry L. Howell. *Surface micromachined force gauges: Uncertainty and reliability*. Journal of Micromechanics and Microengineering, vol. 12, no. 1, pages 13–20, 2002. Compilation and indexing terms, Copyright 2008 Elsevier Inc.

[Yamamoto 03] K. Yamamoto, M. Ishii, K. Hyodo, T. Yoshimitsu & T. Matsuo. *Development of power assisting suit (miniaturization of supply system to realize wearable suit)*. In 6th International Conference on Motion and Vibration Control, volume 46, pages 923–30, Saitama, Japan, 19-23 Aug. 2002 2003. Dept. of Welfare Syst. Eng., Kanagawa Inst. of Technol., Japan, JSME. M1: Copyright 2004, IEE; T3: JSME Int. J. C, Mech. Syst. Mach. Elem. Manuf. (Japan).

[Yoshimitsu 04] T. Yoshimitsu & K. Yamamoto. *Development of a power assist suit for nursing work*. In SICE 2004 Annual Conference, volume 1, pages 577–80, Sapporo, Japan, 4-6 Aug. 2004 2004. Kanagawa Inst. of Technol., Japan, IEEE. M1: Copyright 2005, IEE; T3: SICE 2004 Annual Conference (IEEE Cat. No. 04TH8773).

[Zoss 05] A. Zoss, H. Kazerooni & A. Chu. *On the mechanical design of the Berkeley Lower Extremity Exoskeleton (BLEEX)*. In International Conference on Intelligent Robots and Systems, Proceedings, pages 3465–72. IEEE, 2-6 Aug. 2005 2005.

[Zoss 06a] A. Zoss & H. Kazerooni. *Design of an electrically actuated lower extremity exoskeleton*. Advanced Robotics, vol. 20, no. 9, pages 967–88, 2006. M1: Copyright 2006, The Institution of Engineering and Technology.

[Zoss 06b] A.B. Zoss, H. Kazerooni & A. Chu. *Biomechanical Design of the Berkeley Lower Extremity Exoskeleton (BLEEX)*. IEEE/ASME Transactions on Mechatronics, vol. 11, no. 2, pages 128–138, April 2006.